This is to certify that the

dissertation entitled

DISTAL STERIC AND HYDROGEN BONDING EFFECTS
IN HEME-DIOXYGEN INTERACTIONS

presented by

Michail Kondylis

has been accepted towards fulfillment
of the requirements for

Ph.D. degree in Chemistry

Chris G. Cheng
Major professor

Date 12/12/85

DISTAL STERIC AND HYDROGEN BONDING EFFECTS IN HEME-DIOXYGEN INTERACTIONS

By

Michail Kondylis

A DISSERTATION

Submitted to
Michigan State University
in partial fulfillment of the requirements
for the degree of

DOCTOR OF PHILOSOPHY

Department of Chemistry

1985

ABSTRACT

DISTAL STERIC AND HYDROGEN BONDING EFFECTS IN HEME-DIOXYGEN INTERACTIONS

By

Michail Kondylis

The synthetic analog approach has been used very often to elucidate the structure-function relationships in many proteins. The same approach was also used in this study. The proposed distal steric effect of hemoglobin and myoglobin was probed using specifically designed and synthesized porphyrins with an off-the-center strap on one of the porphyrin faces, and an intramolecularly appended proximal imidazole base on the other. The kinetic and thermodynamic parameters of O_2 and CO binding to these synthetic heme models were determined using the standard flash photolysis and spectrophotometric titration methods. A small distal steric effect was observed reducing the CO association rate by a factor of not more than 3 compared to O_2. This small effect cannot account for the large discrimination against CO binding exhibited by the proteins. On the other hand, the polarity near the binding site was proven to be more important, reducing the affinity ratio (M) by an order of magnitude in the models studied.

In order to quantify hydrogen-bonding effects on dioxygen binding to hemes and thus to understand its importance to proteins, the synthesis of Co(II) porphyrins with functional groups of varying hydrogen-bonding ability near the coordination site was undertaken. The realization of this goal was made possible with the synthesis of meso 1-naphthyl porphyrins substituted at the 8-naphthyl position. The study of meso 1-anthryl porphyrins substituted at the 8-anthryl position was also included. The affinity constants for this series of Co(II) porphyrins were determined at different low temperatures and their thermodynamic parameters (ΔH, ΔS) were calculated. There is a large enhancement in O_2 affinity which correlates well with the hydrogen bond strength of each model. The 3 orders of magnitude variation of the binding constants, gave us a clear picture of the importance of the hydrogen bonding in dioxygen binding.

To my mother Irini

and the memory of my father Panayiotis

ACKNOWLEDGMENTS

First of all I would like to thank Professor C. K. Chang for his constant encouragement and guidance during the course of this work.

I would also like to thank Mr. M. S. Koo and all the present and past members of our group for many helpful discussions and friendship. They are all bery-bery good students, although they could be better.

My deep appreciation is due to my parents and my family who put my education as a very high priority in their lives.

My thanks should also be given to Dr. Nick Leventis and the rest of the Greek students who together with the Greek-American community of Lansing made my stay here a little more enjoyable.

I'm also grateful to Eleni for definitely making my new world adventure worthwhile.

TABLE OF CONTENTS

LIST OF TABLES

LIST OF FIGURES

CHAPTER 1

KINETICS OF CO AND O_2 BINDING TO IMIDAZOLE APPENDED STRAPPED HEMES

Introduction

The ability of the single compound protoheme to either reversibly bind oxygen, catalyze oxidation of organic compounds, decompose hydrogen peroxide or transport electrons, depending upon its environment, is remarkable.[1] Even among the first class of compounds, the oxygen carriers, there are large variations in the kinetics and equilibria of oxygenation, which have been the subject of extensive investigations. Hemoglobin is one of the few extensively studied proteins. It was the first protein crystallized (1849); the first protein with a recognized physiological purpose (O_2 transport 1864; CO_2 transport 1904); one of the first proteins whose molecular weight and primary sequence were established (c. 1930); and one of the first proteins whose tertiary and quartenary structures were determined by x-ray crystallography (1960).[1d] Hemoglobin (Hb) is a tetrameric protein consisting of 2α- and 2β-subunits (141 and 146 amino acids, respectively) with one protoheme IX (iron (ii) protoporphyrin IX complex) per subunit. Myoglobin (Mb) consists of a polypeptide chain of 153 residues and one protoheme, which closely resembles one subunit of a hemoglobin, tetramer. In myoglobin the iron atom is coordinated by four porphyrin nitrogen atoms, and

the nitrogen atom of the proximal imidazole (from a histidine).[2,3] (Fig. 1-1).

To examine the relationships between function and structure of dioxygen binding heme proteins, the proteins themselves offer rather limited possibilities. One productive and thus very useful approach, used very often, is the synthetic analog approach.[2] That is, the design, synthesis, characterization and study of "small" models (<2000 amu) of metalloproteins which are structurally and functionally similar to the active site of metalloproteins. Due to its flexibility, the synthetic analog approach can lead to a better understanding of the active site than can be obtained from the protein itself. It allows us to change the structure of the model and by comparison of its spectroscopic and reactivity properties, to recognize previously unrevealed functions of the protein. The study of metalloproteins many times follows the sequence:[2b]

1. Isolation and purification of the metalloprotein.
2. Measurement of physical properties of the active site.
3. Synthesis and isolation of analog complexes.
4. Characterization of structural, spectroscopic and chemical reactivity properties of the synthetic analogs.
5. Comparison between the protein and the analogs and among the analogs to reveal new structure-function relationships.

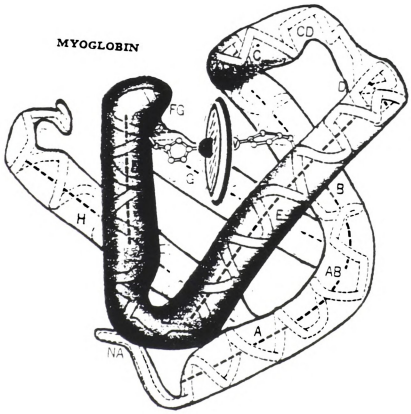

Figure 1-1 Tertiary structure of myoglobin.

One may argue for this sequence that molecular modeling occurs only after a great deal about the proteins is already known. That's because it is difficult to design and synthesize active site model compounds unless one already has enough information about the active site. Synthetic models can provide a detailed understanding of the structure and functioning of the active site which cannot be obtained (or at least not without extreme difficulty) by studying the hemoprotein itself. The modification of the metal reactivity by the protein can also be revealed by the study of simple models where the metal is not influenced by the protein. Finally, the synthetic analogs can give us a better understanding of the function and mechanism of biological systems.

The so-called distal steric effect in Hb and Mb is one of the problems currently being probed by means of synthetic models. The idea that non-bonding interactions with protein residues, like the distal imidazole, can after the binding of ligands to hemoglobin and myoglobin, began with the demonstration by St. George and Pauling[4] of reduced binding of isocyanides (RNC) with increasing steric bulk of the R group. X-ray crystallography showed that the structures of carbon monoxide liganded hemoglobin and myoglobin exhibit a bent or tilted FeCO linkage with respect to the porphyrin ring,[5] whereas in heme model compounds the FeCO bond is linear and perpendicular to the heme plane.[6] The origin of the distorted configuration in the proteins is attributed

primarily to nonbonding steric interactions of the axial ligand with residues at the distal side. An assumption is made that ligands such as O_2, which preferentially form bent complexes, should encounter less steric hindrance when bound in the heme pocket.[7] It has been proposed that in Hb and Mb, the distal side steric effect would decrease the affinity ratio of CO vs. O_2, and is responsible for the detoxification of CO poisoning in respiratory systems.[8] A comparison of ligand binding constants of proteins and model compounds often shows that many heme models have a larger CO vs. O_2 affinity ratio (M value) than the proteins. However, such a comparison does not necessarily constitute a correlation between the distal steric effect and affinity, as the ligand binding constants of heme models can be drastically altered by medium effects.[9] Indeed, Traylor and coworkers have shown that a five-coordinate protoheme-imidazole model binds both O_2 and CO in aqueous suspensions with equilibrium and kinetic parameters almost identical to R-state isolated hemoglobin chains,[9,10] which led them to the conclusion that R-state Hb simply maintains the protoheme five-coordinated, soluble in water and protected against oxidation, without any steric hindrance. In other cases, for example, T-state Hb and notably myoglobins have very small M values which cannot be duplicated by simple heme compounds and so they must be subjected to some distal side steric hindrance.

It is, therefore, of importance to examine the steric

effects on ligand affinity using synthetic models equipped with varying degrees of steric hindrance at the distal side. Several porphyrin models of this kind have been prepared[11] but failed to show the degree of discrimination against CO, that is present in myoglobin. All the existing models have a covalently bound alkyl or aromatic group residing exactly above the center of the porphyrin ring, protecting the distal side of the heme and at the same time providing steric hindrance for the incoming gaseous ligands. And indeed reduced association rate constants for CO and O_2 have been observed for these models, but without being able to reproduce the differentiation, Mb shows, in favor of O_2. The fact that for those models both O_2 and CO association rates are reduced to values that in some cases are even lower than that for myoglobin and yet, the proper differentiation between them is not observed led us to believe that the differentiation may not be proportional to the steric hindrance but that it rather reaches a maximum and then decreases, as the steric effect becomes too great. In order to test this hypothesis new model compounds with more "delicate" steric hindrance should be synthesized. It is reasonable to assume that strapped porphyrins with the strap off-the-center of the ring would impose the desired gentle steric effect (Fig. 1-2). It was with these thoughts that the strapped porphyrins shown in Fig. 1-3 were synthesized and studied.

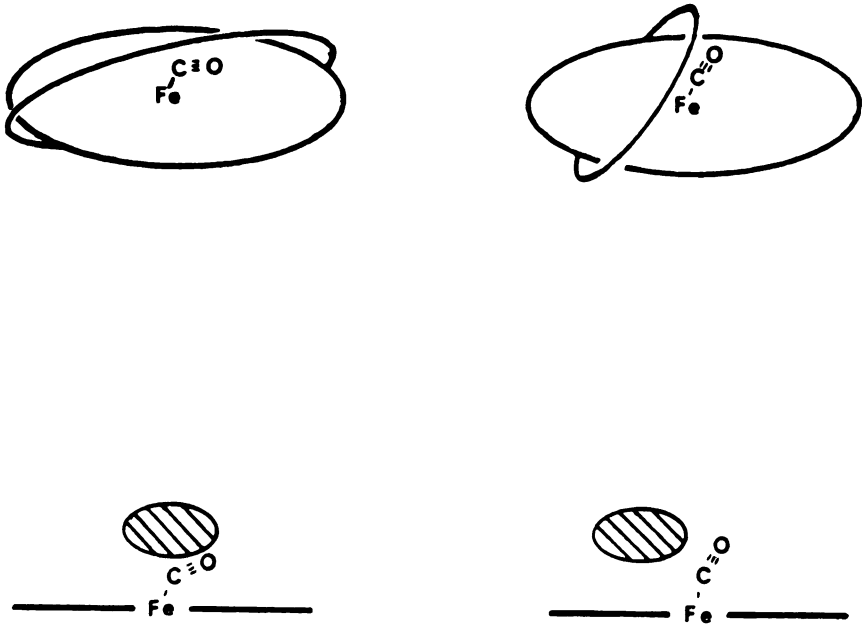

Figure 1-2 Graphic representation of CO distortion in symmetrically and side strapped hemes.

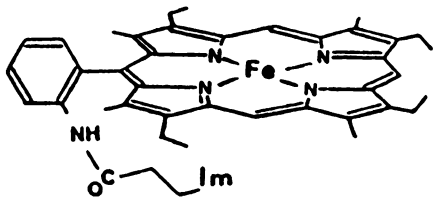

Fe $(CH_2)_2$Im

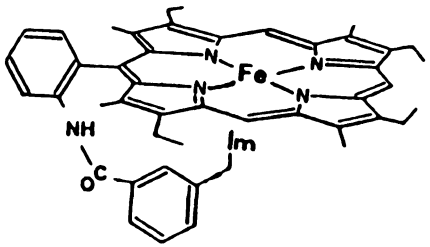

Fe BzIm

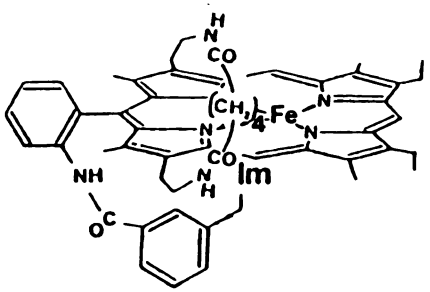

Fe SSP-12

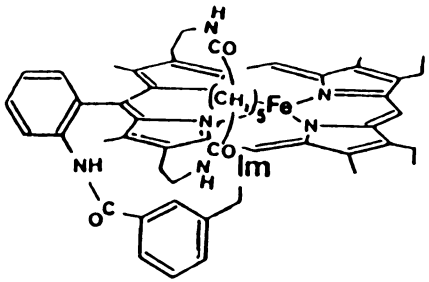

Fe SSP-13

Figure 1-3 Structures of Fe$(CH_2)_2$Im, FeBzIm, FeSSP-12 and FeSSP-13 hemes.

Results and Discussion

Here is presented the equilibria and kinetic rates of CO and O_2 binding of a system which possesses both an off-the-center strap and a covalentely bound imidazole. Two unprotected hemes were also studied for reasons of comparison with the protected system. The equilibria constants for CO binding were determined by means of direct spectrophotometric titrations of a degassed and reduced[16] solution of the hemes in toluene. The CO association rate constants (k^{CO}) were also determined directly by flash photolysis. The CO dissociation rates (k^{-CO}) were calculated from the CO equilibrium constants and the CO association rates. O_2 affinities were determined by CO competition measurements and calculated according to the Gibson equation:[1a]

$$1/R = 1/k^{-O}2 + K^{O}2/k^{CO}[CO]$$

The O_2 association rate constants ($k^{O}2$) were determined directly by means of flash photolysis, while the O_2 dissociation rate constants ($k^{-O}2$) were calculated from the O_2 affinities and the $k^{O}2$. A detailed description of how the kinetic and equilibria values were obtained is described in the "Materials and Methods" section of this chapter. All the rates and equilibrium constants for the model compounds studied and relevant heme proteins, are tabulated in Table 1-1.

The first somewhat unexpected result one can observe is the higher than usual, although not entirely unprecendented,[11f,14b] rate constants for the two unprotected hemes. (Compare for example Tables 1-1 and 1-2). If these values are compared with the very similar series of diaryl substituted hemes studied earlier[12] (Table 1-2), it is apparent that all the rate constants are 2-5 fold larger in the present system. The two heme systems are very similar (same imidazole tail, same solvent and temperature, same electronic effect from the porphyrin periphery), the only difference being the second aryl group. The electronic nature of the porphyrin ring cannot account for this difference simply because there is hardly any difference between the two system, and even more, in cases where appreciable changes in the electronic nature of the heme periphery have been introduced only the O_2 dissociation rate is affected.[14c] For the same reasons one cannot expect differences at either polarity of the ligand binding site or solvation effects to account for this unexpected kinetic behavior of our new models. Another effect which can influence the kinetic behavior of the hemes is the heme deformation effect which is due to a movement of the iron atom either toward (proximal push) or away from (proximal pull), the incoming ligand.[14b] the proximal push, where the iron atom is "pushed" by the proximal base (imidazole) towards the plane of the porphyrin, thus making it more accessible to the incoming sixth ligand, would be expected

Table 1-1 Kinetic and Equilibrium Constants for CO and O_2 Binding to Unsymmetrically Strapped and Unstrapped Five Coordinate Hemes.[a]

Compound	Solv.	k^{CO} ($M^{-1}S^{-1}$) x10^{5}	k^{-CO} (Sec^{-1}) x10^{-2}	$P_{\frac{1}{2}}^{CO}$ (Torr) x10^{-3}	k^{O_2} ($M^{-1}S^{-1}$) x10^{7}	k^{-O_2} (Sec^{-1})	$P_{\frac{1}{2}}^{O_2}$ (Torr)	M[d]	k^{O_2}/k^{CO}
Mb[b]	H_2O	3-5	2-4	14-25	1-2	10-30	0.5-1	20-40	
Hb, isolated α^{SH}	H_2O	40	1.3	24	5	28	0.3	130	
FeBzIm	PhMe	43 ± 3	31 ± 2	7.0 ± 0.2	20 ± 3	(5.9 ± 0.9) x 10^{4}	30±3	4300	47
$Fe(CH_2)_2Im$	PhMe	40 ± 3	31 ± 2	8.0 ± 0.7	18 ± 2	(9.5 ± 1.4)x 10^{4}	52±3	6500	45
FeSSP-13	PhMe	2.8 ± 0.6	4 ± 1	14 ± 3.5	3.4 ± .5	(4.0 ± 0.6) x 10^{3}	11.7 ± 0.2	860	121
FeSSP-12	PhMe	8.2 ± 1.5	5 ± 1	64 ± 1	4.6 ± .2	(3.0 ± 0.3) x 10^{2}	0.73 ± 0.08	110	56

a. Rates were calculated using the following solubilities: 1 torr of CO or O_2 = 1 x 10^{-5} M (Toluene)

b. Reference 1a.

c. Reference 7a.

d. $M = P_{\frac{1}{2}}^{O_2}/P_{\frac{1}{2}}^{CO}$

Table 1-2. CO and O_2 Binding Constants of Diphenyl Five Coordinate Hemes.[a]

Compound	Solvent	k^{O_2} ($M^{-1}S^{-1}$)	k^{-O_2} (Sec^{-1})	$P_{1/2}{}^{O_2}$ (Torr)	k^{CO} ($M^{-1}S^{-1}$)	k^{-CO} (Sec^{-1})	$P_{1/2}{}^{CO}$ (Torr)	M[b]
Cis	toluene	3×10^7	38,000	126	2.3×10^6	0.12	0.0054	23,000
Trans	toluene	2.6×10^7	4,100	16	1.6×10^6	0.072	0.0045	3,550

a. Reference 12.

b. $M = P_{1/2}{}^{O_2}/P_{1/2}{}^{CO}$

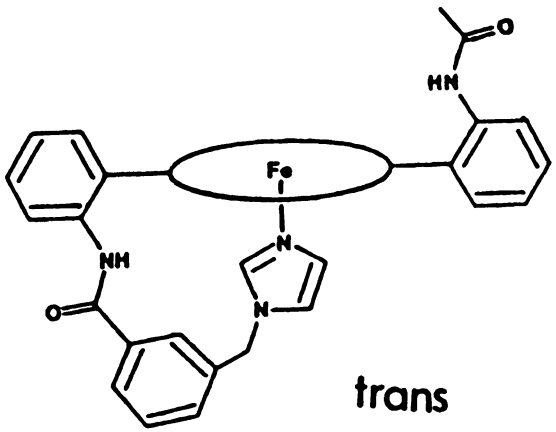

trans

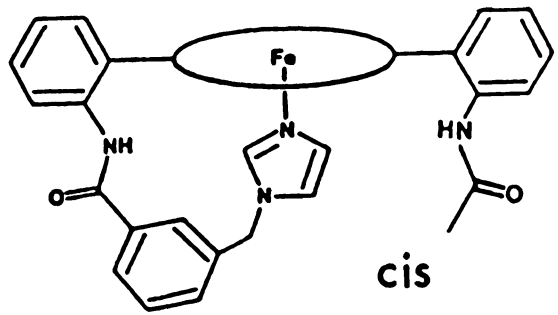

cis

to enhance both CO and O_2 affinities and provide an attractive explanation for the observed rates for FeBzIm. However, this cannot be true. The fact that the two unhindered hemes, FeBzIm and $Fe(CH_2)_2Im$, with the different imidazole tails but very similar kinetic parameters leaves no doubt that the proximal base's position and orientation cannot be responsible for the kinetic behavior of these hemes. So, after all, it seems reasonable to assume that the different kinetic behavior of FeBzIm and $Fe(CH_2)_2Im$ can be attributed to the unsymmetrical substitution of the porphyrin ring which in turn can cause distortion of the porphyrin ring, thus altering its reactivity.[14a] Structural studies have shown that the binding of a ligand to a five-coordinate iron (II) porphyrin is accompanied by movement of the iron into the porphyrin macrocycle. So an "unusual" conformation of the heme ring is reflected in the rate constants. At present there is not sufficient structural data available to unequivocally substantiate this proposal, but it seems the only plausible explanation fitting all the experimental observations.

Comparing now, the unhindered hemes to FeSSP-13, one can clearly see that the CO affinity is decreased while the O_2 affinity increased. And as a result M is reduced from 4300 and 6500 for FeBzIm and $Fe(CH_2)_2Im$ respectively, to 860 for FeSSP-13. This is a significant reduction, but it does not completely reflect the magnitude of the steric effect the strap imposes on the binding site of the heme, as a closer

look at the kinetic parameters reveals. Previous work from our laboratory as well as from others has demonstrated[12,14] that any distal side steric effect will be reflected in the association rates of CO and O_2, leaving the dissociation rates unaffected. In the present case though, even the CO dissociation rate is reduced going from the unprotected systems to the strapped ones. Having in mind that the CO dissociation rate is practically insensitive to any distal steric effect, one has to conclude that the tight strap which is introduced over the porphyrin ring forces it in a different conformation, thus cancelling the effect of its unsymmetrical substitution. So the reduction of the CO dissociation rate can be attributed mainly to a conformational change of the porphyrin ring. If one now considers the change of the O_2 dissociation rate, it is evident that it is reduced too, but reduced 2-3 times more than the CO dissociation rate. There must be a different reason for this greater reduction of the O_2 dissociation rate, in addition to the conformational change of the porphyrin. As it has been shown before[11,12,13] where amide linkages are holding straps or caps over the porphyrin ring, there is a constructive dipolar interaction between the amide dipole and the $Fe-O_2$ dipole which stabilizes the bound O_2 and, of course, reduces its dissociation rate (Fig. 1-4). So it is not surprising that the O_2 dissociation rate is reduced much more than the CO on going from the unhindered heme to the strapped one. So far it has been clear that by

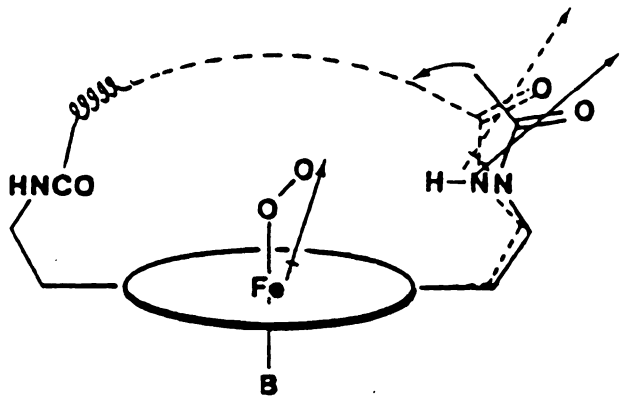

Figure 1-4 The change in dipole orientation upon introduction of a tight strap across the heme face.

comparing only the affinity ratios of different hemes it is impossible to determine the magnitude of the distal steric effect accurately, since many other effects also play important roles in determining M. It would be better to compare the ratio of the association rates of O_2 vs. CO, as Traylor suggested,[14] because it is the association rates that are primarily affected by distal side steric effect. Indeed when the ratios of the association rates for the two models are compared, it is evident that there is a 2-3 fold differentiation against CO (Table 1-1). So for FeSSP-13 there certainly is a small steric differentiation in favor of O_2; and although its magnitude cannot account for the much greater difference in affinity ratios between myoglobins and unhindered heme models it is nevertheless significant. Now if the tighter strapped heme FeSSP-12 which might be expected to show a greater steric hindrance is compared to FeSSP-13, certain important differences can be observed. First of all, M is reduced by almost an order of magnitude to come very close to that of myoglobin. But again a closer look at the individual rate constants reveals that this improvement is not due to an enhanced steric differentiation but rather due to a large stabilization of the bound O_2, which is evident by the more than 10-fold reduction of the O_2 dissociation rate. In fact, although the strap of FeSSP-12 is tighter than FeSSP-13 even the small but significant distal steric effect of FeSSP-13 is completely lost ($k^{O}2/k^{CO}$ for FeSSP-12 is practically the

same with the one of the unprotected hemes). As the study of the CPK models for these two compounds revealed, the reason for this loss of steric effect is that because the tighter strap in FeSSP-12 is forced to assume a conformation with the bulk of it lying away from the center of the heme. The steric interaction between the strap and the incoming gaseous ligands is thus diminished. It is also the fact that the strap of FeSSP-12 consists of an even number of atoms without any carbon at the center of the strap (as opposed to FeSSP-13), combined with the different conformation of the strap, that brings about the complete loss of the distal side steric effect. An alternative explanation for the loss of steric hindrance can be put forward by using Traylor's proposal.[14] This proposal states that the distal side steric effect is not directly related to repulsion in the bound state but is governed by the limited access to the heme face. In other words, the transition state and bound state are equally affected by steric encumbrance, the mechanism comprising a rapid conformational equilibrium among almost equal energy states, some of which deny access to the heme and thus slow down the association rates. In the present case of FeSSP-12 one may argue that the strap is very short for any of its low-energy conformation to reach far enough and protect the heme center. Consequently, no distal steric effect is observed. The validity of this explanation, though, could not be decisively confirmed by this study.

The decrease, now, in the O_2 dissociation rate can be explained in terms of better and stronger dipole-dipole interactions between the bound O_2 and the amide groups of the strap. The shorter strap, on the one hand, changes the orientation of the amide to better align itself with the bound O_2 dipole, and on the other hand, brings the dipoles closer, for a stronger interaction[12] (Fig. 1-4). The result is a greater stabilization of the bound O_2 which is reflected in the reduced O_2 dissociation rate. And it is this reduction of $k^{-O}2$ that overcomes the loss of steric differentiation and which gives rise to a net decrease of the affinity ratio.

Conclusion

At first it is noteworthy that with the exception of the O_2 dissociation rate, FeSSP-13 has CO and O_2 kinetic rate constants very similar to Mb. Secondly, it is also evident from the kinetic parameters of FeSSP-12, that O_2 binding is greatly affected by the constructive, head-to-tail, dipole-dipole, interaction with the polar amide linkages. Hydrogen bonding to the bound oxygen has also been shown to be even more effective in reducing the O_2 dissociation rate.[12] So it is not surprising that FeSSP-13, which does not have the capability to form hydrogen bond(s) to the bound O_2 and in which the dipole-dipole interaction is not very strong, exhibits a much larger $k^{-O}2$ value than does oxomyoglobin, where a hydrogen bond between the bound O_2 and the distal

imidazole NH has been shown to exist.[3a] So from this work, as well as from earlier studies,[12] it is evident that the influence of different factors like the medium, local polarity, hydrogen bonding, porphyrin deformation etc., is greater than the steric effect. So in general our results reaffirm the notion[14] that distal side steric effects cannot account for more than a 3-fold differentiation of CO and O_2 and that the proper differentiation cannot effectively be brought about by distal side steric effect alone.[14] The present study also indicates that it would be a unique synthetic challenge to prepare heme models that match Mb's kinetic behavior. Such a model should possess some distal steric hindrance like the one of FeSSP-13 and at the same time a functional group capable of forming a hydrogen bond (like -OH or $-CONH_2$) with the bound O_2, at the appropriate distance from the center of the heme.

Materials and Methods

The synthesis of the models discussed here is outlined in the synthetic part of this work (Chapter 3). Iron insertions were accomplished by the ferrous bromide method.[15] Toluene was purified by stirring at R.T. with several changes of conc. H_2SO_4 followed by drying over anhydrous sodium carbonate and distillation from lithium aluminum hydride just prior to solution preparation. Sample solutions for kinetics and CO titrations were prepared by dissolving the ferric compounds in approximately 4 mL of

toluene (10^{-5} M) containing 10^{-4} M of benzophenone. The solutions were degassed in a 120 mL tonometer by freeze-pump-thaw cycles at 10^{-5} Torr. The hemin chlorides were reduced by photolysis according to the previously described method.[16] Kinetic rates were measured in toluene at R.T. by flash photolysis[17] according to:

$$\text{B-Fe-CO} \underset{k^{CO}[CO]}{\overset{h\nu}{\rightleftharpoons}} \text{B-Fe} \underset{k^{O}2}{\overset{k^{O}2[O_2]}{\rightleftharpoons}} \text{B-Fe-O}_2$$

Flash photolysis was carried out with either a xenon photographic flash gun (Braun 2000) or a flash lamp pumped dye laser (Phase-RDL2100) with rhodamine 6G dye. Decay constants were calculated from transmittance vs. time measurements at 407 nm (oxyheme appearance). CO association was monitored at 413 nm and the output of the photomultiplier was recorded on a Bascom-Turner recorder through a log amplifier in absorbance units then directly computed as pseudo-first order rate constants. CO and O_2 concentrations ranged from 1 x 10^{-5} M to 2 x 10^{-4} M and 3 x 10^{-5} to 8 x 10^{-4} M, respectively. CO association rates (k^{CO}) were calculated from plots of the observed pseudo-first order rate constants vs. CO concentration which typically had correlation coefficients of 0.996 to 1.000 and varied between experiments by less than 10% O_2 association rates ($k^{O}2$) were calculated from similar plots with

correlation coefficients of not less than 0.92. Oxygen affinities were determined by CO competition measurements and calculated according to the Gibson equation:[1a]

$$1/R = 1/k^{-O}2 + K^{O}2/k^{CO}[CO]$$

where $k^{CO}[CO]$ was the observed pseudo-first order rate constant determined before the introduction of O_2. Oxygen dissociation was calculated from the observed oxygen association rate and equilibrium constant. Carbon monoxide affinities were determined by direct titration of the heme with a gas mixture containing 0.73% CO in argon, at R.T., using a standard spectrophotometric procedure used by Halpern and coworkers[18] (Fig. 1-5). The experimental data for kinetic and thermodynamic constants are tabulated in Table 1-3. CO dissociation rates (k^{-CO}) were calculated from $k^{-CO} = k^{CO}/K^{CO}$. Optical spectra were recorded on a Cary 219 spectrometer.

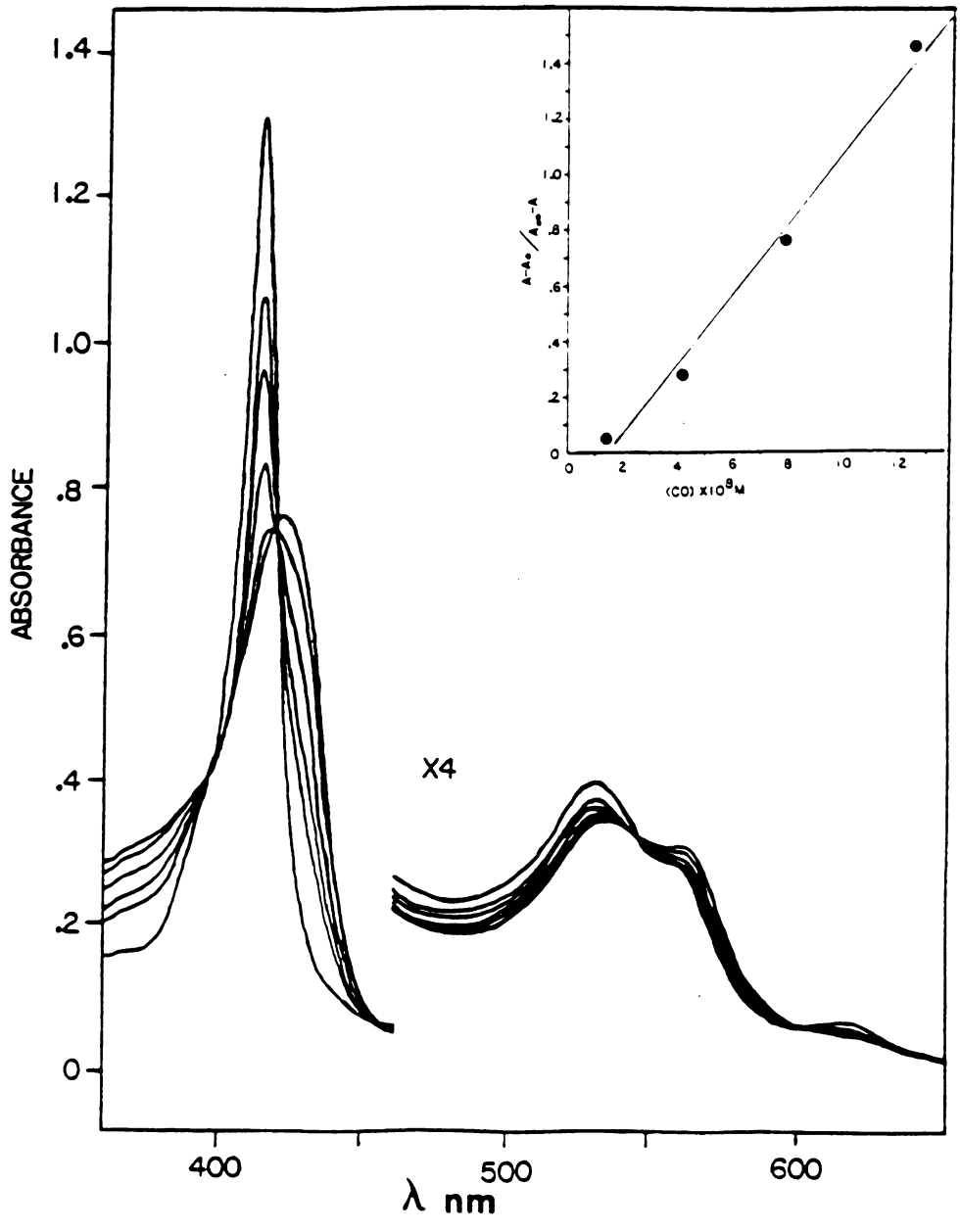

Figure 1-5 Spectrophotometric titration of $Fe(CH_2)_2Im$ in toluene, with CO at R.T.; [CO] x 10^8M = 0.0, 1.40, 4.18, 7.90, 12.54 and 1920 in 1-6 respectively. Inset: plot of $A-A_o/A_\infty-A$ vs. [CO] at 413 nm.

Table 1-3. Experimental Data For Kinetic and Thermodynamic Constants of CO and O_2 Binding to Five-Coordinate Hemes

Compound	$P_{1/2}^{CO}$ Torr	k^{CO} M^{-1} sec^{-1}	$P_{1/2}^{O_2}$ Torr	k^{O_2} M^{-1} sec^{-1}
FeBzIm	0.0069	3.97×10^6	26.0	1.8×10^8
	0.0072	4.23×10^6	33.2	2.2×10^8
		4.63×10^6	30.2	
$Fe(CH_2)_2Im$	0.0074	3.81×10^6	49.6	1.62×10^8
	0.0084	4.19×10^6	54.1	1.97×10^8
FeSSP-13	0.0135	2.56×10^5	11.5	3.73×10^7
	0.0200	2.99×10^5	11.8	3.00×10^7
	0.0094	2.09×10^5		
		3.40×10^5		
FeSSP-12	0.0050	10.30	.787	4.42×10^7
	0.0067	6.36	.677	4.71×10^7
	0.0076	8.02		

CHAPTER 2

INTRAMOLECULAR HYDROGEN BONDING AFFECTING DIOXYGEN BINDING TO COBALT (II) PORPHYRINS

Introduction

The binding of molecular oxygen to cobalt complexes has been the subject of considerable interest in the last 10-15 years.[25,26] During that time the thermodynamic properties of many Co(II) complexes have been investigated. It was well established by the early studies in this field, that the pentacoordinate Co(II) porphyrin complexes (LCoP), where the fifth ligand is an external ligand (pyridine, imidazole, DMF, piperidine, etc.), can reversibly bind O_2 at low temperature in a variety of solvents. Dioxygen has been shown to form a 1:1 adduct with LCoP according to the equation:

$$LCoP + O_2 \xrightarrow{K} LCoP(O_2)$$

The cobalt-oxygen bond was also probed and it was found to be very polar. In fact EPR[25a,d] studies clearly suggest that it is actually more accurately represented by $Co^{III}-O_2^-$, where cobalt is oxydized and O_2 bears a negative charge, than $Co^{II}-O_2$. It is not surprising that the O_2 adduct of $LCo^{II}P$ is stabilized in polar solvents.[27] One also expects to see a much greater effect on the O_2 binding to Co(II) complexes by hydrogen bonding. In addition, the hydrogen

bonding ability of the distal imidazole to CoMb (Myoglobin reconstituted with CoP), may enhance its O_2 binding ability by several orders of magnitude in comparison with CoP.

While direct evidence such as neutron diffraction studies of oxymyoglobin[3a] and oxyhemoglobin[3c] has left no doubt that heme-bound dioxygen has a tendency to form hydrogen-bond with proton donors, quantitative estimation of how much this interaction contributes to the overall stability of the metal-dioxygen complex has been scarce, due to the inavailability of suitable models. Using a cobalt salicylidenimine complex, Drago et al.[33] observed a 400 fold increase in oxygen affinity when trifluoroethanol was added to the CH_2Cl_2 solution, suggesting intermolecular hydrogen-bonding. The abnormally high oxygen affinity observed for Co(II) "picket-fence" porphyrin[26e] was also attributed to a H-bonding effect of the o-anilido groups,[27] although the rather long 4 Å distance separating N-H $\cdots O_2$ seems to render this interpretation less tenable. In an effort to create an ideal environment for such a hydrogen-bond to occur, we have designed porphyrin models in which an intramolecular hydrogen donor is juxtaposed to the terminal oxygen atom of the coordinated dioxygen (Fig 2-1). These models should provide a means of quantitatively determining the influence of H-bond on the formation of dioxygen adducts. Barring electronic effects, the strength of hydrogen-bond is largely dependent on steric constraints. For effective hydrogen-bonding to take place, it is

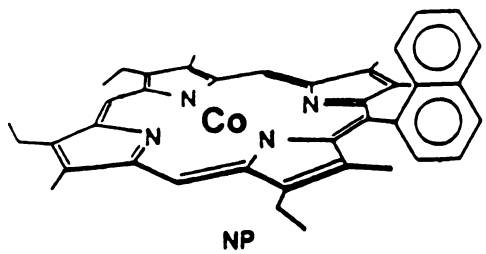

NP

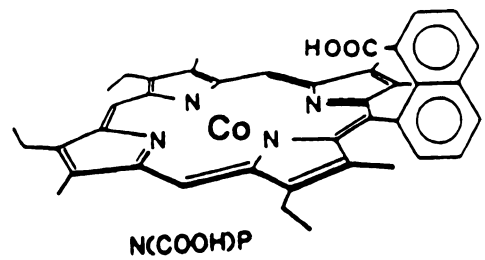

N(COOH)P

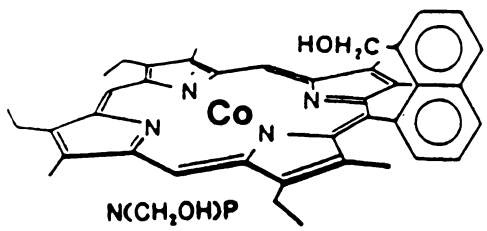

N(CH_2OH)P

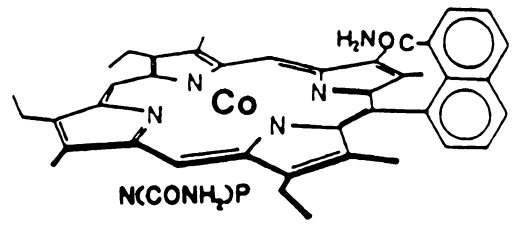

N($CONH_2$)P

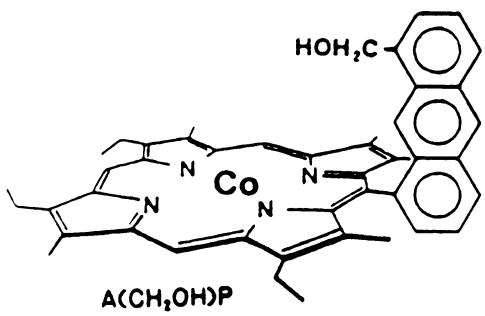

A(CH_2OH)P

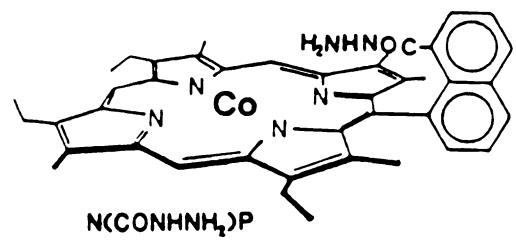

N($CONHNH_2$)P

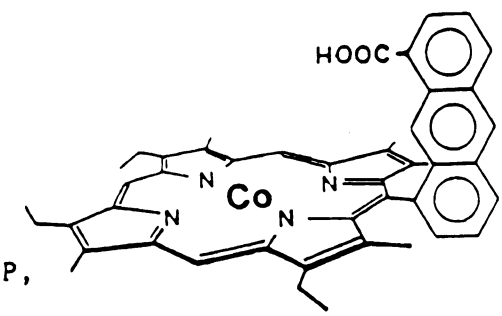

A(COOH)P

Figure 2-1

The structures of NP, N(CO_2H)P, N(CH_2OH)P, N($CONH_2$)P, N($CONHNH_2$)P, and A(CO_2H)P.

essential to minimize the distance and the freedom of motion between the proton source and the acceptor. The realization of this goal was possible with the synthesis and study of intramolecularly hydrogen-bonded cobalt-O_2 complexes.

Results and Discussion

A. Oxygen Binding.

Here is presented the equilibrium constants and thermodynamic parameters of O_2 binding to a series of Co(II) porphyrins with functional groups capable of forming hydrogen-bonds of different strength, at very close proximity to the metal center. For comparison, a similar porphyrin with the same substitution but without any functionality near the metal center was also synthesized and studied. The equilibrium constants were determined at 3 different low temperatures (-42°, -30° and 0°C) in DMF, and in some cases CH_2Cl_2/imidazole. The dioxygen adduct formed in DMF, without extraneous nitrogen base, has a DMF molecule weakly bound trans-axially. In the presence of imidazole base, the O_2 affinity increased significantly as a result of the stronger axial base, but this affinity remained constant throughout the range of base concentration tested (0.1 - 2 mM). The reluctance of Co(II) porphyrins to form a 6-coordinate bis-imidazole complex[25f] thus allows us to relate the O_2 binding of models with that of proteins. The equilibrium constants and thermodynamic parameters of these model compounds were obtained as described in the "Materials

and Methods" section of this chapter. All the equilibrium constants, $P_{1/2}$ and ΔH and ΔS values are tabulated in Table 2-1.

Our results clearly demonstrate that the presence of a protic group near the dioxygen binding site, greatly increases the Co-O_2 formation constant, producing a free energy gain between about 3 kcal/mole for N(CO_2H)P to 1.1 kcal/mol for N(CH_2OH)P, with reference to NP in DMF at -42°C. The enthalpy change (obtained from Van't Hoff plots) for formation of these intramolecular hydrogen-bonded dioxygen complexes also increases significantly. More importantly, both the affinity increase and the enthalpic gain correlate well with the hydrogen-bond strength. Considering the literature thermodynamic parameters of hydrogen-bonding for the following pairs: benzoic-acid and DMSO: ΔH = -8.8 kcal/mole, ΔS = -20.7 eu; benzoic acid and tripropylamine: ΔH = -12.9, ΔS = -26.2; benzyl alcohol and amines: ΔH = -10; the large gain in enthalpy for our model compounds may be entirely attributable to the intramolecular hydrogen bond. The large negative entropy is also consistent with the loss of rotational degree of freedom of the metal-bound O_2.

It is also evident from the results on Table 2-1 that the difference between the naphthalene and anthracene substituted porphyrins is negligible. The anthracene acid and naphthoic acid, as well as the anthracene alcohol and naphthalene alcohol porphyrins have practically indentical

Table 2-1. Thermodynamic Properties for O_2 Binding to Cobalt Porphyrins

Compound	Solvent	T(°C)	K($Torr^{-1}$)	$P_{1/2}$(Torr)	ΔH^a (kcal/mol)	ΔS^a (eu)
CoNP	DMF	-42	$(4.76 \pm .09) \times 10^{-2}$	21 ± 0.4	-11 ± 0.4	-52 ± 2
		-30	$(1.43 \pm .03) \times 10^{-2}$	70 ± 2		
$CoN(CO_2H)P$	DMF	-42	36 ± 6	0.028 ± 0.005	-22 ± 1.3	-88 ± 5
		-30	1.4 ± 0.1	0.73 ± 0.06		
		0	$(2.0 \pm 0.3) \times 10^{-2}$	49 ± 7		
$CoA(CO_2H)P$	DMF	-42	50 + 7	0.020 ± 0.003		
$CoN(CONH_2)P$	DMF	-42	3.3 ± 0.6	0.30 ± 0.06		
		-30	0.25 ± 0.01	4.0 ± 0.2	-16 ± 1.6	-70 ± 7
		0	$(1.1 \pm 0.03) \times 10^{-2}$	91 ± 2.5		
$CoN(CONHNH_2)P$	DMF	-42	13 ± 1	0.080 ± 0.007		
$CoN(CH_2OH)P$	DMF	-42	$(5.1 \pm 0.6) \times 10^{-1}$	1.9 ± 0.2		
		-30	$(2.4 \pm 0.1) \times 10^{-1}$	4.1 ± 0.25	-12 ± 1	-52 ± 4
		0	$(1.1 \pm 0.02) \times 10^{-2}$	91 ± 2		

$CoA(CH_2OH)P$	DMF	-42	$(4.5 \pm 0.5) \times 10^{-1}$	2.2 ± 0.2		
		-30	$(2.0 \pm 0.1) \times 10^{-1}$	4.9 ± 0.1	-12 ± 0.5	-52 ± 2
		0	$(1.1 \pm 0.02) \times 10^{-2}$	91 ± 3		
CoNP	Ph_3CIm/CH_2Cl_2	-42	1.0 ± 0.2	1.0 ± 0.2		
$CoN(CO_2H)P$	Ph_3CIm/CH_2Cl_2	-42	$(76.9 \pm 2.5) \times 10^{-1}$	$(1.3 \pm 0.04) \times 10^{-3}$		
		-30	28 ± 6	0.036 ± 0.008	-23 ± 1	-88 ± 4
		0	$(2.7 \pm 0.1) \times 10^{-1}$	3.7 ± 0.14		
		(15		40)[b]		
CoMb (sperm whale)[c]		25		57	-13.3	-53
CoMb (horse)[c]		25		57	-11.3	-46
$CoHb_{\alpha}^{-SH}$		15		24.3	-13.9	-54.4
$CoHb_{\beta}^{-SH}$		15		24.5	-16.5	-63.8

a. Standard state, 1 torr;

b. Extrapolated from ΔH and ΔS.

c. From reference 36.

d. From reference 37.

binding constants. This fact, first, is surprising because one would expect to see some differentiation due to the longer distance between the metal center and the functional group is located in the anthracene case. Nevertheless, a closer look at the structure of these compounds reveals that the distance difference is not critical and the anthracene substituted porphyrins have the same capability to form hydrogen-bond with the bound oxygen as their naphthalene counterparts (Fig. 2-2).

The O_2 binding affinity of $N(CO_2H)P$ and NP was also studied in CH_2Cl_2 using a substituted imidazole as the fifth ligand for the Co complex. This system resembles the proteins because an imidazole is the proximal base in the protein case, too. The difference between the O_2 binding affinity at the two solvent systems, is about an order of magnitude and it is attributed to the fact that imidazole is a much stronger ligand than DMF. So the strong hydrogen-bonding ability of **23** provided the necessary stabilization for the bound O_2 and for the first time the equilibrium constant of CoMb can be reproduced by a simple model. Nevertheless, an important difference between the model and protein cannot escape attention. While the high O_2 affinity exhibited by CoMb and CoHb using a single hydrogen-bond in model porphyrins has been duplicated, the thermodynamic data suggest that the enhanced O_2 affinity of the protein has more subtle cause than the mere formation of a hydrogen-bond with the distal histidine. It has been pointed out[36] that

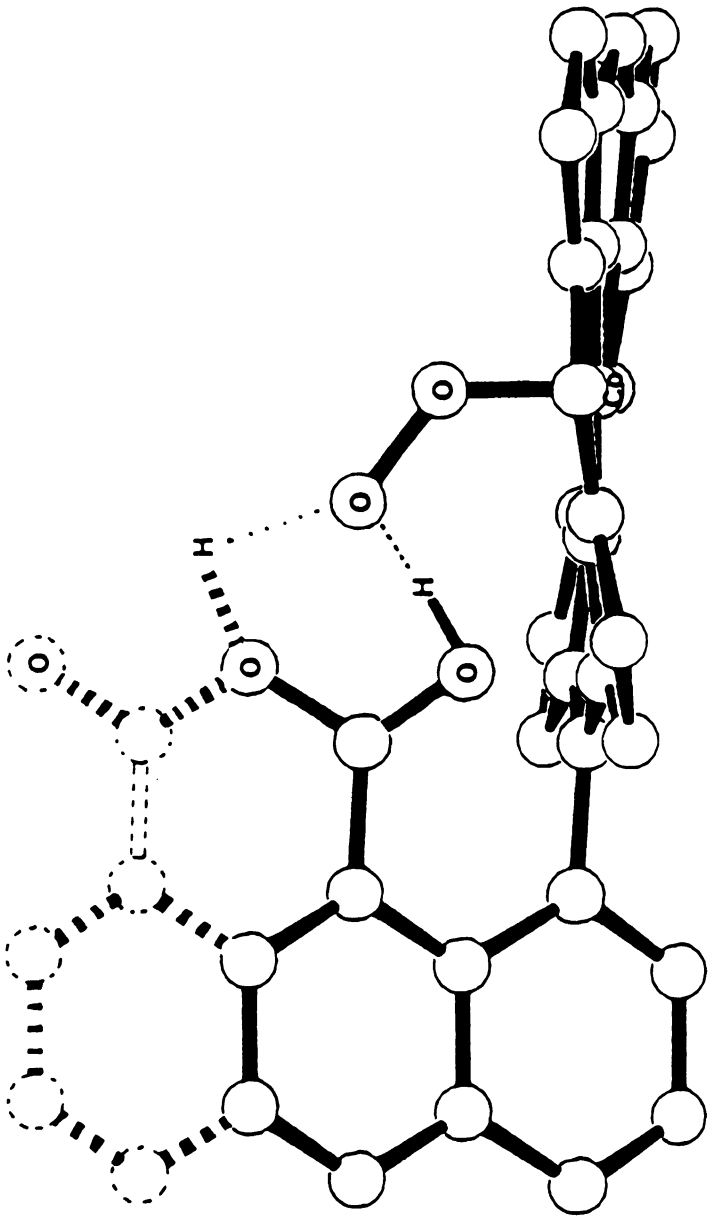

Figure 2-2 Graphic representation of the proximity of the acidic proton to the bound O_2 in $N(CO_2H)P$ and $A(CO_2H)P$.

the enhancement of O_2 affinity caused by the apoprotein can be the result of a delicate balance between enthalpic and entropic components which differ from protein to protein. This study makes it very clear that a moderate hydrogen-bond involving the histidine N-H can easily supply the 3 kcal/mole ΔH(negative) needed for stabilizing the O_2 adduct. However, the accompanying loss in ΔS observed in models is not present in the protein, possibly because of other compensatory factors. Some of the positive entropy may come from conformational changes distributed throughout the protein. Also unlike models, a pre-formed protein pocket has the advantage of not showing the solvent reorganization entropic loss upon oxygenation. Indeed, these seemingly small contributions are often the major obstacles, as well as challenges, in our quest for mimicking enzymes with synthetic models.

B. Decomposition of the Co(II) Naphthoic Acid Porphyrin.

From the numerous studies of O_2 binding to Co(II) porphyrin complexes it is well established that for a Co(II) porphyrin to bind oxygen it must be 5-coordinate and even then low temperatures are needed to achieve appreciable binding. The tetracoordinate Co(II) - porphyrins are very stable at ambient temperatures when dissolved in non-coordinating solvents such as methylene chloride.[26,27] It is, thus, a unique property of the Co(II) naphthoic acid porphyrin ($N(CO_2H)P$) not only to become oxydized in CH_2Cl_2

at R.T., but to decompose as well. The activation of dioxygen by a Co(II) porphyrin under such mild conditions and the complete destruction of the porphyrin ring, are completely unprecedented. This intriguing phenomenon was studied and efforts to elucidate its mechanism were made.

In this effort to understand the mechanism, the necessity of the dioxygen had to be established. And indeed, when the Co(II) complex of $N(CO_2H)P$ was kept dissolved in CH_2Cl_2 under argon, no decomposition took place, even after prolonged periods of time. As soon as this solution was exposed to air, the decomposition (evident from the color change) would start immediately. So it is beyond any doubt that oxygen is needed for the decomposition. The second piece of experimental evidence that indicates that the carboxylic acid group is essential is that if ammonia is passed through the methylene chloride solution before it is exposed to air, $N(CO_2H)P$ is perfectly stable. That means that the acidic proton of the porphyrin sitting close to the metal is necessary. That should not be surprising though, since the difference between this unstable Co(II) porphyrin and all the other ones is exactly this carboxylic group, so that is only natural that it does participate in the reaction. The solvent is also important for the decomposition. If DMF is used instead of methylene chloride, then, the porphyrin ligand does not decompose although the cobaltous ion oxidized to Co^{III} immediately. This solvent effect can be attributed to the mild basicity

of DMF and its polarity which effectively "diffuse" the strength of the acidic proton rendering it unable to promote the decomposition.

The effect of external acid on the system is also very profound. The decomposition takes place significantly faster when a strong acid is present. In the presence of HCl gas in CH_2Cl_2, the decomposition takes place with a $t_{1/2}$ of about 1 min. while in the case of the untreated solution $t_{1/2}$ is about 10 min.

Another important finding is that radical traps, such as duroquinone and galvinoxyl, do not inhibit the reaction, so that any radical chain mechanism can be ruled out.

The most important result, though, is the isolation and characterization of one of the major products of this decomposition, namely the Etiobiliverdin IV (EBV IV, Fig. 2-3) which suggests that one of the major pathways of the reaction involves an attack of the meso position of the porphyrin where the napthyl group is attached by the activated O_2. This is contradictory to the previous examples of metallo-porphyrins' decomposition by H_2O_2 where the phenyl-substituted meso positions are the most stable towards oxygen attack (because of steric reasons).[38] In a separate experiment, when the Co(II) complex of meso-monophenyl porphyrin was decomposed in methylene chloride with H_2O_2 and the H^1 NMR of the mixture of the colored products was taken, the phenyl group could be seen attached to the tetrapyrroles. That means that O_2 attacks preferably

at the unsubstituted meso positions as opposed to the $N(CO_2H)P$ case, where no napthyl protons were detected. The importance of the position of the carboxyl group is also demonstrated by the inability of $A(CO_2H)P$ to initiate the same sequence of reactions, although it, too, binds to dioxygen with the same affinity as $N(CO_2H)P$ (Table 2-1). This observation clearly shows that the carboxyl group being so close to the ring cleavage position is not coincidental but that it should play a dominant role in the sequence of reactions. A plausible mechanism for the decomposition of $N(CO_2H)P$ consistent with the experimental facts is thus proposed, and is outlined in Fig. 2-3. The first step is the O_2 binding to the Co center and the intramolecularly protonation of the bound oxygen by the carboxylic proton. We suggest that in the presence of an acid catalyst, the carboxylic group would react with the metal-bound $\cdot O_2H$ species much the same way as it would reaction with hydrogen peroxide to yield a peracid.

The peracid, being closer to the substituted meso position of the porphyrin will, of course, preferentially hydroxylate this methine position rather than any of the other three, to cause the collapse of the porphyrin ring. The actual mechanism of the ring cleavage cannot be determined at this time but may involve a reaction sequence very similar to the biodegradation of heme molecules that lead to the formation of bile pigments.[39]

In conclusion, it is evident that the strength of a

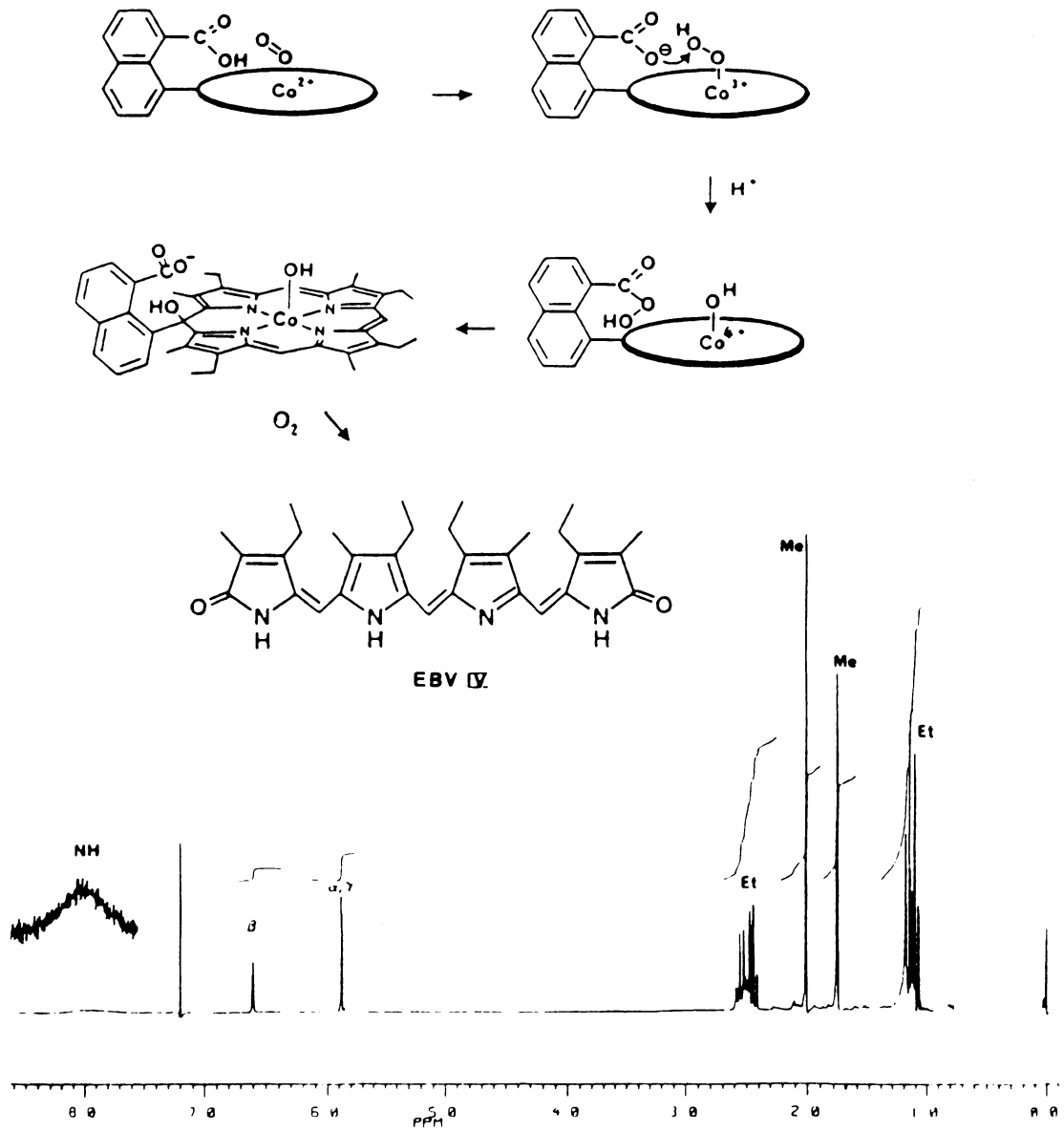

Figure 2-3 Decomposition of $N(CO_2H)P$.

hydrogen donor, as well as its position relative to the binding site of O_2, have a very large effect on the stability of the O_2 adduct and the activation of dioxygen.

Experimental

A. Dioxygen Binding to Co(II) Porphyrins.

The synthesis of the porphyrin-nathoic acid (N(COOH)P) and its derivatives is outlined in the synthetic part of this work (Chapter 3). The synthesis of the porphyrin anthracene acid and its derivatives as well as the naphthalene porphyrin is described elsewhere.[23] Cobalt ion was incorporated into the prophyrins as follows: 5 mg of porphyrin free base were dissolved in CH_2Cl_2 (10 mL) and the solution was degassed by passing argon through it for 5 min. Then a solution of excess $CoCl_2$ and anhydrous sodium acetate in CH_3OH (5 mL) was added. The mixture was heated on a steam bath under argon, until all the solvent was evaporated. CH_2Cl_2 was added ($\sim$5 mL) and the CoP was transferred to a syringe containing a degassed solution of sodium dithionite in H_2O. The reduced Co(II) porphyrins were then dissolved anaerobically in freshly distilled DMF (approximately 4 mL, 1 x 10^{-5} M). The solutions were degassed in a 60 mL tonometer by freeze-pump-thaw cycles at 10^{-5} Torr. Oxygenation was monitored spectrophotometrically at several temperatures. Binding constants in 1 mM solution of 1-tritylimidazole in CH_2Cl_2 were similarly determined. (CH_2Cl_2 was distilled over LAH just prior to use.) The low

temperatures were achieved by immersing the tonometer in a dewar filled with liquid propane (b.p.: -42°C) liquid freon-12 (b.p.: -30°C) or water/crushed ice (0°C). The dioxygen adducts were very stable at -42°C but underwent autoxidation rapidly at room temperature (half lifes at 0°C in most cases were about 4 min.). The O_2 affinities were determined by direct titration of CoP with either pure O_2 or air, using a standard spectrophotometric procedure used by Halpern and coworkers[18] (Fig. 2-4). The O_2 binding constant of NP at 0°C was impossible to determine because even at higher than atmospheric O_2 pressures the complex is not fully oxygenated. This observation, though, is in agreement with previous studies of simple Co(II) porphyrins.[25,26] The solubility of O_2 in DMF at low temperatures is not known and all the equilibrium constants are calculated at the standard state of 1 Torr. The titration curves typically had correlation coefficients of .990 to .999 and varied between experiments by less than 18% (given the instability of the cobalt dioxygen adducts at 0°C the error margin is somewhat larger than usual). The equilibrium constants given on Table 2-1 are the average value of 2-4 runs(Table 2-2). Since the UV-vis spectrum of the oxygenated complexes is very similar with the one of the oxydized Co(III) complex, in order to prove that no oxidation had taken place it was necessary to pump the solution again after the titration to see the spectrum returning to its original form.

The values of the thermodynamic parameters (ΔH, ΔS) were

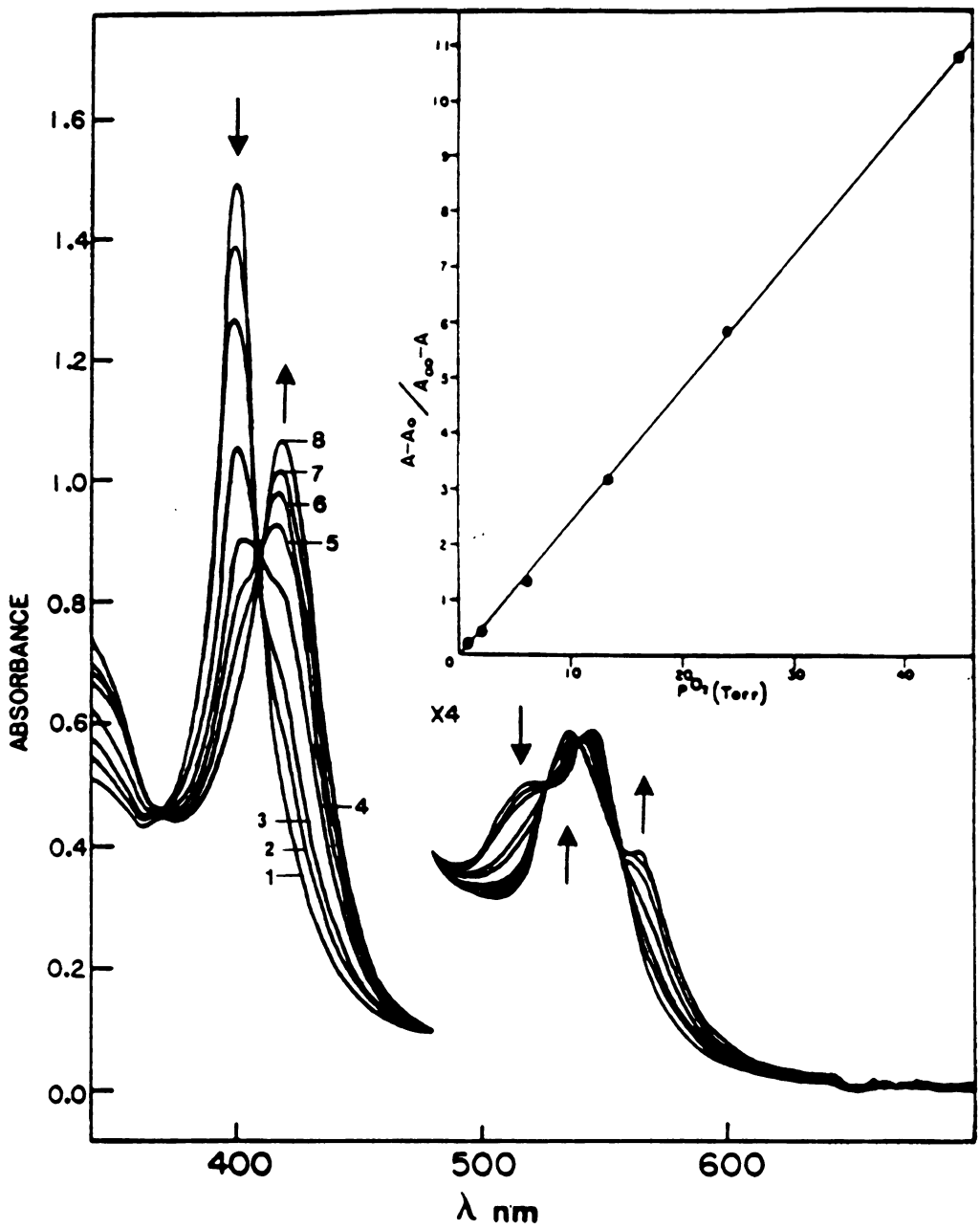

Figure 2-4 Spectrophotometric titration of $A(CH_2OH)P$ in DMF with O_2 at -30°C; P^O2 (Torr) = 0.0, 0.79, 2.09, 6.28, 13.61, 24.1, 45.0, and >760 in 1-8 respectively. Inset: plot of $A-A_o/A_\infty-A$ Vs. P^O2 at 419 nm.

obtained by the Van't Hoff plots of 1/T vs ln k (Fig 2-5). In the case of NP, although the Van't Hoff plot consists of only two points, the ΔH and ΔS values agree very nicely with those of previously studied simple Co(II) porphyrins.[25,26]

Optical spectra were recorded on a Cary 219 spectrometer.

B. Decomposition of the Co(II) Naphthoic Acid Porphyrin [$N(CO_2H)P$].

$CoN(CO_2H)P$ (10 mg., 0.015 mmol) was dissolved in methylene chloride (5mL) under Ar, and this solution was then added to CH_2Cl_2 (5 mL) containing one drop of benzoyl chloride. The mixture was left for 30 min., open to air, during which time a very characteristic color change from pinkish-red to dark green, took place. The green solution was washed with 25% NaOH (3 x 10 mL), conc. HCl (2 x 10 mL) and saturated aq. $NaHCO_3$. The organic layer was then separated, dried over anhydrous Na_2CO_3 and evaporated to dryness under reduced pressure. TLC revealed many colored bands; the major band was separated on a preparative silica gel plate and proved to be Etiobiliverdin IV by means of NMR, MS, and UV-vis spectroscopies (15%). The isolated product was identical in all respects to an authentic sample; MS m/e 498 (13, M^+); NMR δppm 1.17 (6H, t, Et), 1.22 (6H, t, Et), 1.83 (6H, S, Me), 2.08 (6H, S, Me), 2.53 (4H, q, Et), 2.60 (4H, q, Et), 5.94 (2H, S, meso), 6.66 (2H, S, meso), 8.3 (br, NH).

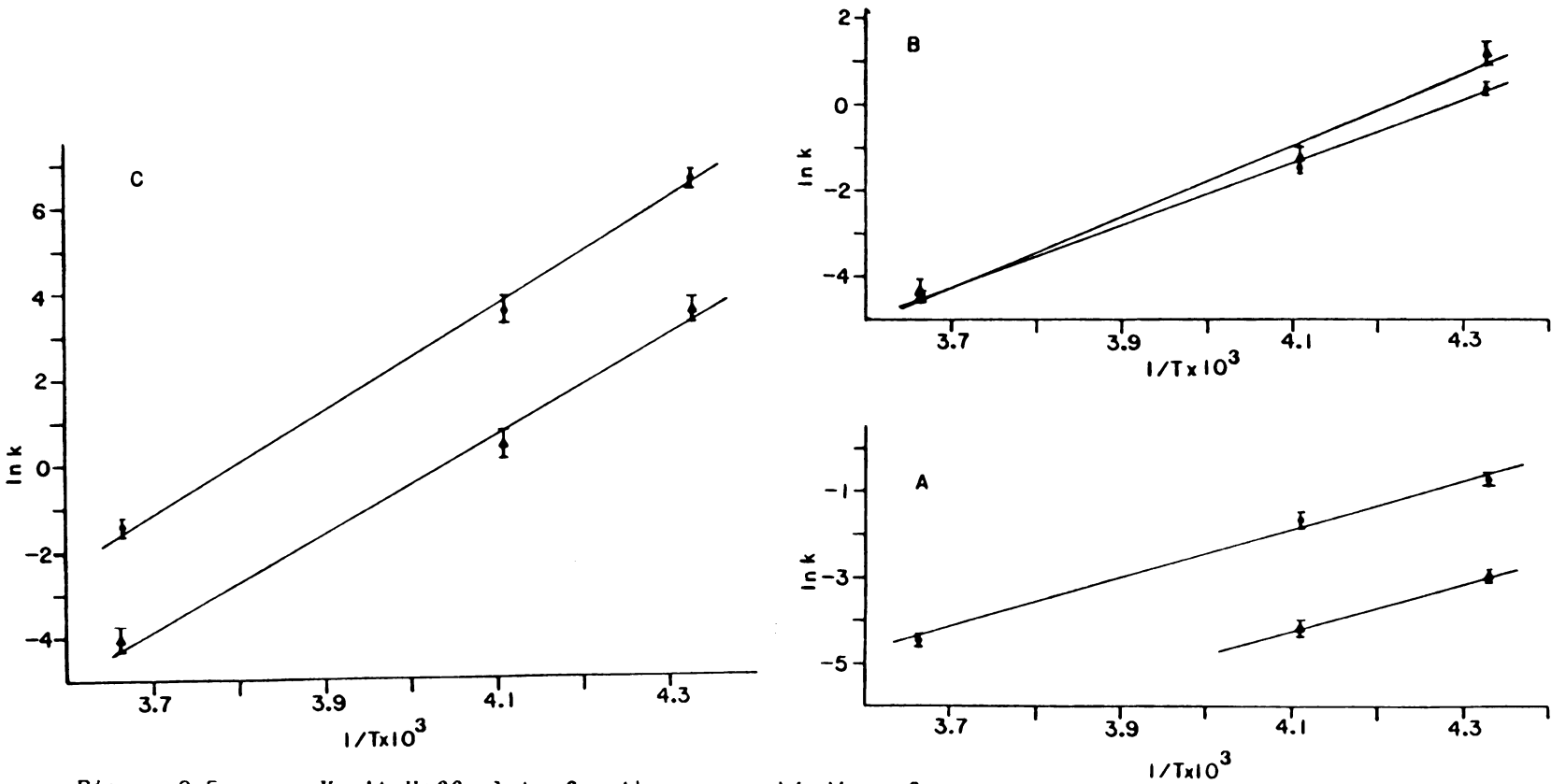

Figure 2-5 Van't Hoff plots for the oxygen binding of cobalt porphyrins:

A. ●: NP in DMF; ▲: $A(CH_2OH)P$ in DMF.

B. ●: $N(CONH_2)P$ in DMF; ▲ : $N(CH_2OH)P$ in DMF

C. ●: $N(CO_2H)P$ in DMF; ▲ : $N(CO_2H)P$ in Ph_3CIm/CH_2Cl_2

Table 2-2. Experimental Data For the Thermodynamic Properties For O_2 Binding to Cobalt Porphyrins

Compound	Solvent	T(°C)	$P_{1/2}$(Torr)
CoNP	DMF	-42	21.5 20.9
		-30	68.7 71.1
$CoN(CO_2H)$	DMF	-42	0.0280 0.0349 0.0225 0.0271
		-30	0.770 0.691
		0	43.0 47.0 57.3
$CoA(CO_2H)P$	DMF	-42	0.0179 0.0229
$CoN(CONH_2)P$	DMF	-42	0.26 0.34
		-30	3.90 4.13
		0	92.8 89.3
$CoN(CONHNH_2)P$	DMF	-42	0.0758 0.0851
$CoN(CH_2OH)P$	DMF	-42	1.75 2.07
		-30	3.93 4.28
		0	89.7 91.9

$CoA(CH_2OH)P$	DMF	-42	2.08 2.30
		-30	4.83 5.00
		0	89.3 92.8
CoNP	Ph_3Im/CH_2Cl_2	-42	0.893 1.141
$CoN(CO_2H)P$	Ph_3Im/CH_2Cl_2	-42	0.00128 0.00134
		-30	0.030 0.042
		0	3.61 3.81

C. Fe Insertion To Naphthoic Acid Prophyrin.

Porphyrin (20 mg) was dissolved in 1:1 THF/benzene (20 mL), containing collidine (2 drops) and $FeBr_2$ (40 mg). The solution was heated under argon for ca. 30 min. and the solvent was removed in vacuo. The residue was redissolved in CH_2Cl_2, extracted twice with 10% HCl washed with H_2O and eluted on silica gel column. To obtain the ferric chloride form, the solution was washed with saturated NaCl in 0.1 N HCl. UV-vis λmax 645, 541, 505, 388.

CHAPTER 3

SYNTHESIS OF NOVEL PORPHYRINS

A. SYNTHETIC MODELS OF MYOGLOBIN

Introduction

The construction of synthetic metalloporphyrin complexes which mimic heme containing proteins has been one of the most powerful methods in studying reaction mechanisms and structure-function relationships, of hemoproteins and especially myoglobin. Most model systems trying to mimic the distal steric hindrance that myoglobin exhibits are based on two families of porphyrins; the β-substituted porphyrins (e.g. protoporphyrin) and the meso-substituted tetraphenyl (TPP) and diphenyl (DPE) derivatives. These two types of porphyrins have been manipulated extensively and in the last 10-15 years a large number of interesting model systems with colorful names, have been created.[12,19] The β-substituted compounds resemble more closely the naturally occurring hemes. However, the excessive floppiness of the side chains used in functionalization is often undesirable. The tetraphenyl systems, particularly those functionalized with o-anilido groups (e.g. "picket fence" heme) are structurally more rigid. Nevertheless, they suffer from the fact that synthetically it is very difficult to derivatize one particular phenyl group (out of four in TPP) on the porphyrin ring in order to attach special appendaces. The

diphenyl systems, although a little easier to derivatize, offer little control over systematic change of the steric hindrance at the distal side of the porphyrin. For that reason, meso-monophenyl and at the same time β-substituted systems were designed and synthesized in an attempt to prepare better models, which on one hand would be easier to selectively derivatize at the proper position and on the other hand would give us a greater flexibility in the design of the kind and magnitude of the steric hindrance.

The strapped porphyrins **2**, **3** and **4** (Scheme I) were at first synthesized from the easily obtained β-substituted porphyrin (1),[20] but proved to be unsuitable for kinetic and equilibria studies of CO and O_2 binding, since even the bulky external bases used to form the penta-coordinate heme necessary for these studies formed hexa-coordinate complexes instead. So the more lengthy synthesis of the elaborate porphyrins **5** and **6** (Scheme III) was undertaken. The new system should have a rather rigid imidazole linkage from the opposite side of the strap in order to form a stable five-coordinate heme and to thus allow a detailed study of O_2 and CO kinetic and equilibria parameters. At the same time two more unprotected porphyrins with no strap were prepared for reason of comparison to the stericly hindered ones (Scheme II). These synthetic hemes were indeed applied in modeling studies of myoglobin and the results are discussed elsewhere in this work.

Synthesis

The parent compound **1** for the simple strapped porphyrins was synthesized according to the literature.[20] The porphyrin was converted to its diacid-chloride and then, without isolation, coupled with equivalent amount of the proper diamine (Scheme I). The two reactants were dissolved separately in CH_2Cl_2 and mixed slowly under high-dilution conditions in order to reduce di- and oligomerization. The purification of the final product was carried out on silica gel plates.

For the synthesis of the meso-(o-aminophenyl) porphyrin **9** the 5,5'-unsubstituted dipyrromethane **7** had to be prepared first (Scheme II). This was accomplished by the acid catalysed reaction of α-free pyrrole **5** with o-acetamido-benzaldehyde. The 5,5'-unsubstituted dipyrromethane was obtained from an one pot hydrolysis and decarboxylation of **7**. So by condensing **7** and 5,5'-diformyldipyrromethane **15** in CH_2Cl_2 with a catalytic amount of p-toluenesulfonic acid in the presence of zinc acetate, Zn-porphyrin (**9**) was produced which was demetalated after purification (it is easier to purify the Zn-porphyrin as it travels on silica gel faster than its free base). The two different imidazole tails were finally attached to the porphyrin according to a high yield literature procedure.[15]

A different dipyrromethane had to be designed for the synthesis of porphyrins with imidazole tail, as well as, strap. Pyrrole **12** equipped with an ethyl propionate group

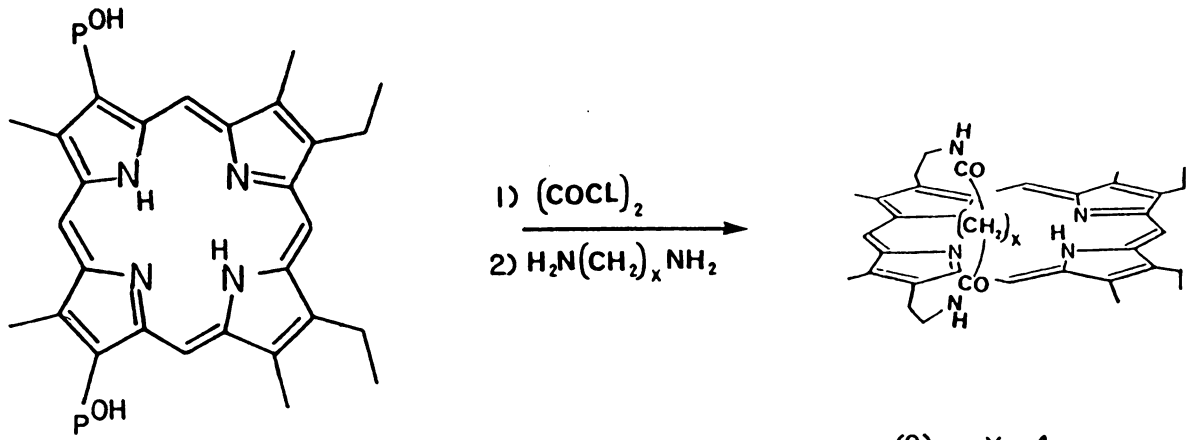

(2) X = 4

(3) X = 5

(4) X = 6

SCHEME I

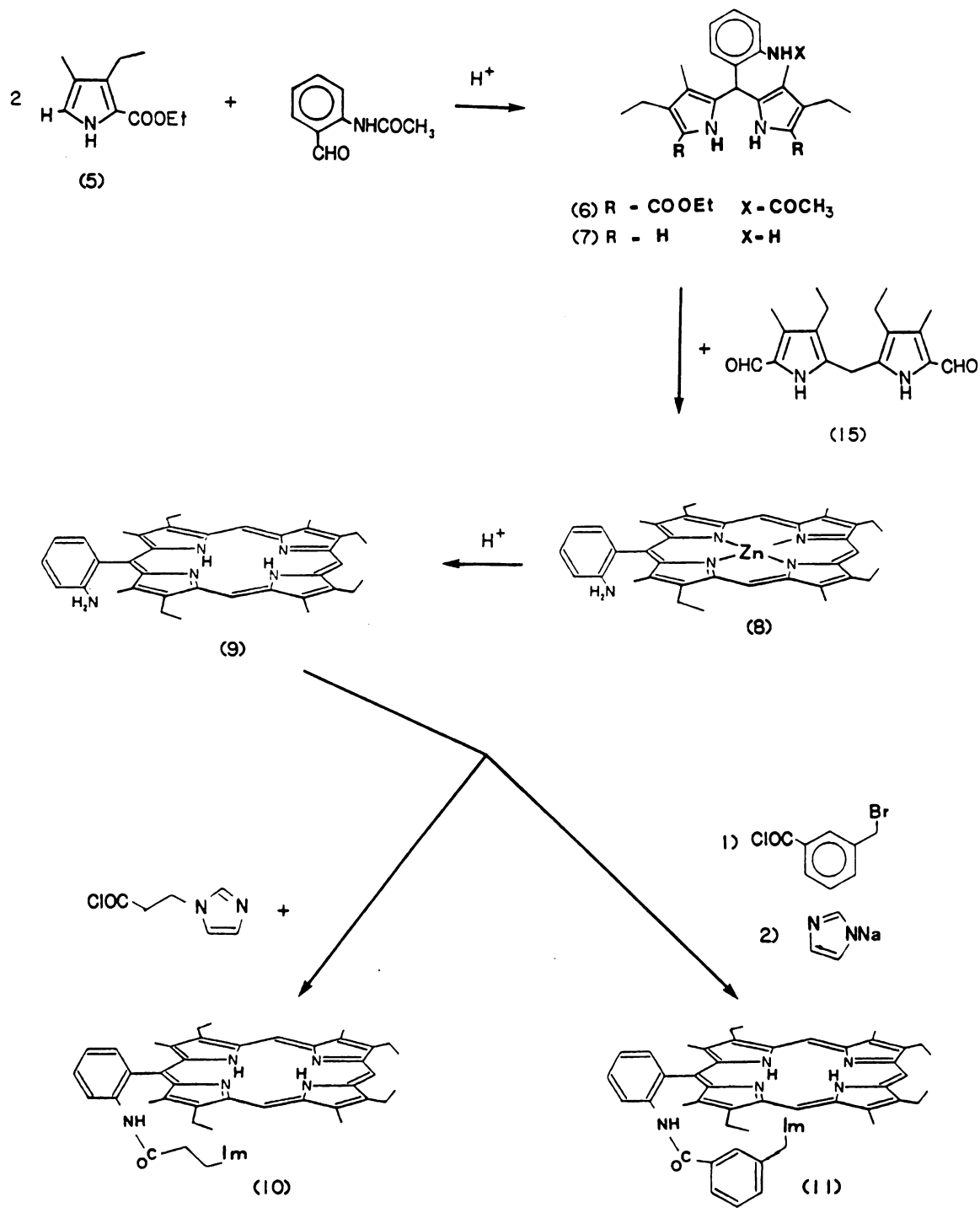
2
COOEt
NHCOCH3
CHO
H+
(5)
NHX
R
H
(6) R - COOEt X - COCH3
(7) R - H X - H
OHC
CHO
(15)
Zn
H2N
(8)
(9)
ClOC
Br
1) ClOC
2)
NNa
NH
Im
(10)
(11)

SCHEME 2

served this purpose. It was condensed with o-acemido benzaldehyde in a similar fashion with the previous case (Scheme III). The hydrolysis and decarboxylation of the diester dipyrromethane **13** was once again done in one step. The condensation of the two dipyrromethanes was in this case done in methanol because **14** was insoluble in CH_2Cl_2. To the mono-anilido porphyrin **16**, the tail was attached first so that its bulkyness would force the strap to "close" from the opposite face of the porphyrin. Finally the ester groups were acid hydrolyzed (the amide bond was unaffected), the so produced di-acid porphyrin was converted to the di-acid chloride in situ, and subsequently coupled to the diamine, followed by the attachment of imidazole without isolation of the intermediate.

Experimental

'H NMR spectra were recorded on a Bruker WM-250 MHz instrument in $CDCl_3$. Absorption spectra were measured in CH_2Cl_2 using a Cary 219 spectrometer. Mass spectra were measured with a Finnigan 4021 GC-MS (direct insertion probe, 70 eV, 200-300°C), or a Varian MAT CH5 equipped with ionteck FAB gun, operated at 8 KV. Methylene chloride was distilled from CaH_2 and THF from $LiAlH_4$ before use.

(3,7-Diethyl-2,8,13,17-tetramethylporphyrin-12,18)-butane-1,4-[4(1-aza-2-oxo),4(1-aza-2-oxo)-Cyclophane] (2).

Diacid-porphyrin **1**[20] (190 mg, 0.34 mmol) was suspended

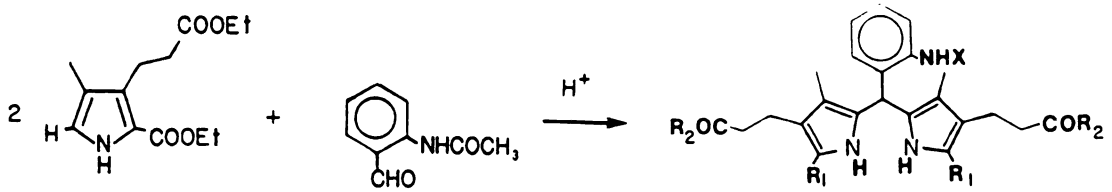

(12)

(13) R_1 - COOEt R_2 - OEt X - $COCH_3$
(14) R_1 - H R_2 - OH X - H

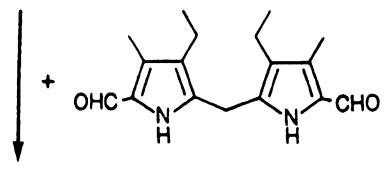

(15)

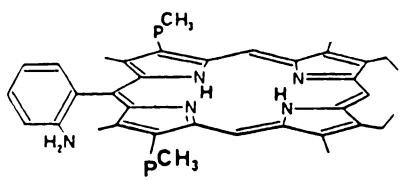

(16)

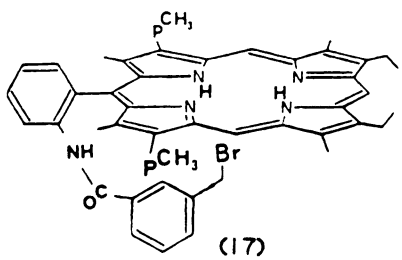

(17)

1) HCOOH/HCL
2) $(COCL)_2$
3) $H_2N(CH_2)_xNH_2$
4) Na Im

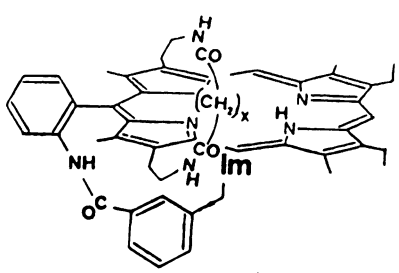

(18) X = 4
(19) X = 5

SCHEME 3

in 30 mL dry methylene chloride, excess oxalyl chloride (1 mL) was added and the mixture was refluxed gently on an oil bath for 2 h. protected from the moisture. The homogenized solution was then evaporated to dryness under vacuum, and the diacyl-chloride porphyrin was redissolved in dry methylene chloride (50 mL) and used without isolation for the coupling reaction. This solution was placed under argon in one syringe of a two-syringe drive. In the other one was placed under argon a solution of 1,4-diamino-butane (35.5 mg, 0.40 mmol) and 0.5 mL of triethylamine, in methelene chloride (50 mL). These two solutions were injected at a rate of 1 mL/min per syringe at R. T. into 400 mL of dry methylene chloride with magnetic stirring. The stirring continued overnight in the dark and then the solvent was evaporated under reduced pressure. The residue was taken in CH_2Cl_2 (100 mL) washed with 10% HCl (2 x 50 mL), H_2O (50 mL) and saturated $NaHCO_3$ (2 x 50 mL). Finally the organic layer was chromatographed on silica gel plate (3% CH_3OH-CH_2Cl_2). The crude product was recrystallized from CH_3OH/CH_2CL_2; (40 mgr, 19.3%); MS, m/e 618 (10, M^+); NMR δppm - 3.51 (2H, S, pyr. NH), -1.0, -0.7 (each 2H, br, -NHCH$_2$**CH$_2$**-), 1.6 (2H, br, NH**CH$_2$**-), 1.88 (6H, t, Et), 2.3 (2H, m, -CH_2CO-), 2.42 (2H, br, -CONH-), 2.6 (2H, br,-NH**CH$_2$**-), 2.9 (2H, d,-CH_2**CH$_2$**CO-), 3.57 (6H, S, Me), 3.62 (6H, S, Me), 4.10 (4H, q, Et), 4.11 (4H, q, Et), 4.3 (2H, m, -**CH$_2$**CH_2CO-), 4.6 (2H, d, -**CH$_2$**CH_2CO-), 9.93 (2H, S, meso), 10.02 (1H, S, meso), 10.09 (1H, S, meso); UV-vis λmax (ε_M) 620 nm (5600), 565 (7200), 533

(11100), 497 (13200), 399 (165400).

(3,7-Diethyl-2,8,13,17-tetramethylporphyrin)-pentane-1.5-[5(1-aza-2-oxo), 5(1-aza-2-oxo)-cyclophane]. (**3**)

This strapped porphyrin was prepared in a manner analogous to **2** using 1,5-diamino-pentane; (yield 18.9%), MS m/e 632(10,M^+); NMR δppm - 3.7 (2H, br, pyr NH), -2.8, -1.6 (each: 2H, br, $-NHCH_2\mathbf{CH_2}-$), -1.1, -0.6 (each: 1H, br, $-NHCH_2CH_2\mathbf{CH_2}-$), 1.2 (2H, br, $-NH\mathbf{CH_2}-$), 1.90 (6H, t, Et), 2.5 (2H, br, $-NH\mathbf{CH_2}-$), 3.1 (4H, m,$-CH_2CO-$), 3.5 (2H, br, -CONH-), 3.61 (6H, S, Me), 3.65 (6H, S, Me), 4.10 (4H, q, Et), 4.4 (2H, m,$-CH_2CH_2CO-$), 4.6 (2H, m, $-\mathbf{CH_2}CH_2CO-$), 10.01 (2H, S, meso), 10.06 (1H, S, meso), 10.12 (1H, S, meso); UV-vis λmax (ε_M) 620 nm (6700), 563 (8600), 531 (12800), 496 (15900), 398 (152600).

(3,7-Diethyl-2,8,13,17-tetramethylporphyrin)-hexane-1,6-[6(1-aza-2-oxo), 6(1-aza-2-oxo)-cyclophane] (**4**)

This strapped porphyrin was prepared in a manner analogous to **2** using 1,6-diamino-hexane; (yield 16%); MS m/e 646 (16, M^+); NMR δppm -3.7 (2H, br, pyr NH), -0.9 (2H, br, $-NHCH_2CH_2\mathbf{CH_2}-$), -0.6 (4H, br $-NHCH_2\mathbf{CH_2}CH_2-$), 0.2 (2H, br, $-NHCH_2\mathbf{CH_2}-$), 1.8 (2H, br,$-NH\mathbf{CH_2}-$), 1.89 (6H, t, Et), 3.0-3.3 (6H, m, $-\mathbf{CH_2}CONH\mathbf{CH_2}$), 3.57 (6H, S, Me), 3.64 (6H, S, Me), 3.8 (2H, br, -CONH-), 4.12 (2H, q, Et), 4.13 (2H, q, Et), 4.4 (2H, m, $-\mathbf{CH_2}CH_2CO-$), 4.6 (2H, d, $-CH_2CH_2CO-$), 10.02 (3H, S, meso), 10.12 (1H, S, meso); UV-vis λmax (ε_M) 620 nm

(5900), 565 (7600), 530 (11300), 496 (14400), 398 (157100).

Zinc 5-[6-amino-1-phenyl)-3,7,12,18-tetramethyl-2,8,13,17-tetraethylporphyrin (**8**).

Ethyl 3-ethyl-4-methyl-2-pyrrolecarboxylate[21] (5.0 g, 27.6 mmol) and o-acetamido benzaldehyde (2.25 g, 13.8 mmol) were dissolved in ethanol (100%, 100 mL); catalytic amount of concentrated H_2SO_4 was added and the solution was refluxed for 5 h. on a steam bath. The pressumably formed dipyrromethane diethyl ester **6** was hydrolyzed and decarboxylated in the same pot, as follows: To the above reaction mixture a 30% aq. KOH solution was added (100 mL) and refluxing continued for 3 h. on an electric heating mantle. The condenser was then removed and the volume of the solution was reduced to 1/2 by evaporation. Vigorous refluxing continued overnight during which a dark brown viscous oil separated from the solution. The oil solidified upon cooling to R. T. The bulk of the solution was dicanted carefully and what remained in the flask was partioned between saturated NaCl and CH_2Cl_2. The organic layer was evaporated to dryness and the crude product was used in the next reaction without purification.

Diformyl-dipyrromethane **15**[22] (180 mg, 0.63 mmol) and the above crude 5,5'-unsubstituted dipyrromethane **7** (230 mg) were dissolved in CH_2Cl_2 (100 mL) and a solution of p-toluolo-sulfonic acid (0.5 g) in CH_3OH (5 mL) was added. After stirring for 6 h. in the dark at R. T., 5 mL of

saturated methanolic zinc acetate was added to the reaction mixture and stirring continued overnight. The reaction mixture was then washed with water (2 x 30 mL), evaporated to dryness and chromatographed on silica gel. The product was finally recrystallized from CH_2Cl_2-CH_3OH; (40 mg, 10% based on **15**); MS m/e 631/633/635 (31/19/17, M^+); NMR δppm 1.75 (6H, t, Et), 1.77 (6H, t, Et), 2.56 (6H, S, Me), 3.25 (2H, br, NH_2), 3.48 (6H, S, Me), 3.84 (4H, q, Et), 3.95-4.06 (4H, m, Et), 6.79 (1H, d, Ar), 7.15 (1H, t, Ar), 7.52 (1H, t, Ar), 7.61 (1H, d, Ar), 9.66 (1H, S, meso), 9.97 (2H, S, meso), UV-vis λmax (ε_M) 569 nm (19300), 532 (19200), 405 (364500).

5-(6-Amino-1-phenyl)-3,7,12,18-tetramethyl-2,8,13,17-tetraethylprophyrin (**9**).

Zinc porphyrin **8** was dissolved in CH_2Cl_2 and washed with 15% HCl twice, H_2O and saturated $NaHCO_3$. The organic layer was dried over anhydrous Na_2SO_4 and evaporated to dryness under reduced pressure. The residue was recrystalized from CH_2Cl_2/CH_3OH to afford a practically quantitative yield of **9**; MS m/e 569 (17, M^+), 285 (20, M^{2+}); NMR δppm -3.27 (2H, br, pyr NH), 1.77 (6H, t, Et), 1.88 (6H, t, Et), 2.71 (6H, S, Me), 3.63 (6H, S, Me), 4.02 (4H, q, Et), 4.10 (4H, q, Et), 7.06-7.68 (4H, m, Ar), 9.98 (1H, S, meso), 10.17 (2H, S, meso).

5-{o-[3-(N-Imidazolyl)-propylamido]phenyl}-2,8,13,17-

tetraethyl-3,7,12,18-tetramethylprophyrin (**10**).

Excess 3-(N-Imidazolyl)propionic acylchloride[15] was dissolved in CH_3CN (20 mL) and added dropwise to a refluxing solution of porphyrin **9** (40 mg, 0.07 mmol) in CH_2Cl_2 (50 mL), containing 2 drops of triethylamine. After 3 h. the reaction mixture was poured into ice, the organic layer separated and washed successively with 5% HCl (30 mL), H_2O (30 mL), saturated $NaHCO_3$ (30 mL) and H_2O (30 mL). After drying over anhydrous Na_2SO_4 the organic layer was evaporated to dryness and the crude product purified on a thick layer silica gel plate with 3% MeOH-CH_2Cl_2. The major band was porphyrin (**10**); MS m/e 691 (M^+); NMR δppm -3.25 (2H, br, pyr NH), 1.76 (6H, t, Et), 1.90 (6H, t, Et), 2.48 (6H, S, Me), 3.67 (6H, S, Me), 3.79 (2H, t, CH_2), 4.07 (4H, q, Et), 4.09 (4H, q, Et), 6.27, 6.67, 6.84, 7.03 (each: 1H, S, 3 Im-H and -CONH-), 7.54 (1H, t, Ar), 7.80-7.92 (2H, m, Ar), 8.72 (1H, d, Ar), 10.01 (1H, S, meso), 10.20 (2H, S, meso); UV-vis λmax (ε_M) 622 nm (2900), 568 (12300), 536 (9900), 503 (11500), 403 (139100).

5-{o-[m-[a-N-Imidazolyl)-toluamido]phenyl}-2,8,13,17-tetraethyl-3,7,12,18-tetramethylporphyrin (**11**).

A solution of the o-amino-phenyl prophyrin **9** (40 mg, 0.070 mmol) in CH_2Cl_2 (20 mL) was added to an excess of α-bromo-m-toluic acyl chloride[15] (0.4 mmol) and heated to reflux for 2 h. An even greater excess of sodium imidazolate (135 mg, 1.5 mmol) in CH_3CN (20 mL) was then added all at

once. The mixture refluxed for 3 h. after which it was diluted with water, the organic layer separated and successively extracted with 5% HCl (100 mL), H_2O (100 mL), saturated $NaHCO_3$ (100 mL) and H_2O (100 mL). After drying over anhydrous Na_2SO_4 the organic layer was evaporated to dryness and the crude product purified on a thick layer silica gel plate with 3% CH_3OH-CH_2Cl_2. The major band was porphyrin **11**; MS m/e 753 (M^+); NMR δppm -3.15 (2H, br, pyr NH), 1.72 (6H, t, Et), 1.87 (6H, t, Et), 2.56 (6H, S, Me), 2.98 (2H, S, $ArCH_2$), 3.61 (6H, S, Me), 4.03 (4H, q, Et), 4.09 (4H, q, Et), 5.24 (1H, S, Im-H), 5.45 (1H, S, Im-H), 6.30 (1H, S, Im-H), 6.2-6.6 (4H, m, ArNH), 7.5-8.2 (4H, m, Ar), 8.95 (1H, d, Ar), 9.99 (1H, S, meso), 10.16 (2H, S, meso).

Methyl 5-(6-amino-1-phenyl)-13,17-diethyl-3,7,12,18-tetramethyl-2,8,-dipropionateporphyrin (**16**).

Ethyl 4-methyl-3-(2-methoxycarbonyl ethyl)-2-pyrrole carboxylate **12** (6.0 g, 33.1 mmol) and o-acetamido benzaldehyde (2.70 g., 16.6 mmol) were dissolved in 100% ethanol (100 mL), catalytic amount of conc. H_2SO_4 was added and the solution was refluxed for 5 h. on a steam bath. The pressumably formed dipyrromethane diethyl ester **13** was hydrolyzed and decarboxylated in the same pot without isolation, as follows: To the above reaction mixture a 30% KOH solution was added (100 mL) and refluxing continued for 3 h. on an electric heating mantle. The condenser was then

removed and the solution's volume was reduced to 1/2 by evaporation. Vigorous refluxing continued overnight. The dark red solution was then cooled down in an ice-bath and carefully neutralized with acetic acid. The precipitate that formed was filtered, washed with water and air dried. An attempt to positively identify this crude product was unsuccessful, and so it was used without purification for the next reaction.

Diformyl-dipyrromethane **15** (500 mg, 1.75 mmol) and the above crude product (700 mg) were dissolved in methanol (300 mL) and p-toluolo-sulfonic acid (1.0 g) was added. After the reaction mixture was stirred for 6 h. in the dark at R.T., 5 mL of saturated methanolic zinc acetate were added and stirring continued overnight. The reaction mixture was then evaporated to dryness under reduced pressure. The residue was dissolved in methylene chloride (150 mL) and washed successively with H_2O (50 mL), 15% HCl (50 mL), H_2O (50 mL and saturated $NaHCO_3$ (50 mL). The organic layer was then chromatographed on a silica gel column (3% CH_3OH-CH_2Cl_2). The desired product, **16** was the only porphyrin in the reaction mixture (41 mg, 3.5% based on **15**); NMR δppm -3.32 (1H, br, pyr NH), -3.18 (1H, br, pyr NH), 1.87 (6H, t, Et), 2.69 (6H, S, Me), 3.15 (4H, t,-$\mathbf{CH_2}CO_2Me$), 3.65 (6H, S, Me), 3.68 (6H, S, Me), 4.07 (4H, q, Et), 4.37 (4H, t, -$\mathbf{CH_2}CH_2CO_2Me$), 6.35-8.35 (4H, m, Ar), 9.96 (1H, S, meso), 10.16 (2H, S, meso).

Methyl 5-{o-[m-(α-Bromo)-tuluamido]phenyl]-13,17-diethyl-3,7,12,18-tetramethyl-2,8-dipropionateporphyrin (**17**)

Porphyrin **16** (50 mg, 0.073 mmol) in CH_2Cl_2 (50 mL) was added to an excess of α-Bromo-m-tuluic acyl chloride[15] (.4 mmol), and the mixture was heated to reflux for 2 h. It was then washed with saturated $NaHCO_3$ (30 mL) and chromotographed on a thick silica gel plate (3% CH_3OH-CH_2Cl_2), the desired product being the only major band; NMR δppm; 1.89 (6H, t, Et), 2.58 (6H, S, Me), 3.06 (2H, S, -CH_2Br), 3.12 (2H, t, -$\mathbf{CH_2}CO_2Me$), 3.65 (12H, S, Me), 4.08 (4H, q, Et), 4.35 (4H, t, -$\mathbf{CH_2}CH_2CO_2Me$), 6.2-9.0 (9H, m, Ar and -CONH-), 10.00 (1H, S, meso), 10.21 (2H, S, meso).

(5-{o-[m-(α-N-Imidazolyl)-toluamido]phenyl}-13,17-diethyl-3,7,12,18-tetramethylporphyrin)-butane-1,4[4(1-aza-2-oxo), 4(1-aza-2-oxo)-cyclophane) (**18**)

Porphyrin **17** (20 mg, 0.023 mmol) was dissolved in 88% formic acid (50 mL) and 2 mL of conc. HCl was added. The mixture was heated on a steam bath for 3 h. and evaporated to dryness under reduced pressure. The residue was suspended into dry methylene chloride (30 mL) and 0.5 mL of oxalyl chloride was added. The mixture was refluxed gently on an oil bath for 1-1/2 h. during which it was homogenized. It was then once again evaporated to dryness and the crude diacyl chloride porphyrin was used without purification for the coupling reaction with 1,4-diamino-butane using the high dilution method described earlier (see synthesis of 2).

After the coupling was completed the crude product was dissolved in CH_2Cl_2 (20 mL) and an excess of sodium imidazolate (10 mg, 0.1 mmol) in CH_3CN (20 mL) was added all at once. The mixture was heated to refluxing for 3 h. after which the solution was diluted with H_2O. The organic layer was separated and successively extracted with 5% HCl (100 mL), H_2O (100 mL), saturated $NaHCO_3$ (10 mL), H_2O (100 mL) and evaporated to dryness. The product was separated on a thick silica gel plate (5% CH_3OH-CH_2Cl_2); MS m/e 892 (M^+); NMR δppm -2.5 (2H, br, pyr NH), -1.0, -0.8 (each: 2H, br, -$NHCH_2CH_2$), 1.4 (2H, br, -$NH\mathbf{CH_2}$-), 1.88 (6H, t, Et), 2.5-2.85 (8H, m, -$\mathbf{CH_2}CONH\mathbf{CH_2}$-), 2.75 (6H, S, Me), 3.60 (6H, S, Me), 4.06 (4H, q, Et), 4.12 (2H, S, $ArCH_2$-), 4.25, 4.6 (each: 2H, br, -$\mathbf{CH_2}CH_2CO$-), 5.05 (1H, S, Im-H), 5.9-8.8 (10H, m, Ar and 2 Im-H), 9.94 (1H, S, meso), 10.06 (2H, S, meso); UV-vis λmax (ε_M) 624 nm (2500), 571 (5600), 539 (6900), 506 (10100), 405 (179900).

<u>(5-{o-[m-(α-N-Imidazolyl)-toluamido]phenyl}-13,17-diethyl-3,7,12,18-tetramethylprophyrin)-pentane-1.5-[5(1-aza-2-oxo),5-(1-aza-2-oxo)-cyclophane]</u> (**19**)

This strapped porphyrin was prepared in a manner analogous to the previous one **18**, using 1,5-diamino-pentane. The final product in this case, was the only major product of this sequence of reactions; MS m/e 907 (M^+); NMR δppm -2.9 (2H, br, pyr NH), -2.2, -2.0 (each: 2H, br, -$NHCH_2\mathbf{CH_2}$-), -1.0 (2H, br, -$NHCH_2CH_2\mathbf{CH_2}$-), 1.55 (4H, br, -$NH\mathbf{CH_2}$-), 1.87

(6H, t, Et), 2.59 (6H, S, Me), 2.92 (4H, t, $-CH_2CO-$), 3.59 (6H, S, Me), 3.65 (2H, S, $ArCH_2-$), 4.04 (4H, q, Et), 4.20, 4.61 (each: 2H, m, $-\mathbf{CH_2}CH_2CO-$), 5.05 (1H, S, Im-H), 6.0-8.9 (10H, m, Ar and 2Im-H), 9.95 (1H, S, meso), 10.13 (2H, S, meso); UV-vis λmax (ε_M) 624 nm (2000), 570 (4300), 539 (5100), 505 (8900), 405 (110300).

B. SYNTHESIS OF MESO-NAPHTHYL SUBSTITUTED PORPHYRINS

Introduction

Hydrogen bonding has been thought to play a very important role in the ability of cobalt (II) macrocyclic complexes to reversibly bind dioxygen.[25] So far, although many Co (II) porphyrin complexes have been prepared over the last 15 years,[25b-f,26] and their O_2 binding abilities studied, the effect of hydrogen bonding was not fully investigated because of the lack of appropriate models, and it was left open to speculations[25c-e] as to how significant it can be. Only recently Jameson and Drago[27] have studied the effect of weak H-bonding present in the "picket fence" porphyrin. In order for one to systematically examine the effect of hydrogen bonding, a series of porphyrin models should be available with substituents which, on the one hand, would have functional groups capable of forming hydrogen bonds of different strength to be bound O_2 and on the other hand, would be in the right position, close to the

center of the porphyrin for maximum effect. For those reasons, meso substituted porphyrins with a naphthyl group possessing a functional group at its 8th position, seemed to be ideal. As CPK models suggest, the functional group of this system would be held over the porphyrin ring and in very close proximity to its center. The synthesis of such a series of porphyrins was undertaken and is described here.

Synthesis

The recently developed method for the synthesis of mono-aryl substituted porphyrins[23] had to be modified in order to prepare the naphthyl porphyrin **23** because the 8-formyl-1-naphthoic acid[24] first used was unreactive. The loss of its reactivity was attributed to its tautomeric form where the formyl group is lost. So to overcome this problem acenaphthaquinone was first condensed with the α-free pyrrole **5** (Scheme IV), to give the meso substituted dipyrromethane **21** which is a very stable X'talline solid. For the cleavage of the C-C bond to form the 8-dipyrromethane-1-naphthoic acid, the method of basic hydrolysis by Fuson and Munn,[24] for the cleavage of acenaphthaquinone was used. This method turned out to be very convenient because at the same time the C-C bond cleaves, the carboxylic esters of the dipyrromethane are hydrolyzed and decarboxylated, too. So the dipyrromethane **22** produced from this reaction was ready to use for the one step synthesis of the porphyrin. The coupling reaction of

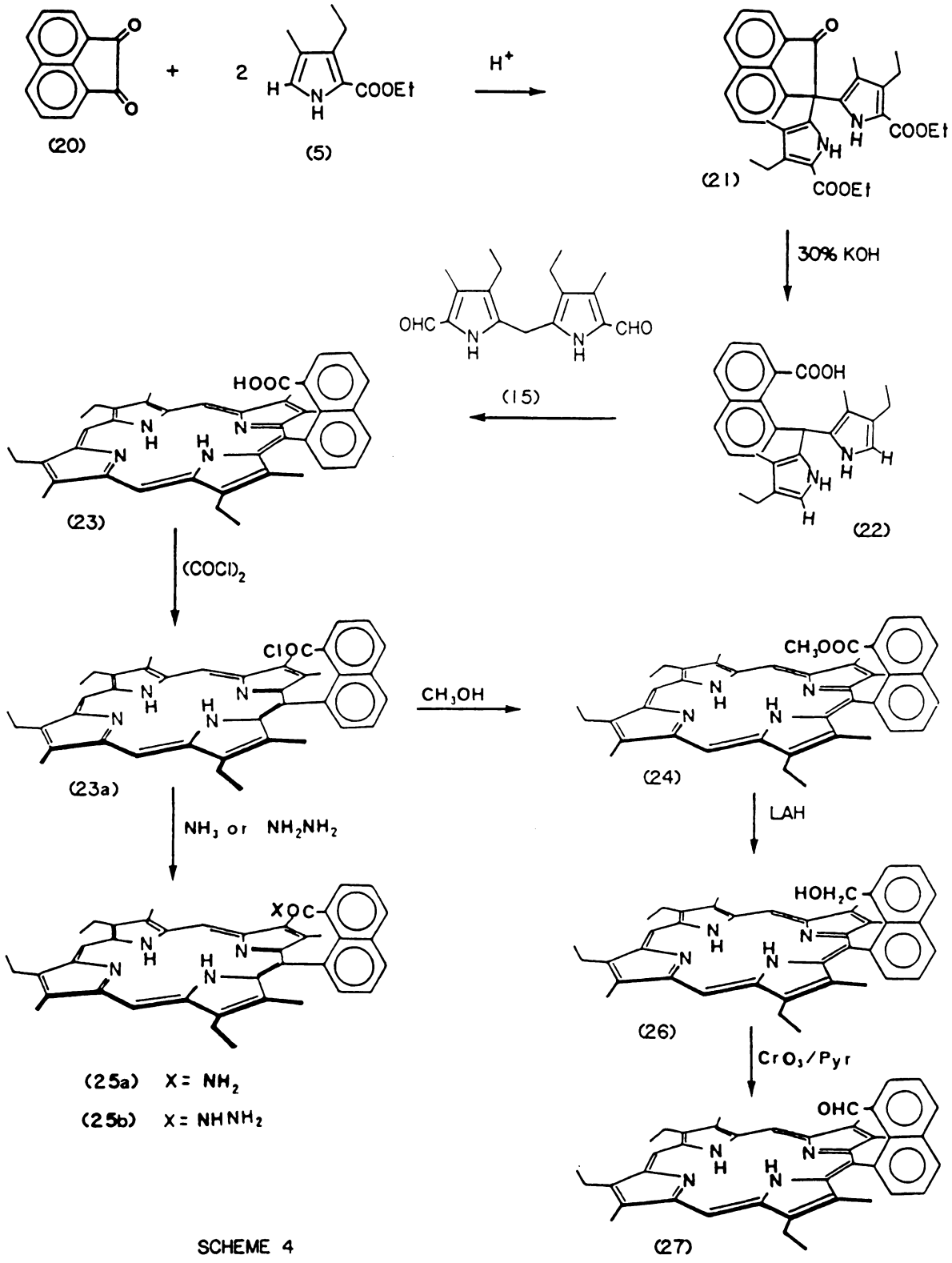
(20)
(5)
H+
(21)
30% KOH
(15)
(22)
(23)
(COCl)2
(23a)
CH3OH
(24)
LAH
NH3 or NH2NH2
(25a) X = NH2
(25b) X = NHNH2
(26)
CrO3/Pyr
(27)

SCHEME 4

the two dipyrromethanes was carried out smoothly, under mild conditions and the desired porphyrin produced in good yield. The polar carboxylic group inevitably renders this porphyrin slow moving on silica gel and its purification tedious. Nevertheless, it can be converted to its acyl chloride without purification and separated after it is derivatized to a less polar, easier to purify amides or esters.

The esterification of the carboxylic group of the parent compound **23** was surprisingly difficult when the CH_3OH/conc. H_2SO_4 method was used. At the same time the hydrolysis of the methyl carboxylate **24** was also very slow and incomplete. The reason for this peculiarity is not clearly understood but it seems possible that the carboxylic group, being enclosed in the hydrophobic pocket of the aromatic porphyrin ring and the naphthyl group, is not easily accessible to other polar groups. So **23**, had to be first converted to its acyl chloride **23a** which then could be quenched by CH_3OH to give the methyl ester **24** in good yield. From this compound one could also prepare the alcohol **26** and aldehyde **27**, using standard procedures. Finally quenching of the acyl chloride with ammonia produced a small amount of the corresponding amide, while most the porphyrin decomposed.

An even more functionalized system was also synthesized by condensing dipyrromethane **22** with another meso-aryl substituted one **28c** (Scheme V). The new system's behavior and handling was identical to the previous one. The cis-trans isomers of this comound were impossible to separated

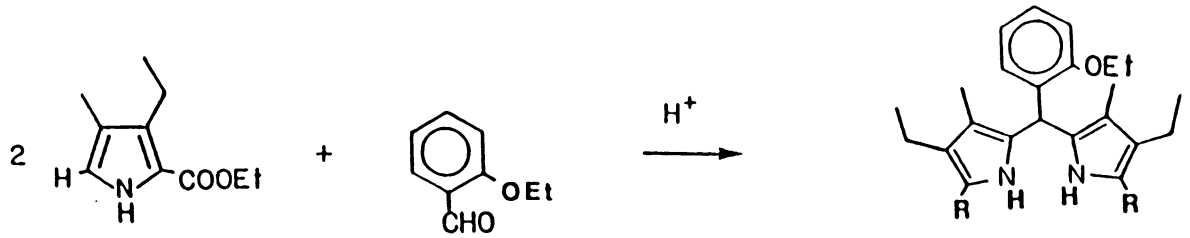

(5)

(28) R - COOEt
(28a) R - COOH
(28b) R - H
(28c) R - CHO

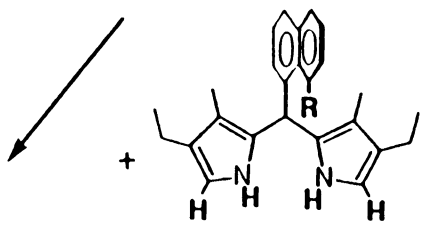

(22) R=COOH

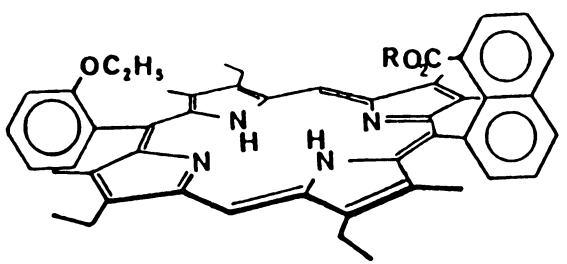

(29) R = CH_3

(29a) R = H

SCHEME 5

even in small scale. However if this porphyrin is derivitized, such a separation should be possible, as our experience with similar systems dictate.[15]

Experimental

1,1-Bis(5-ethoxycarbonyl-4-ethyl-3-methyl-2-pyrryl)-2-oxo-acenaphthene (21)

To a suspension of acenaphthenequinone **20** (10.0 g, 55.0 mmol) in 100% ethanol (700 mL) was added ethyl 3-ethyl-4-methyl-2-pyrrole carboxylate[21] **5** (20.0 g, 110.0 mmol) and concentrated H_2SO_4 (1 mL). The mixture was refluxed overnight on a steambath and **20** was completely dissolved. The solution was then reduced to 250-300 mL under reduced pressure and cooled in an ice-bath. The yellow crystilline solid which precipitated was collected by filtration and washed with 30% H_2O in ethanol (3 x 30 mL) (15.0 g). The filtrate was concentrated to one half of its volume and cooled again to give a second darker crop (2.5 g), (total yield 17.5 g, 61%); m.p. 108-110°C; MS m/e 526 (100, M^+), 480 (53), 453 (40), 437 (61), 346 (88), 240 (78), 217 (94); NMR δ ppm 1.06 (6H, t, Et), 1.28 (6H, t, Et), 1.62 (6H, S, Me), 2.68 (4H, q, Et), 4.24 (4H, q, OEt), naphthyl: 7.49 (1H, d), 7.69 (1H, t), 7.80 (1H, t), 7.95 (1H, d), 8.03 (1H, d), 8.19 (1H, d), 8.44 (2H, br, NH).

8-[(4,4'-diethyl-3,3'-dimethyl-2,2'-dipyrryl)methyl]-1-naphthoic acid (22)

Dipyrromethane **21** (10.0 g, 19.1 mmol) was suspended in 30% KOH (100 mL) and refluxed overnight under Argon. The resulted dark red, homogeneous solution was poured into acid and was neutralized by the careful addition of acetic acid. Dipyrromethane **22** precipitated as pink amorphous solid, collected by suction filtration and washed with water and several times (6.5 g, 85%). This solid was used in the next step without further purification; NMR δ ppm 1.1 (6H, t, Et), 1.6 (6H, S, Me), 2.4 (4H, q, Et), 6.4 (1H, S, methane CH), 7.2 (2H, d, 5,5'-pyrrole) 7.4-8.4 (8H, m, naphthyl and 2NH).

5-(8-carboxyl-1-naphthyl)-2,8,13,17-tetraethyl-3,7,12,18-tetramethylporphyrin (**23**)

To a solution of the decarboxylated dipyrrylmethane **22** (2.1 g, 5.2 mmol) and the diformyldipyrromethane **15**[22] (1.5 g, 5.2 mmol) in dry methylene chloride (900 mL) was added a solution of p-toluenesulfonic acid monohydrate (5 g) in methanol (40 mL). The solution was stirred for 6 h. at R.T. in the dark; after which a saturated solution of zinc acetate in methanol (40 mL) was added, and stirring in the dark continued for another 8 h. This solution was then washed with H_2O (2 x 100 mL) and evaporated to dryness, under reduced pressure. The crude product was chromatographed from silica gel column twice (starting with pure CH_2Cl_2 and slowly increasing the percentage of methanol up to 10%). After the purification, a methylene chloride

solution of the porphyrin was shaken with 15% HCl (100 mL) to demetalate it, washed with saturated $NaHCO_3$ dried over anhydrous Na_2SO_4 and evaporated to dryness (500 mg, 14.8%); NMR δ ppm -2.3 (1H, br, NH), -1.1 (1H, br, NH), 1.7 (6H, t, Et), 1.9 (6H, t, Et), 2.1 (6H, S, Me), 3.7 (6H, S, Me), 3.9 (2H, q, Et), 4.0 (2H, q, Et), 4.1 (4H, q, Et), naphthyl: 7.0 (1H, d), 7.5 (1H, t), 7.9 (1H, t), 8.2 (1H, d), 8.2 (1H, d), 8.3 (1H, d), meso: 10.1 (1H, S), 10.3 (2H, S); UV-vis λmax (ε_M) 626 nm (2800), 571 (7600), 538 (7600), 504 (11400), 407 (157100).

5-[8-(methoxycarbonyl)-1-naphthyl]-2,8,13,17-tetraethyl-3,7,12,18-tetramethylporphyrin (**24**)

Porphyrin **23** (100 mg, 0.15 mmol) was dissolved in dry methylene chloride (70 mL) and excess oxalyl chloride (1 mL) was added. The solution was refluxed for 1-1/2 h. and the solvent together with the excess of oxalyl chloride, was removed under reduced pressure. The acyl chloride porphyrin produced was immediately quenched with large excess of anhydrous methanol (50 mL). After stirring the mixture for 5 min., methanol was removed and the residue dissolved in CH_2Cl_2 (100 mL), washed with saturated $NaHCO_3$ (30 mL) and purified by recrystallization from CH_2Cl_2/CH_3OH to give purple crystals in quantitative yield; MS m/e 662 (60, M^+), 331 (g, M^{2+}); NMR δ ppm -3.14, -3.07 (each: 1H, br, NH), 0.09 (3H, S, -OMe), 1.70 (6H, t, Et), 1.89 (6H, t, Et), 2.11 (6H, S, Me), 3.64 (6H, S, Me), 3.96 (4H, q, Et), 4.08 (4H,

q, Et), naphthyl: 7.30 (1H, d), 7.60 (1H, t), 7.85 (1H, t), 8.03 (1H, d), 8.27 (1H, d) 8.35 (1H, d), meso: 9.97 (1H, S), 10.14 (2H, S); UV-vis λmax (ε_M) 625 nm (2900), 572 (5900), 537 (6900), 503 (13900), 405 (178000).

5-[8-(Hydroxymethyl)-1-naphthyl]-2,8,13,17-tetraethyl-3,7,12,18-tetramethylporphyrin (**26**)

The methyl ester porphyrin **24** (100 mg, 0.15 mmol), was dissolved in dry THF (150 mL) and a 3-fold excess of $LiAlH_4$ was added carefully. The mixture was magnetically stirred at R.T. for 2 h. (The progress of the reaction can easily be monitored by TLC, as the product's R_f value is significantly smaller than that of the starting material). The solvent was then evaporated almost to dryness and the residue was carefully partitioned between CH_2Cl_2 and 10% HCl. The organic layer was then washed with saturated $NaHCO_3$, dried over anhydrous Na_2SO_4 and evaporated to dryness. Recrystallization of the crude product from CH_2Cl_2/CH_3OH gave **26** as purple crystals (67 mg, 70%); MS m/e 634 (16, M^+); NMR δ ppm -3.17 (1H, br, NH), -2.98 (1H, br, NH), 0.19 (1H, t, OH), 1.70 (6H, t, Et), 1.87 (6H, t, Et), 2.12 (6H, S, Me), 3.09 (2H, d, $-\mathbf{CH_2}OH$), 3.64 (6H, S, Me), 3.93 (2H, q, Et), 3.99 (2H, q, Et), 4.08 (4H, q, Et), naphthyl: 7.60 (1H, S), 7.62 (1H, d), 7.78 (1H, t), 8.00 (1H, d), 8.16 (1H, t), 8.34 (1H, d), meso: 9.96 (1H, S), 10.15 (2H, S); UV-vis λmax (ε_M) 625 nm (2100), 572 (6400), 538 (6500), 503 (15000), 405 (190000).

5-(8-Formyl-1-naphthyl)-2,8,13,17-tetraethyl-3,7,12,18-tetramethylporphyrin (**27**)

Porphyrin **26** (45 mg, 0.08 mmol) was dissolved in dry pyridine (3 mL) and it was added in one portion to an ice-cooled solution of CrO_3 (27 mg) in pyridine. The mixture was stirred for 20 min. after which the ice-bath was removed and stirring continued for 2 more h., at R. T. Then the solution was partitioned between CH_2Cl_2 and H_2O. The organic layer was first washed with 10% HCl (2 x 20 mL), and then with saturated $NaHCO_3$. Finally it was evaporated to dryness and the product separated on a thick silica gel plate (1% CH_3OH-CH_2Cl_2), to afford **27** in practically quantitative yield; NMR δ ppm -3.08 (2H, br, NH), 1.69 (6H, t, Et), 1.87 (6H, t, Et), 2.10 (6H, S, Me), 3.63 (6H, S, Me), 3.93 (4H, m, Et), 4.08 (4H, q, Et), 5.82 (1H, S, -CHO), 7.3-8.5 (6H, m, naphthyl), 9.96 (1H, S, meso), 10.15 (2H, S, meso).

5-(8-Acetamido-1-naphthyl)-2,8,13,17-tetraethyl-3,7,12,18-tetramethylporphyrin (**25a**)

Porphyrin **23** (100 mg, 0.15 mmol) was dissolved in dry methylene chloride (70 mL), and oxalyl chloride (1 mL) was added. The solution was refluxed for 1-1/2 h. and the solvent together with the excess of oxalyl chloride was removed under reduced pressure. The residue was redissolved in dry methylene chloride (70 mL) and dry ammonia was

briefly passed through the stirred solution. The reaction mixture was then washed with water (30 mL), dried over anhydrous Na_2SO_4 and evaporated to dryness. The crude product was chromatographed on a silica gel column (3% CH_3OH-CH_2Cl_2) and then recrystallized from CH_3OH-CH_2Cl_2 (10 mg, 10%); MS m/e 647 (12, M^+); NMR δ ppm -3.15 (2H, br, NH), 1.69 (6H, t, Et), 1.87 (6H, t, Et), 2.12 (6H, S, Me), 2.60 (2H, br, $-CONH_2$), 3.62 (6H, S, Me), 3.90 (4H, m, Et), 4.07 (4H, q, Et), naphthyl: 7.30 (1H, d), 7.56 (1H, t), 7.89 (1H, t), 8.17 (1H, d), 8.23 (1H, d), 8.35 (1H, d), 9.95 (1H, S, meso), 10.12 (2H, S, meso); UV-vis λmax (ε_M) 627 nm (2800), 573 (7100), 541 (7300), 506 (8800), 409 (106500).

5-(8-Acetohydrizide-1-naphthyl)-2,8,13,17-tetraethyl-3,7,12,18-tetramethylporphyrin (**25b**)

Porphyrin **23** (100 mg, 0.15 mmol) was dissolved in dry methylene chloride (20 mL) and excess oxalyl chloride (1 mL) was added. The solution was refluxed for 1 to 1-1/2 h. and the solvent together with the excess of oxalyl chloride was removed under reduced pressure. The residue was redissolved in dry methylene chloride (50 mL) and hydrazine monohydrate (0.5 mL) was added. The mixture was stirred for 5 min. washed with water (30 mL), dried over anhydrous Na_2SO_4 and evaporated to dryness. The crude product was chromatographed on a silica gel column (3% CH_3OH-CH_2Cl_2). The desired product eluted first and the unreacted starting material second. The final product was recrystallized from

CH_3OH-CH_2Cl_2 (45 mg, 44%); MS m/e 662 (M^+); NMR δppm - 1.79, -1.30 (each: 2H, br, pyr -NH), 1.76, 1.94 (each: 6H, t, Et), 2.01, 3.52 (each: 6H, S, Me), 3.92 (4H, q, Et), 4.09 (4H, q, Et), 7.5 - 8.5 (6H, m, naphthyl), 10.16 (1H, S, meso), 10.28 (2H, S, meso). UV-vis λmax (ε_M) 625 (2900), 572 (6900), 541 (7800), 506 (13000), 407 (169200).

6-Ethoxy-1-[(5,5'-dicarboxyl-4,4'-diethyl-3,3'-dimethyl-2,2'-dipyrryl)methyl]benzene (**28a**)

Ethyl 3-ethyl-4-methyl-2-pyrrolecarboxylate (**5**)[21] (4.83 g, 26.7 mmol) and o-ethoxybenzaldehyde (2 g, 13.3 mmol) were dissolved in 100% Ethanol (50 mL), conc. H_2SO_4 was added (5 drops) and the solution was refluxed on a steam bath overnight. Then, without isolation of the intermediate, dipyrromethane **28**, a 30% solution of potassium hydroxide was added in the same flask (50 mL) and the mixture was refluxed on an electric heating mantle for another 5 h. The solution was then poured into crushed ice, neutralized carefully by the slow addition of acetic acid and the precipitated pink amorphous solid was collected by suction filtration washed with H_2O several times and air dried (5 g, 86%). This product was used in the next step without further purification. MS m/e 394 (2, M^+-CO_2), 350 (29, M^+-$2CO_2$), 44 (100, CO_2^+); NMR δ ppm 1.13 (6H, t, Et), 1.32 (3H, t, -OEt), 1.88 (6H, S, Me), 2.75 (2H, q, Et), 2.78 (2H, q, Et), 4.00 (2H, q, -OEt), 5.68 (1H, S, methane CH), 6.89-7.24 (4H, m, Ar), 8.85 (2H, S, NH).

6-Ethoxy-1-[(4,4'-diethyl-3,3'-dimethyl-2,2'-dipyrryl)methyl] benzene (**28b**)

Dipyrromethane **28a** (5 g, 11.4 mmol), was dissolved in ethanolamine (20 mL) and refluxed for 2 h. The solution was then poured into crushed ice and the mixture extracted with CH_2Cl_2 (3 x 30 mL). The organic layer was then evaporated to dryness and the crude product - a brown oil - was purified by passing it through a short silica gel column (CH_2Cl_2). The purified product was a yellow viscous oil (2.8 g, 70%); NMR δ ppm 1.15 (6H, t, Et), 1.23 (3H, t, -OEt), 1.79 (6H, S, Me), 2.41 (4H, q, Et), 3.90 (2H, q, -OEt), 5.74 (1H, S, methane CH), 6.33 (2H, d, 5,5'-pyrrole), 6.80-7.20 (4H, m, Ar), 7.55 (2H, br, NH).

6-Ethoxy-1-[(4,4'-diethyl-3,3'-dimethyl-5,5'-diformyl-2,2'-dipyrryl)methyl]benzene (**28c**)

Phosphoryl chloride (1.5 mL) was added dropwise over a period of 15 min. to a stirred, ice-cooled, solution of dipyrromethane **28b** (5 g, 14.3 mmol), in N,N'-dimethylformamide (10 mL). The solution was then stirred at R. T. for 1.5 h. and then poured into ice and H_2O. To the acidic solution, saturated $NaHCO_3$ was slowly added until it became basic. Then it was heated on a steam bath for 15 min. and the product precipitated upon standing for 2-3 days, as brown amorphous crystals (75%); MS m/e 406 (100, M^+), 377 (53, M^+-CHO); NMR δ ppm 1.19 (6H, t, Et), 1.25 (3H,

t, -OEt), 1.85 (6H, S, Me), 2.69 (4H, q, Et), 3.98 (2H, q, -OEt), 5.76 (1H, S, methane CH), 6.87-7.30 (4H, m, Ar), 9.15 (2H, br, NH), 9.48 (2H, S, -CHO).

Cis/trans 5-[8-(Methoxycarbonyl)-1-naphthyl]-15-[6-ethoxy-1-phenyl]-2,8,12,18-tetraethyl-3,7,13,17-tetramethyl-porphyrin (**29**)

To a solution of diformyl dipyrromethane **28c** (2 g, 4.9 mmol) and 5,5'-unsubstituted dipyrromethane **22** (1.97 g, 4.9 mmol) in dry methylene chloride (900 mL) was added a solution of p-toluene sulfonic acid monohydrate (5 g) in methanol (40 mL). The solution was magnetically stirred for 6 h. at R. T. in the dark, after which a saturated solution of zinc acetate in methanol (40 mL) was added and stirring continued in the dark for another 8 h. at R. T. The solution was then washed with H_2O (2 x 100 mL) and evaporated to dryness under reduced pressure. The crude product was passed through a silica gel column (5% CH_3OH-CH_2Cl_2) to separate the porphyrin from most but not all the impurities. This partially purified porphyrin was dissolved in dry CH_2Cl_2 (100 mL), excess oxalyl chloride was added (2 mL) and the mixture refluxed on an oil bath for 2 h. Then it was evaporated to dryness under reduced pressure and the acyl chloride was quenched by anhydrous methanol (100 mL). The solution was once again evaporated to dryness, the residue redissolved in CH_2Cl_2 washed with saturated $NaHCO_3$ and chromatographed on a silica gel column (CH_2Cl_2).

Finally the product was recrystallized from CH_3OH-CH_2Cl_2 (50 mg, 13%). The final product was a mixture of the cis and trans isomers as expected. Attempts to separate the two isomers even in small scale (preparative silica gel TLC plate) were unsuccessful. If we assume that for steric reasons the trans isomer should be the major product then the cis/trans ratio is 1/1.4 as the NMR reveals; MS m/e 391 (22, M^{2+}); NMR δ ppm -2.20 (2H, br, NH), 0.25 (S, Co_2Me cis), 0.34 (S, CO_2Me trans), 0.80 (t, -OEt cis), 1.00 (t, -OEt trans), 1.72 (6H, t, Et), 1.79 (6H, t, Et), 2.15 (6H, S, Me), 2.57 (6H, S, Me), 3.96 (2H, q, Et), 4.01 (2H, q, Et), 4.15 (4H, q, Et), 7.26-8.40 (10H, m, Ar), 10.18 (2H, S, meso).

C. SYNTHESIS OF NOVEL HIGHLY FUNCTIONALIZED PORPHYRINS

Introduction

A plethora of synthetic porphyrins have been prepared over the last 25 years from simple highly symmetric ones to more complicated unsymmetric ones. Depending on the complexity of the target molecule syntheses can be approached from a variety of directions.[28] If laborious separation of mixtures are to be avoided, totally unsymmetrical porphyrins must usually be synthesized by cyclization of a preformed open-chain tetrapyrrole.[29] In this procedure (Scheme VII) an unsymmetrically substituted

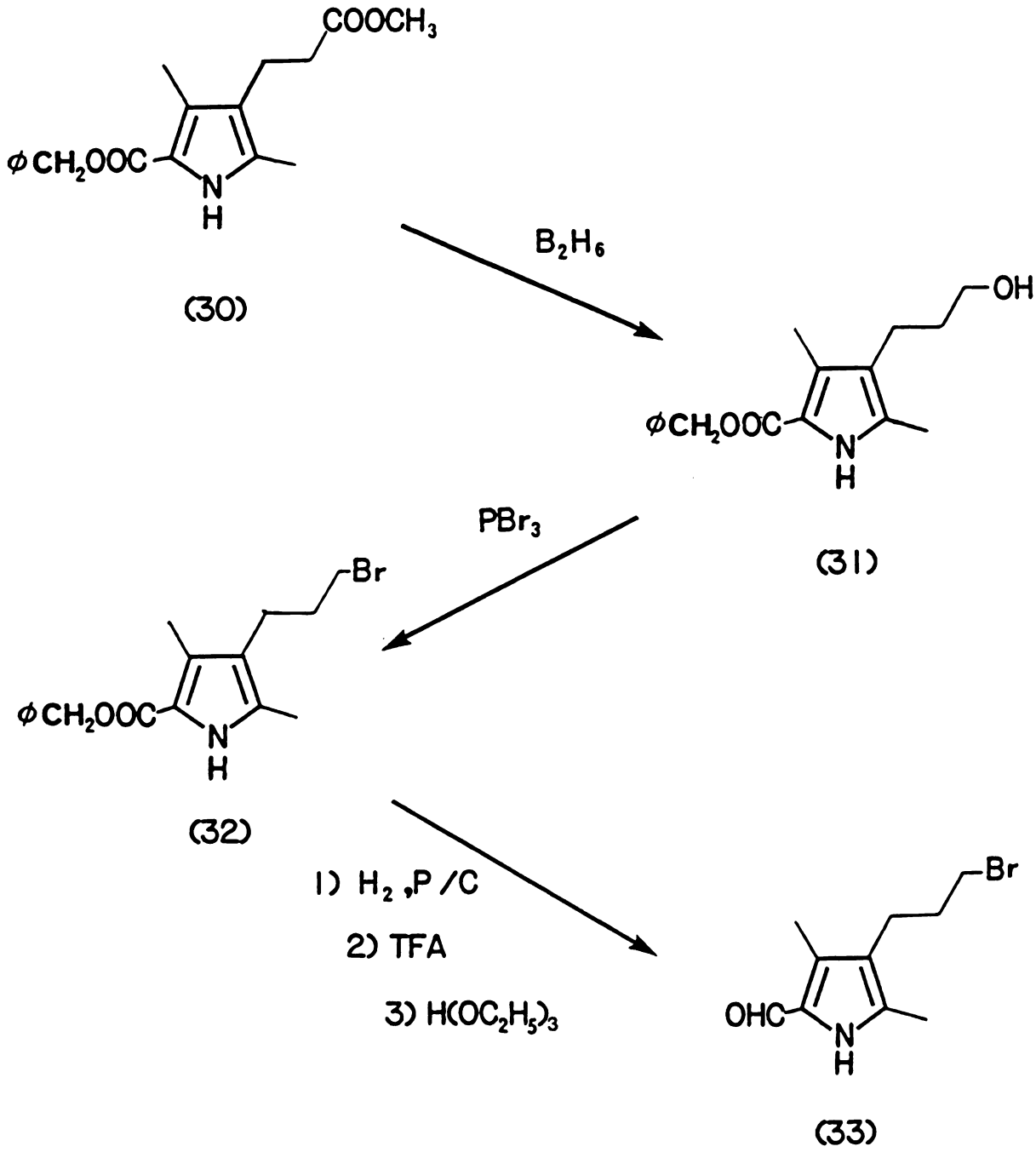
COOCH3
φCH2OOC
N
H
(30)
B2H6
OH
φCH2OOC
N
H
(31)
PBr3
Br
φCH2OOC
N
H
(32)
1) H2 ,P /C
2) TFA
3) H(OC2H5)3
Br
OHC
N
H
(33)

SCHEME 6

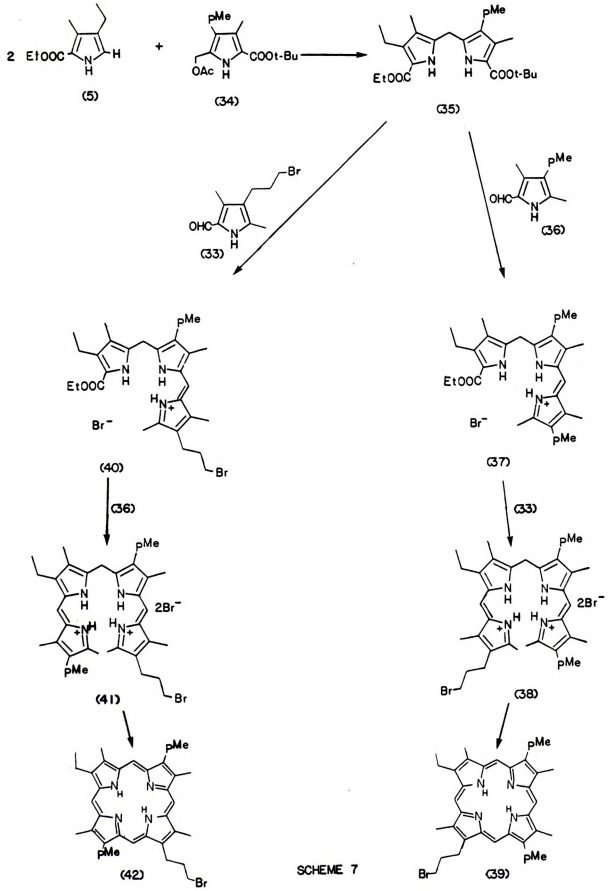
2 EtOOC
(5)
pMe
OAc
COOt-Bu
(34)
(35)
Br
OHC
(33)
OHC
(36)
Et00C
Br⁻
(40)
(37)
(36)
(33)
2Br⁻
(41)
(38)
(42)
(39)

SCHEME 7

and differentially protected ethyl tert-butyl pyrromethane-5,5'-dicarboxylate (**35**) is selectively hydrolysed and decarboxylated to give pyrromethane **35a** which in turn, can be transformed into a tripyrrin salt by condensation with a 2-formylpyrrole. Condesnation with a second 2-formylpyrrole, after hydrolysis and decarboxylation of the second ester, gives an a,c-biladiene salt. Changing the sequence of the introduction of the two formylpyrroles, one can get the a,c-biladiene salt with a different geometry. Cyclization of the two 1',8'-dimethyl-a,c-biladiene salts gave the two isomeric porphyrins **39** and **42**.

These two porphyrins were designed in this way so that either symmetric or asymmetric straps of different lengths could be built across the prophyrin plane. Such a flexibility was hoped to give us a better control over the magnitude of steric hindrance at the binding site of the heme. By functionalizing one side chain of the prophyrin periphery with the bromide one can later attach an imidazole tail necessary for myoglobin models. Unfortunately, although the incorporation of the straps went smoothly following the same pathway described in part A of this chapter, the substitution of the bromide as well as the physical studies of those models did not work quite as smoothly. The substitution of the bromide by $(CH_3)_2CHNH(CH_2)_3Im$ was carried out in refluxing xylenes with excess of the substituted imidazole present. The product was very hard to purify though, because it was nearly

impossible to elute on silical gel or alumina columns. Nevertheless, the NMR of the small quantities that were purified, although very complex and difficult to assign, did show the imidazole hydrogen peaks between 5.5 - 7.5 ppm as expected. That let us believe that the right compounds were made. But the even more disappointing result was that these hemes, when an attempt to measure their CO association was made, did not show first order kinetics. The reason for this behavior is believed to be the high flexibility of the imidazole tail which on one hand cannot discriminate between the two different heme faces and on the other can also form an intermolecular complex with a second heme. So the completion of the synthesis of these models was abandoned and the emphasis was shifted to the construction of models with a more rigid imidazole tail which indeed proved to be successful (see part A).

Finally, the recently developed method for the synthesis of monoaryl-substituted porphyrins was also used for the preparation of o-methoxy phenyl porphyrin **44**.

Synthesis

The stepwise synthesis of porphyrins **39** and **42**, requires the use of four pyrroles (Scheme VII). Three of them **5**,[21] **34**[30] and **36**[31] were synthesized according to the literature while for the fourth one **33**, the modification of Benzyl 4-(2-ethyl carboxymethyl)-3,5-dimethyl-2-pyrrolecarboxylate (**30**)[32] was necessary. In the first step the methyl ester

was converted to the corresponding alcohol in quantitative yield using B_2H_6. Reaction of the alcohol with phosphorous tribromide yields the bromopropylpyrrole **32**. The catalytic cleavage of the benzyl ester was finally followed by decarboxylation in trifluoroacetic acid and formylation with triethyl orthoformate in one pot, to afford the 2-formyl-4-(3-bromopropyl)pyrrole (**33**), in good yield.

For the synthesis of the a,c-biladienes, Smith's procedure was followed.[29] The t-butyl ester of dipyrromethane **35** (Scheme VII) was firstly cleaved in TFA and a formyl pyrrole was added, and condensed with it to afford the corresponding tripyrrolic salt. In a similar step, the second ester was cleaved (under much more rigorous conditions), and the fourth pyrrole was added. Finally, the a,c-biladiene salts were heated briefly in DMF, in the presence of Cu(II) chloride to produce the porphyrins **39** and **42**, each one as the major poryphyrin product.

For the synthesis of the o-methoxy-phenyl porphyrin **44**, dipyrromethane **43b** had to be synthesized first. This was done in ethanol in the presence of an acid catalyst, followed by basic hydrolysis. The diacid-dipyrromethane **43a** was finally decarboxylated in refluxing ethanolamine and was coupled to diformyldipyrromethane **15** to afford porphyrin **44** in relatively good yield (Scheme VIII).

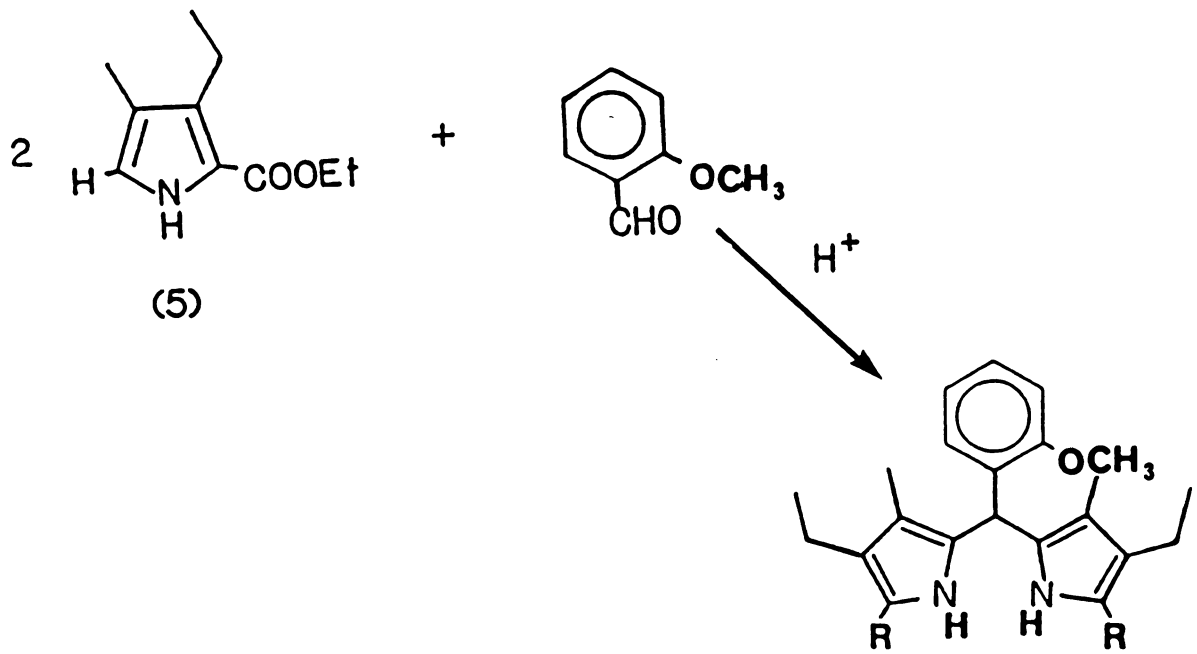

(5)

(43) R - COOEt

(43a) R - COOH

(43b) R - H

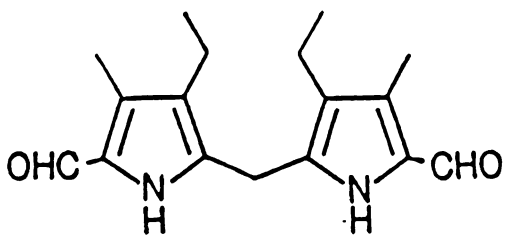

(15)

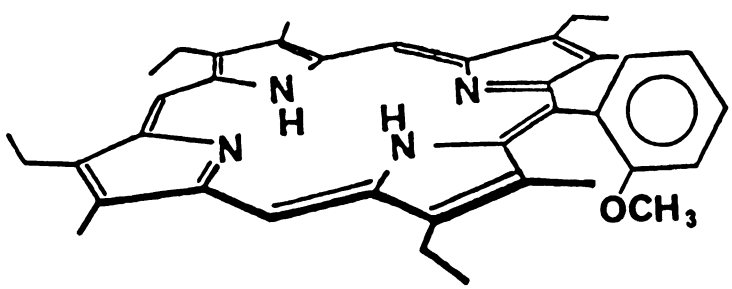

(44)

SCHEME 8

Experimental

Benzyl 4-(3-hydroxypropyl)-3,5-dimethyl-2-pyrrolecarboxylate (**31**)

In a three-neck, round bottom, flask, was placed sodium boron hydride (3.6 g, 95 mmol) and THF (25 mL). Boron trifluoride etherate (1M, 17.4 mL) diluted in anhydrous ether (100 mL) was then added dropwise through a dropping funnel, to the stirred suspension of $NaBH_4$. A slow stream of Argon transferred the generated diborane into another R. B. flask, containing a solution of Benzyl 4-(2-methoxy carbonylethyl)-3,5-dimethyl-2-pyrrolecarboxylate (**30**)[32] in anhydrous THF (200 mL). The solution of the pyrrole was stirred throughout the addition of diborane and was continued for 1 more hour. The reaction was easily monitored by means of TLC (the product moves slower than the starting material). The excess of the diborane was destroyed by cautiously adding methanol. The solvents were then removed under reduced pressure and the crude product was recrystallized from CH_3OH to give white crystals, in quantitative yield; m.p. 95°-96°C; MS m/e 287 (14, M^+), 242 (17, $M^+ - (CH_2)_2OH$), 91 (100, ΦCH_2^+); NMR δ ppm 1.70 (2H, m, $-CH_2\mathbf{CH_2}CH_2OH$), 1.72 (1H, br, -OH), 2.18 (3H, S, Me), 2.28 (3H, S, Me), 2.44 (2H, t, $-\mathbf{CH_2}-CH_2CH_2OH$), 3.62 (2H, t, $-\mathbf{CH_2}OH$), 5.28 (2H, S, $-\mathbf{CH_2}\Phi$), 7.3-7.5 (5H, m, Ar), 8.90 (1H, br, NH).

Benzyl 4-(3-bromopropyl)-3,5-dimethyl-2-pyrrolecarboxylate (**32**)

Benzyl 4-(2-methoxy carbonylethyl)-3,5-dimethyl-2-pyrrolecarboxylate (**31**), (6 g, 20.9 mmol) was dissolved in dry methylene chloride (50 mL). Pyridine (2 mL) was added and the protected from the moisture solution was cooled down in an ice-salt bath. To the cooled, magnetically stirred solution, an excess of phosphorous tribromide (11.3 g, 41.7 mmol), was added dropwise over a period of 30 min., and stirring continued overnight with gradual warming up of the mixture. It was then washed with 2N HCl (2 x 20 mL), and saturated $NaHCO_3$ (2 x 20 mL), and the organic layer was dried over anhydrous Na_2SO_4 and evaporated to dryness under reduced pressure to give a green oil. This crude product was passed through an alumina column (CH_2Cl_2), and the new - lighter colored - oil, solidified upon standing for a few hours. Finally the product was recrystallized from methanol to give pale-white crystals (1.54 g, 21%); m.p. 96-97°C; MS m/e 349/351 (48/58, M^+), 242 (90, $M^+ - CH_2CH_2Br$), 91 (100, ΦCH_2^+); NMR δ ppm 1.98 (2H, quintet, $-\mathbf{CH_2}CH_2Br$), 2.21 (3H, S, Me), 2.28 (3H, S, Me), 2.53 (2H, t, $-\mathbf{CH_2}CH_2CH_2Br$), 3.37 (2H, t, $-CH_2Br$), 5.29 (2H, S, ΦCH_2-), 7.2 - 7.5 (5H, m, Ar), 8.81 (1H, br, NH).

4-(3-Bromopropyl)-3,5-dimethyl-2-formylpyrrole (**33**)

In a solution of Benzyl 4-(3-bromopropyl)-3,5-dimethyl-2-pyrrolecarboxylate (**32**), (5.8 g, 16.6 mmol), in THF (150 mL), was suspended 10% Pd on Carbon (4 g) and the mixture stirred under H_2 until the uptake of 1 equivalent of H_2 was

complete (about 1 h.). The suspension was then gravity filtered to separate the catalyst and the solvent of the clear solution was evaporated under reduced pressure. The resulting yellow oil was used in the next reaction without any purification. To the above crude product, trifluoroacetic acid was added (17 mL), and the solution was magnetically stirred fro 5 min. at 40°C (oil bath), under Ar. The evolution of a gas was evident (CO_2). Triethylorthoformate was then added (5.1 mL) in one portion and stirring continued at 40°C for another 5 min. After that 85 mL of water were added to the reaction mixture and the separated oil which soon, solidified was collected and dissolved in ethanol (55 mL). Aqueous ammonia (2N, 35 mL), was added slowly with stirring, followed by water (50 mL), 10 min. later. Finally, the product was collected by suction filtration as yellow crystals. (Overall: 7.6 g, 64%); m.p. 123-125°C; MS m/e 243/245 (26/25, M^+), 136 (100, $M^+ - CH_2CH_2Br$); NMR δ ppm 2.00 (2H, quintet, $-CH_2\mathbf{CH_2}CH_2Br$), 2.28 (6H, S, Me), 2.55 (2H, t, $-\mathbf{CH_2}CH_2CH_2Br$), 3.39 (2H, t, $-CH_2Br$), 9.46 (1H, S, -CHO), 10.05 (1H, br, NH).

Ethyl 3,4'-dimethyl-4-ethyl-3'-(2-methoxycarbonylethyl)-5'-t-butoxycarbonyl-dipyrromethane-5-carboxylate (**35**)

A suspension of ethyl 3-ethyl-4-methyl-2-pyrrolecarboxylate (**5**)[21] (225 mg, 1.24 mmol) and t-Butyl 2-acetoxymethyl-3-(2-methoxycarbonylethyl)-4-methyl-5-pyrrolecarboxylate (**34**)[30] (421 mg, 1.24 mmol) in methanol (5

mL), was added p-toluolosulfonic acid monohydrate (10 mg) and heated with stirring under argon at 40°C for 5 h. The homogenized mixture was then partitioned between H_2O (20 mL) and methylene chloride (30 mL) and the organic layer was dried over anhydrous Na_2SO_4 and evaporated to dryness. The product was used in the next reaction without further purification; MS m/e 460 (16, M^+), 194 (74, $C_{11}H_{16}NO_2^+$), 57 (100, t-but$^+$); NMR δ ppm 1.1 (3H, t, Et), 1.3 (3H, t, $-CO_2Et$), 1.6 (9H, S, t-But), 2.0 (3H, S, Me), 2.2 (3H, S, Me), 2.5 (2H, t, $-CH_2-$), 2.6 (2H, t, $-CH_2-$), 2.7 (2H, q, Et), 3.6 (3H, S, $-CO_2Me$), 3.8 (2H, S, methane CH_2), 4.2 (2H, q, $-CO_2Et$), 8.8 (1H, br, NH), 9.1 (1H, br, NH).

Ethyl 1',2,3,5-tetramethyl-1,4-di(2-methoxycarbonylethyl)-6-ethyltripyrrin-a-6'-carboxylate Hydrobromide (**37**)

Dipyrromethane **35** (4.12 g, 8.95 mmol), was treated with trifluoro acetic acid (30 mL) under Argon atmosphere at ambient temperature, for 5 min. A solution of formyl pyrrole **36**[31] (1.88 g, 9.0 mmol) in methanol (200 mL) was then added all at once and the dark red solution was stirred an additional 90 min., followed by addition of a 30% HBr-CH_3COOH solution (1.5 mL) and ether (250 mL). Continued stirring for 15 min. resulted in the formation of orange-crystals which were collected by means of suction filtration and washed thoroughly with ether (1.74 g, 31.7%). The mother liquor was evaporated to approximately 100 mL, and ether (200 mL) was added to give a second crop of the

product (1 g, 17.6%) (overall: 49.3%); m.p.: decomposes at 221-223°C; MS m/e 551 (2, M^+ -HBr); NMR δ ppm 1.07, 1.36 (each: 3H, t, Et), 2.04, 2.26, 2.31, 2.72 (each: 3H, S, Me), 2.48 (2H, t, $-\mathbf{CH_2}CO_2Me$), 2.73 (8H, m, $-\mathbf{CH_2}CH_2CO_2Me$ and Et), 3.67 (6H, S, $-CO_2Me$), 4.28 (2H, q, $-CO_2Et$), 4.37 (2H, S, meso CH_2), 7.09 (1H, S, methine bridge), 10.22 (1H, br, NH), 13.21 (2H, br, NH).

6-Ethyl-1',8',2,3,5,7-hexamethyl-1,4-di(2-methoxycarbonyl-ethyl)-8-(3-bromopropyl)-a,c-biladiene Dihydrobromide (**38**)

Tripyrrin **37** (3.45 g, 5.46 mmol) was stirred in a mixture of 48% HBr (30 mL), acetic acid (20 mL) and trifluoroacetic acid (30 mL) under N_2, at 65-70°C for 6 h. A solution of formylpyrrole **33** (1.41 g, 5.78 mmol) in methanol (300 mL) was then added all at once and stirring continued for 1 h. at R. T. The reaction mixture was evaporated under reduced pressure and the residue was partitioned between CH_2Cl_2 and saturated NaBr. The organic layer was evaporated to dryness, the residue redissolved in the minimum amount of methanol possible (about 60 mL) and ether was added (500 mL). This mixture was stirred for 10 min. during which the product precipitated as brown crystals, which were collected by suction filtration, washed with ether and air dried (3.4 g, 72%); NMR δ ppm 1.14 (3H, t, Et), 2.05 (2H, m $-CH_2\mathbf{CH_2}CH_2Br$), 2.29, 2.32, 2.33, 2.71, 2.72, 3.45 (each: 3H, S, Me), 2.50 (2H, t, CH_2), 2.6-2.85 (10H, m, CH_2), 3.42 (2H, t, $-CH_2Br$), 3.70 (6H, S, $-CO_2Me$),

5.22 (2H, S, meso CH_2), 7.12, 7.13 (each: 1H, S, methine bridge), 13.20, 13.28 (each: 1H, br, NH), 13.40 (2H, br, NH).

2-Ethyl-3,8,12,18-tetramethyl-7,13-di(2-methoxycarbonylethyl)-17-(3-bromopropyl)porphyrin (**39**)

a,c-Biladiene dihydrobromide **38** (164 mg, 0.19 mmol), was dissolved in dry DMF (19 mL) containing copper (II) chloride (1.07 g, 8.0 mmol). The solution was stirred for 4 min. at 145°C (oil bath) under argon. After cooling, the solution was poured into water and extracted with methylene chloride. The organic layer was then dried over anhydrous sodium sulfate and evaporated to dryness, followed by column chromatography (silica gel -CH_2Cl_2). The red eluants were evaporated to dryness and the residue was treated with conc. H_2SO_4 (30 mL) in order to dimetalate the copper-porphyrin which is the initial product of the reaction. The mixture was then partitioned very carefully between CH_2Cl_2 and water. The organic layer was washed with water (2 x 20 mL) and saturated $NaHCO_3$ (2 x 20 mL), dried over anhydrous Na_2SO_4 and evaporated to dryness. This crude product was further purified by column chromatography (silica gel - CH_2Cl_2) and recrystallized from CH_3OH-CH_2Cl_2 (30 mg, 23%); MS m/e 686/688 (2/2, M^+), 606 (41, M^+ -HBr); NMR δ ppm -3.8 (2H, br, NH), 1.87 (3H, t, Et), 2.86 (2H, quintet, -**CH_2**CH_2Br), 3.27 (2H, t, -**CH_2**CO_2Me), 3.28 (2H, t, -**CH_2**CO_2Me), 3.62, 3.64, 3.67, 3.68 (each: 3H, S, Me), 3.74 (2H, t, -

CH_2Br), 4.10 (2H, q, Et), 4.25 (2H, t, -$\mathbf{CH_2}CH_2CH_2Br$), 4.39 (2H, t, -$\mathbf{CH_2}CH_2CO_2Me$), 4.43 (2H, t, -$\mathbf{CH_2}CH_2CO_2Me$), 10.06 (1H, S, meso), 10.08 (2H, S, meso), 10.14 (1H, S, meso).

Ethyl 1',2,3,5-tetramethyl-4-(2-methoxycarbonylethyl)-6-ethyl-1-(3-bromopropyl)-tripyrrin-a-6'-carboxylate Hydrobromide (**40**)

Tripyrrin **40** was synthesized in a manner analogous to the synthesis of tripyrrin **37** using formyl pyrrole **33** (overall yield: 45.7%); NMR δ ppm 1.07 (3H, t, Et), 1.36 (3H, t, $-CO_2Et$), 2.01 (2H, quintet, $-CH_2\mathbf{CH_2}CH_2Br$), 2.05, 2.27 (each: 3H, S, Me), 2.30 (2H, t, -$\mathbf{CH_2}CH_2CH_2Br$), 2.32 (3H, S, Me), 2.59 (2H, t, -$\mathbf{CH_2}CH_2CO_2Me$), 2.72 (3H, S, Me), 2.62-2.76 (4H, m, Et and $-CH_2\mathbf{CH_2}CO_2Me$), 3.40 (2H, t,$-CH_2Br$), 3.67 (3H, S, $-CO_2Me$), 4.27 (2H, q, CO_2Et), 4.37 (2H, S, meso CH_2), 7.10 (1H, S, meso CH), 10.23 (1H, br, NH), 13.20 (2H, br, NH).

6-Ethyl-1',8',2,3,5,7-hexamethyl-4,8-di(2-methoxycarbonyl-ethyl)-1-(3-bromopropyl)-a,c-biladiene Dihydrobromide (**41**)

a,c-Biladiene salt **41** was prepared in a manner analogous to the synthesis of a,c-Biladiene salt **38** using formylpyrrole **37** instead (overall yield: 76.9%); NMR δ ppm 1.14 (3H, t, Et), 2.06 (2H, quintet, $-CH_2\mathbf{CH_2}CH_2Br$), 2.01, 2.49, 2.82 (each: 2H, t, CH_2), 2.67 (4H, t, CH_2), 2.87 (2H, q, Et), 3.42 (2H, t, $-CH_2Br$), 2.26, 3.45 (each: 3H, S, Me), 2.34, 2.73 (each: 6H, S, Me), 3.48, 3.71 (each: 3H, S, $-CO_2Me$), 5.22 (2H, S, meso CH_2), 7.13, 7.16 (each: 1H, S,

methine bridge), 13.35, 13.44 (each: 1H, br, NH), 13.57 (2H, br, NH).

2-Ethyl-3,8,12,18-tetramethyl-7,17-di(2-methoxycarbonylethyl)-13-(3-bromopropyl)porphyrin (**42**)

Porphyrin **42** was synthesized in a manner analogous to the syntehsis of porphyrin **39** using a,c-biladiene salt **41** instead (yield: 24.4%); MS m/e 606 (4, M^+ -HBr); NMR δ ppm -3.79 (2H, br, NH), 1.89 (3H, t, Et); 2.87 (2H, quintet, $-CH_2\mathbf{CH_2}CH_2Br$), 3.29 (4H, t, $-\mathbf{CH_2}CO_2Me$), 3.64, 3.65, 3.67 (3H, 3H, 6H, each: S, Me), 3.72 (6H, S, CO_2Me), 3.88 (2H, t, $-CH_2Br$), 4.14 (2H, q, Et), 4.30 (2H, t, $-\mathbf{CH_2}CH_2CH_2Br$), 4.41, 4.44 (each: 2H, t, $-\mathbf{CH_2}CH_2CO_2Me$), 10.10 (3H, S, meso), 10.16 (1H, S, meso); UV-vis λmax (ε_M) 619 nm (5500), 565 (8000), 530 (11100), 496 (16100), 399 (174400).

6-Methoxy-1-[(4,4'-diethyl-3,3'-dimethyl-2,2'-dipyrryl)methyl]benzene (**43b**)

α-Free pyrrole **5**[21] (5.32 g, 29.4 mmol) and o-anisaldehyde (2 g, 14.7 mmol) were dissolved in ethanol (100%, 50 mL), 0.5 mL conc. HCl was added and the solution was refluxed on a steam bath for 2 h. Then without isolation of the intermediate dipyrryl methane diethyl ester **43**, a 30% NaOH solution (50 mL), was added and refluxing continued on an electric heating mantle for another 5 h. The mixture was poured into crushed ice and neutralized carefully by the slow addition of glacial acetic acid. The

solid, which precipitated was collected by suction filtration washed with H_2O several times and air dried. This product (without purification) was dissolved in ethanolamine (20 mL) and refluxed for 2 h. The solution was then poured into crushed ice, extracted with methylene chloride (2 x 30 mL) and the organic layer was evaporated under reduced pressure. The product was a brown oil and was used without purification in the subsequent reaction (3 g, 60%); MS m/e 336 (42, M^+), 228 (100); NMR δ ppm 1.15 (6H, t, Et), 1.77 (6H, S, Me), 2.40 (4H, q, Et), 3.66 (3H, S, -OMe), 5.77 (1H, S, methane CH), 6.26 (2H, d, 5,5'-pyrrole), 6.8-7.20 (4H, m, Ar), 7.40 (2H, br, NH).

5-(6-methoxy-1-phenyl)-2,8,13,17-tetraethyl-3,7,12,18-tetramethylporphyrin (**44**)

5,5'-Diformyldipyrromethane **15**[22] (286 mg, 1 mmol), and 5,5-free-dipyrromethane **43b** (336 mg, 1 mmol) were dissolved in CH_2Cl_2 (300 mL). To this solution, methanolic p-toluolosulfonic acid (1 g in 20 mL CH_3OH) was added and after stirring for 6 h. in the dark, it was treated with saturated methanolic zinc acetate (20 mL), and was set aside overnight. It was then washed with 15% HCl (2 x 50 mL), saturated $NaHCO_3$ (2 x 50 mL), and chromatographed on silica gel column (CH_2Cl_2). The product which was the only porphyrin in the reaction mixture was recrystallized from CH_2Cl_2-CH_3OH. (205 mg, 30%); MS m/e 585 (100, M^+), 292 (12, M^{2+}); NMR δ ppm -3.2 (2H, br, NH), 1.76 (6H, t, Et), 1.88

(6H, t, Et), 2.53 (6H, S, Me), 3.63 (6H, S, Me), 3.73 (3H, S, $-OCH_3$), 4.0-4.2 (8H, m, Et), 7.3-7.9 (4H, m, Ar), 9.93 (1H, S, meso), 10.13 (2H, S, meso); UV-vis λmax (ε_M) 622 nm (3000), 568 (6800), 533 (7700), 498 (15000), 403 (168400).

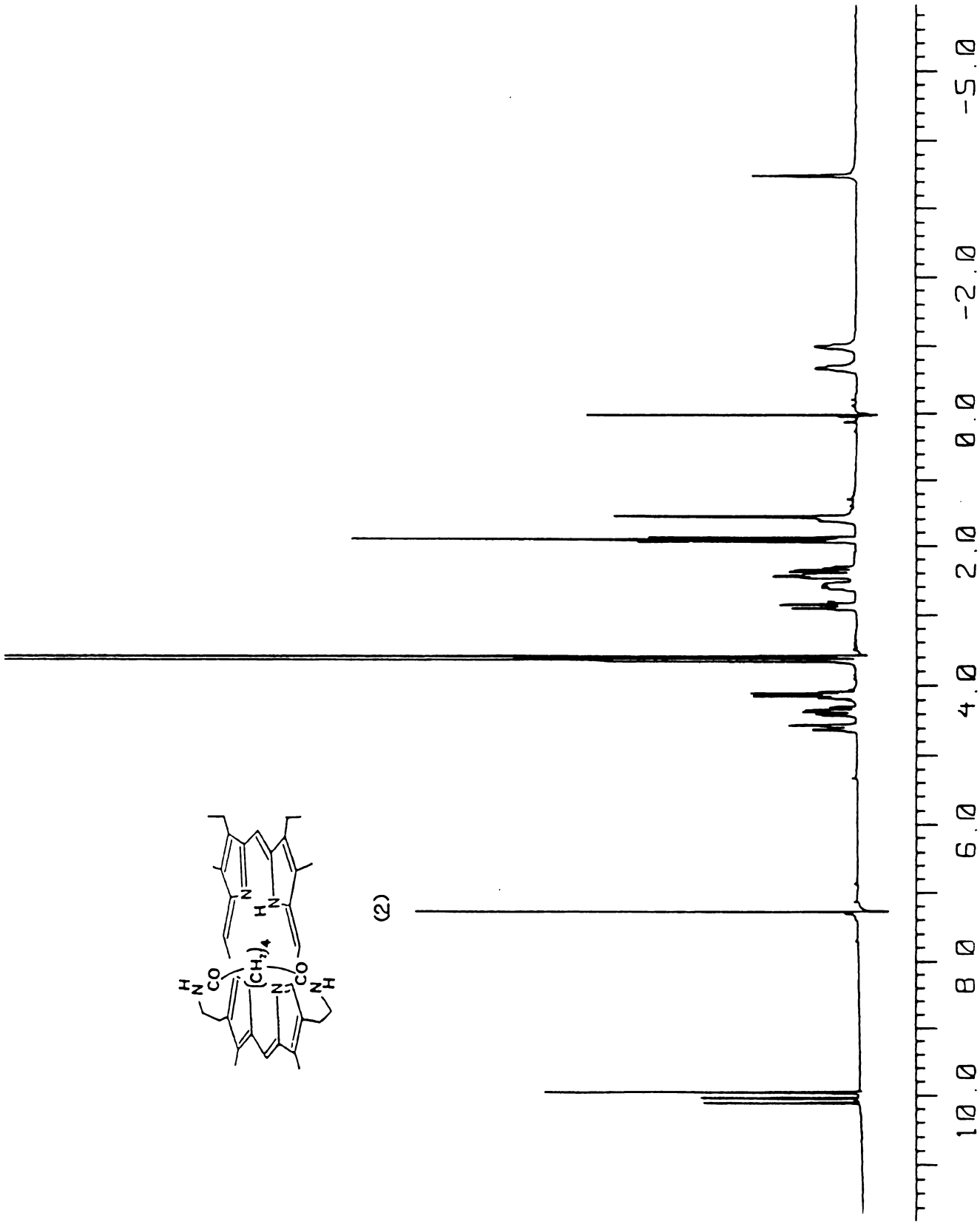

(2)

Figure 3-1 'H-NMR spectrum of porphyrin 2

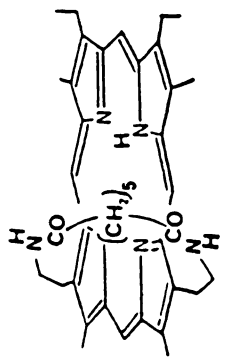

(3)

Figure 3-2 'H-NMR spectrum of porphyrin 3

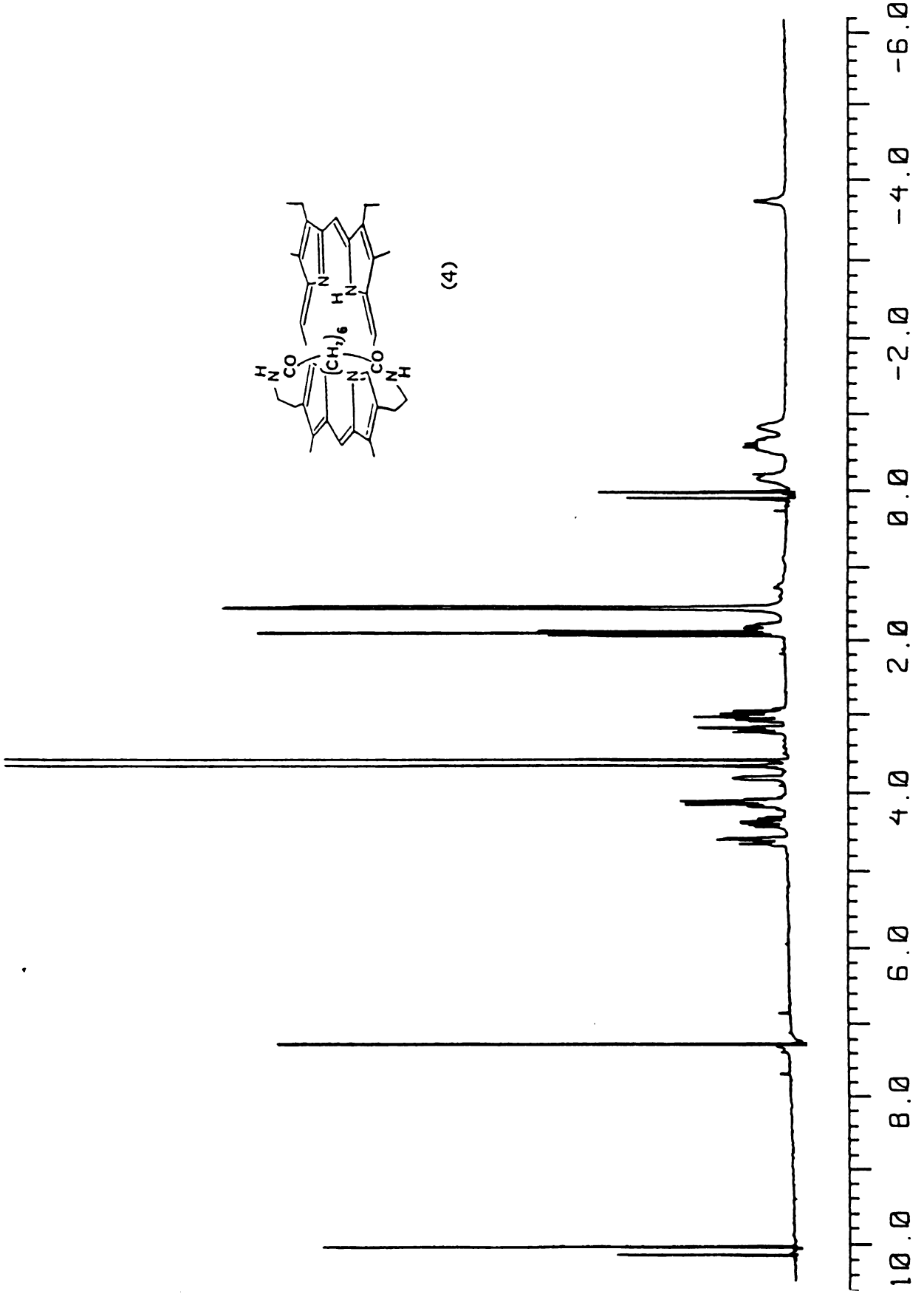

(4)

Figure 3-3 ^{1}H-NMR spectrum of porphyrin 4

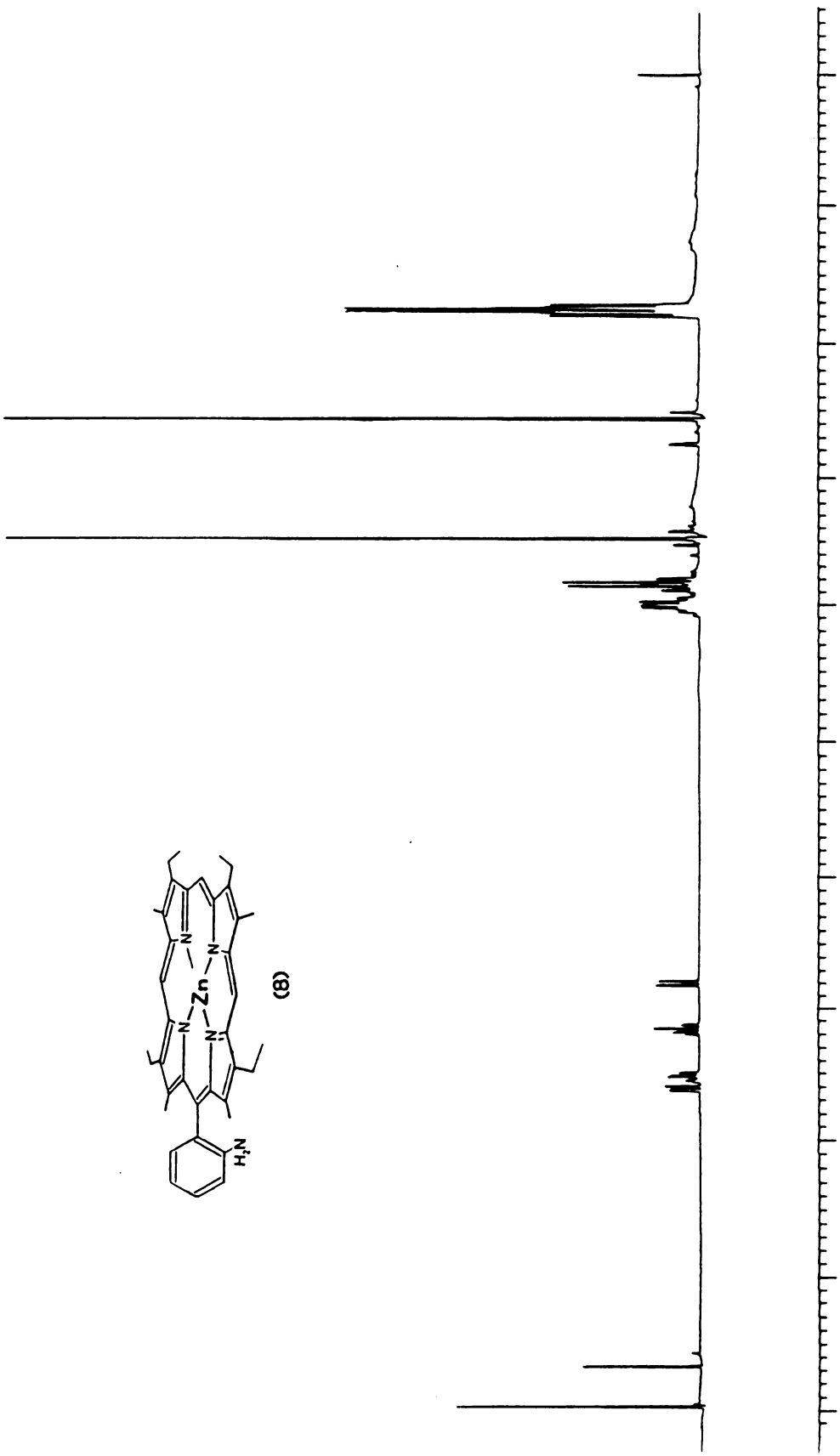

Figure 3-4 'H-NMR spectrum of porphyrin 8

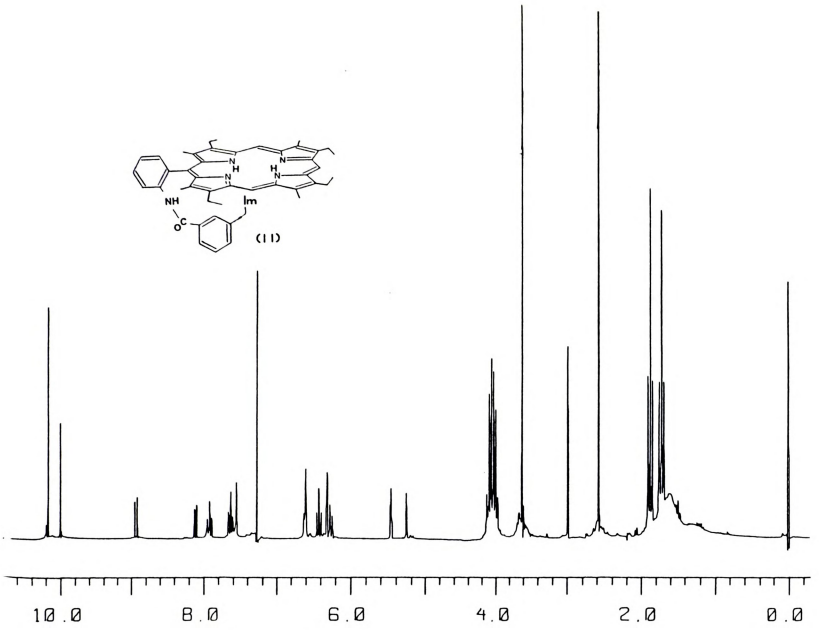

Figure 3-5 'H-NMR spectrum of porphyrin 11

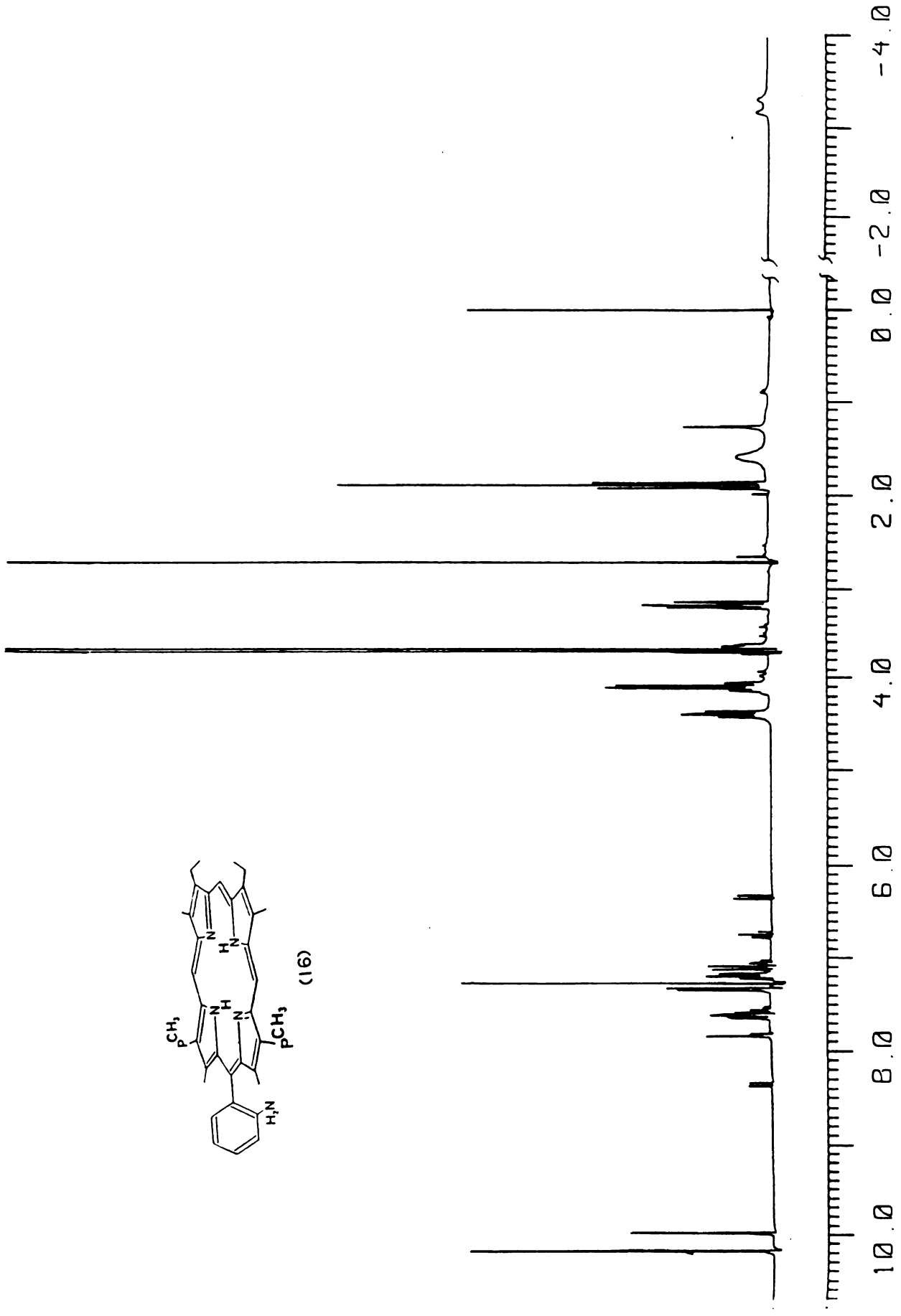

Figure 3-6 'H-NMR spectrum of porphyrin 16

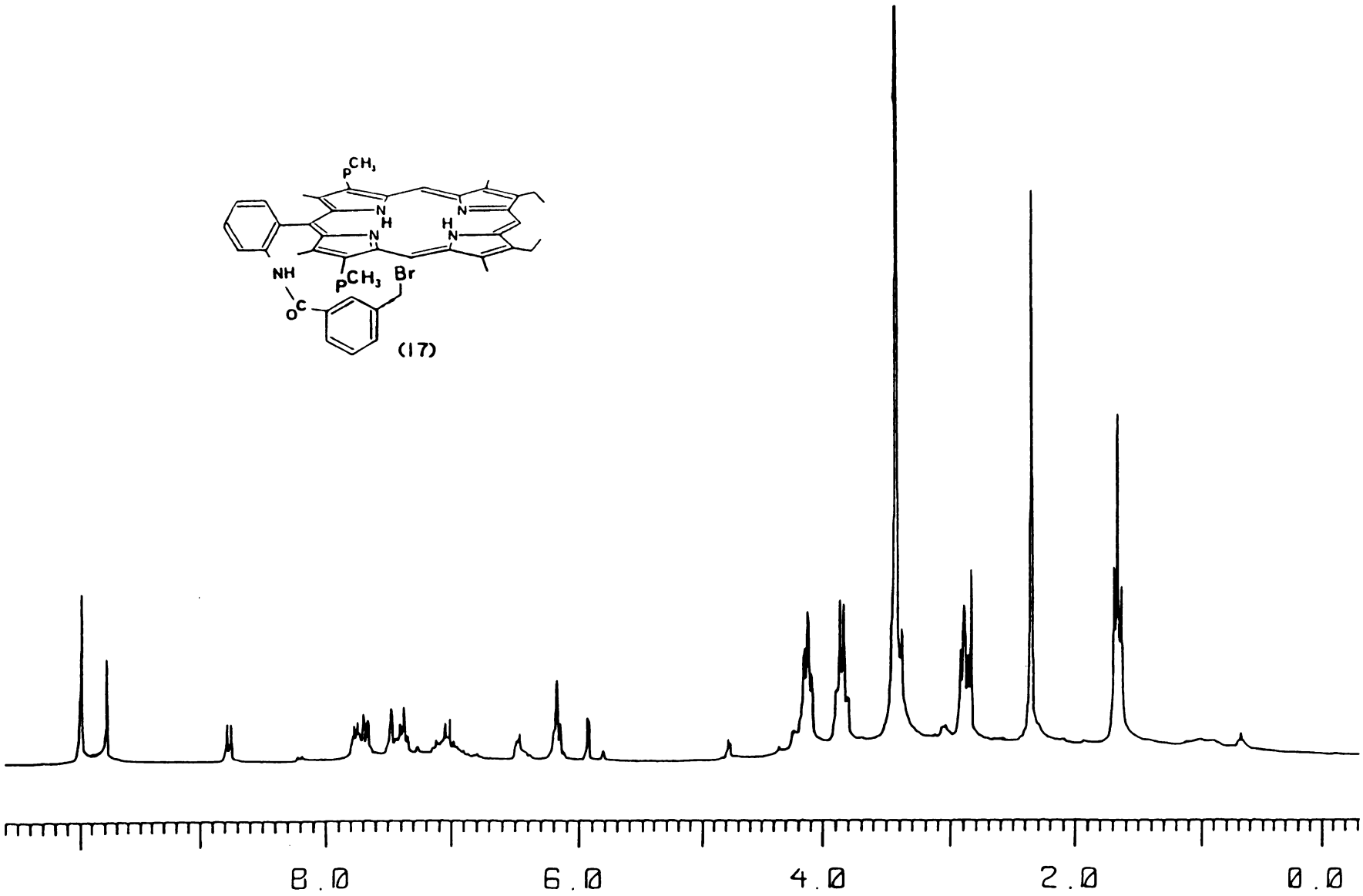

Figure 3-7 'H-NMR spectrum of porphyrin 17

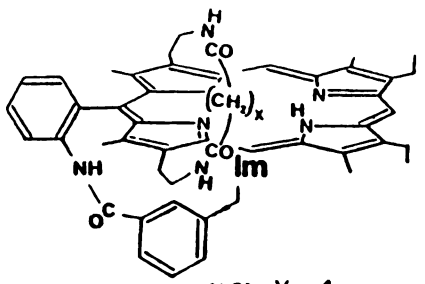

(18) X = 4

Figure 3-8 ^{1}H-NMR spectrum of porphyrin 18

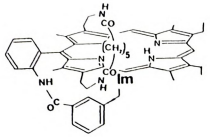

(19)

Figure 3-9 ^{1}H-NMR spectrum of porphyrin **19**

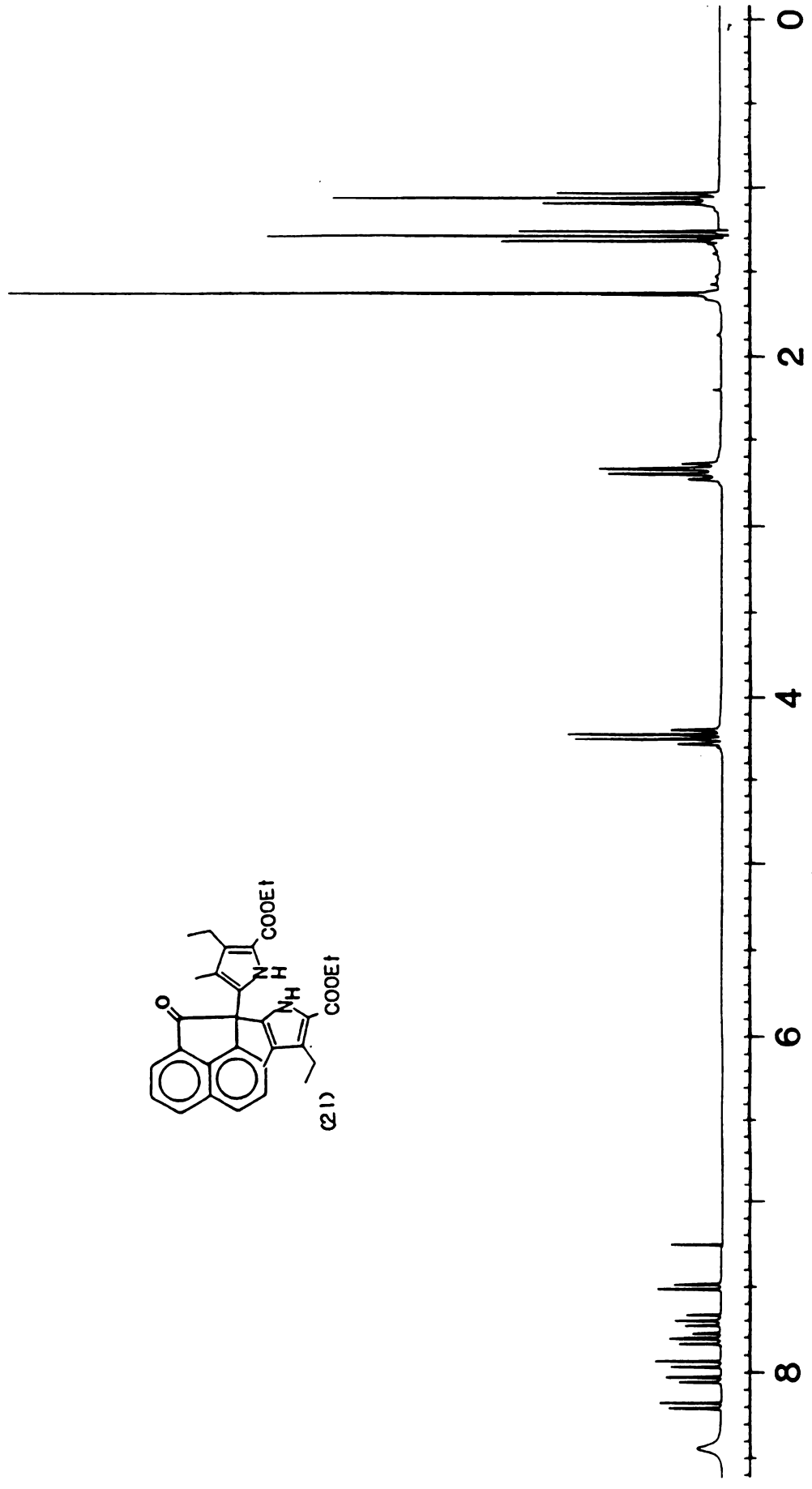

(21)

Figure 3-10 'H-NMR spectrum of Dipyrromethane 21

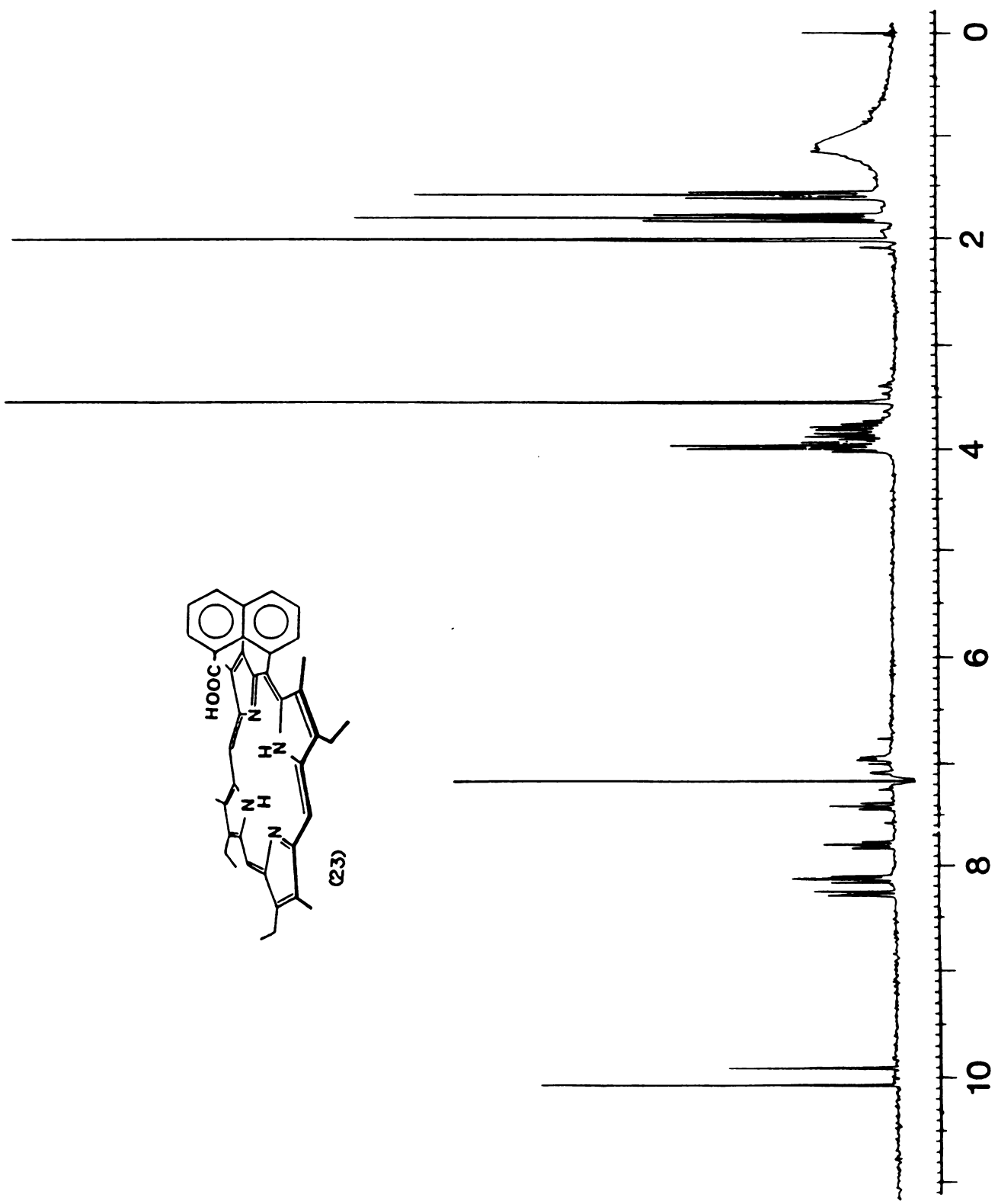

Figure 3-11 'H-NMR spectrum of porphyrin 23

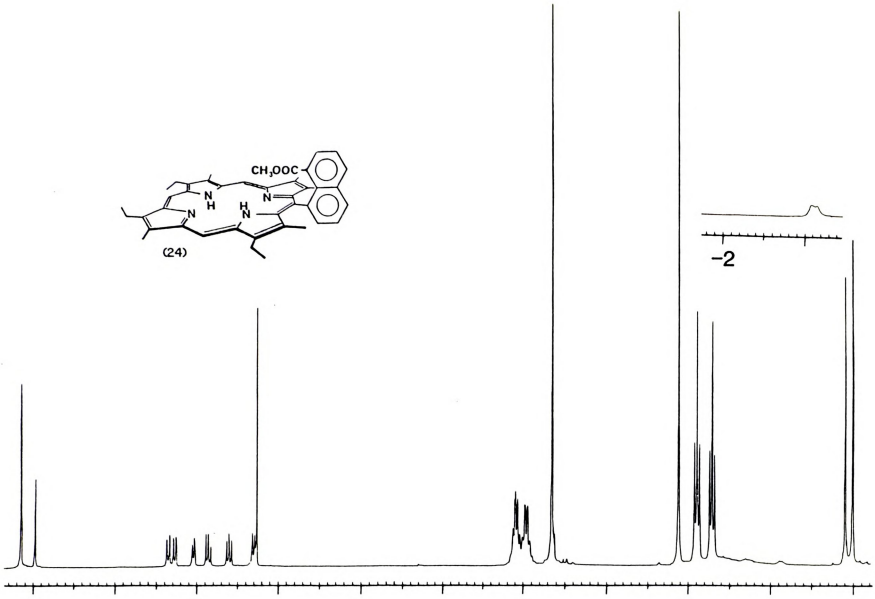

Figure 3-12 ^{1}H-NMR spectrum of porphyrin 24

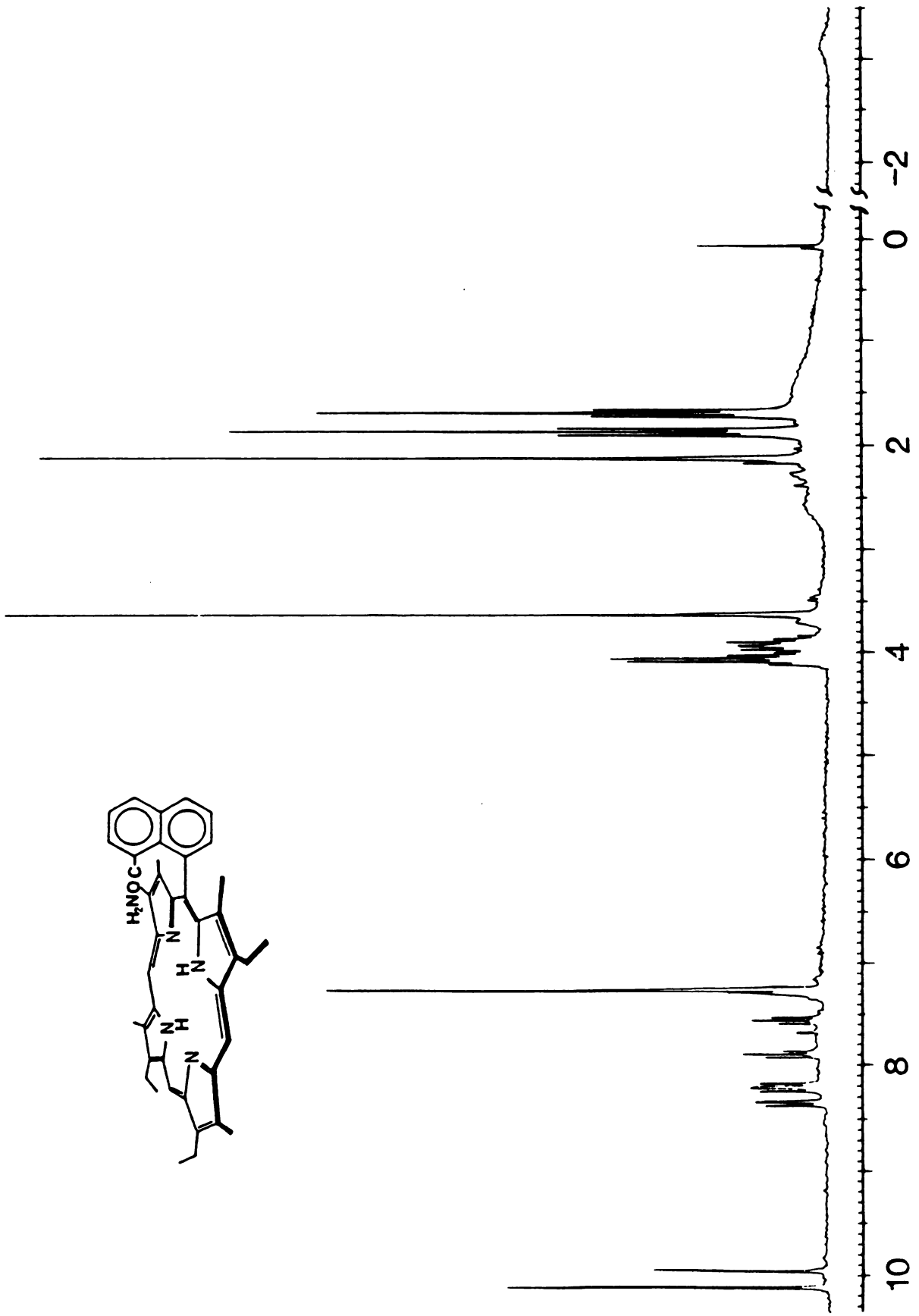

Figure 3-13 'H-NMR spectrum of porphyrin 25a

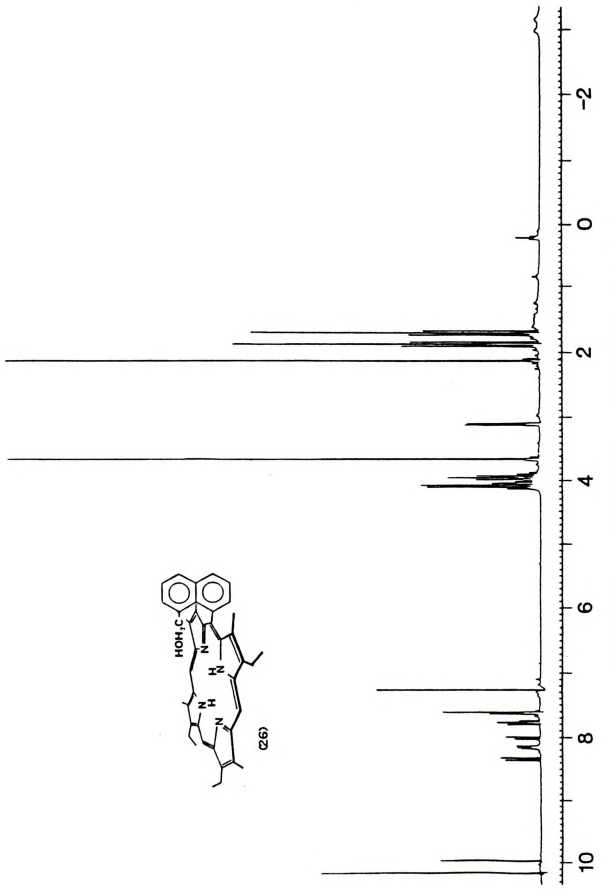

Figure 3-14 ^{1}H-NMR spectrum of porphyrin 26

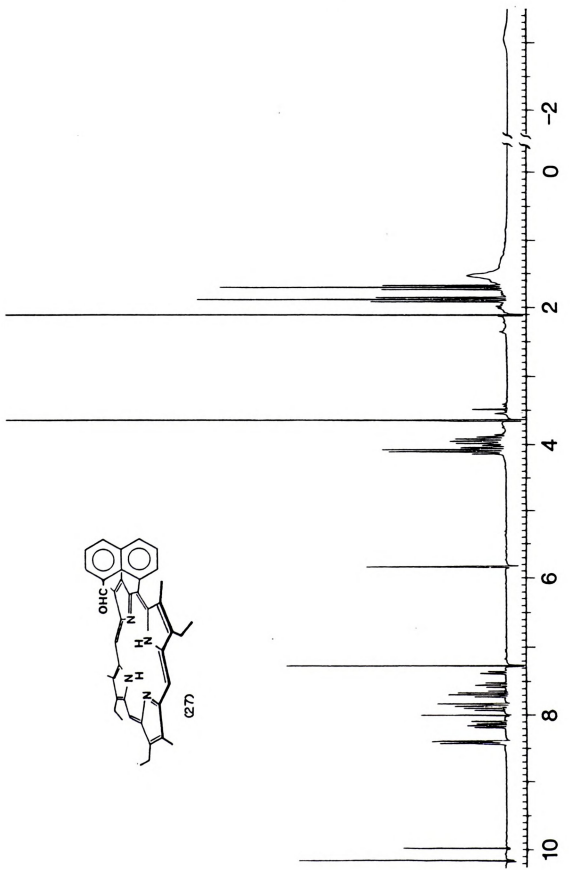

(27)

Figure 3-15 ^{1}H-NMR spectrum of porphyrin 27

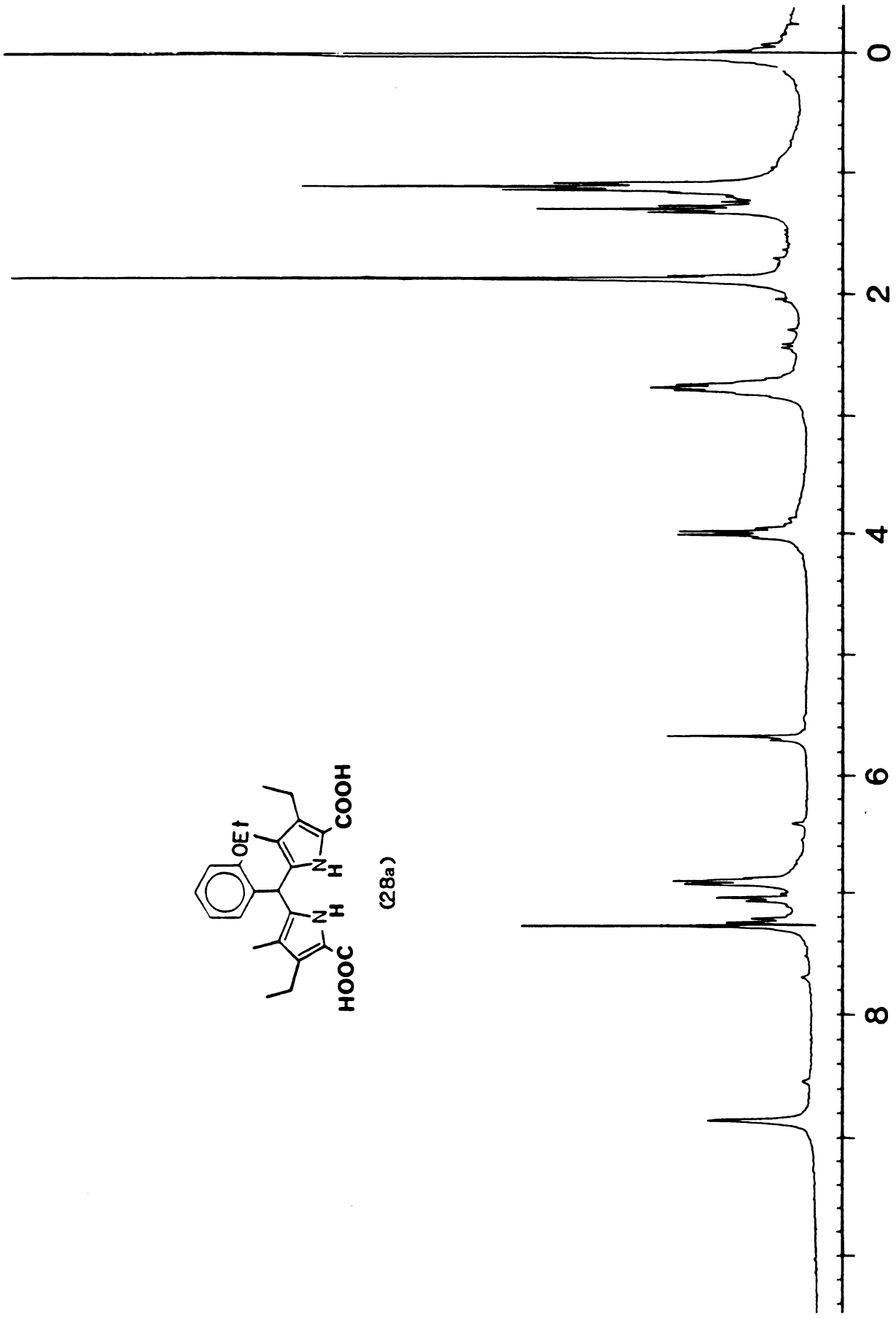

Figure 3-16 'H-NMR spectrum of dipyrromethane 28a

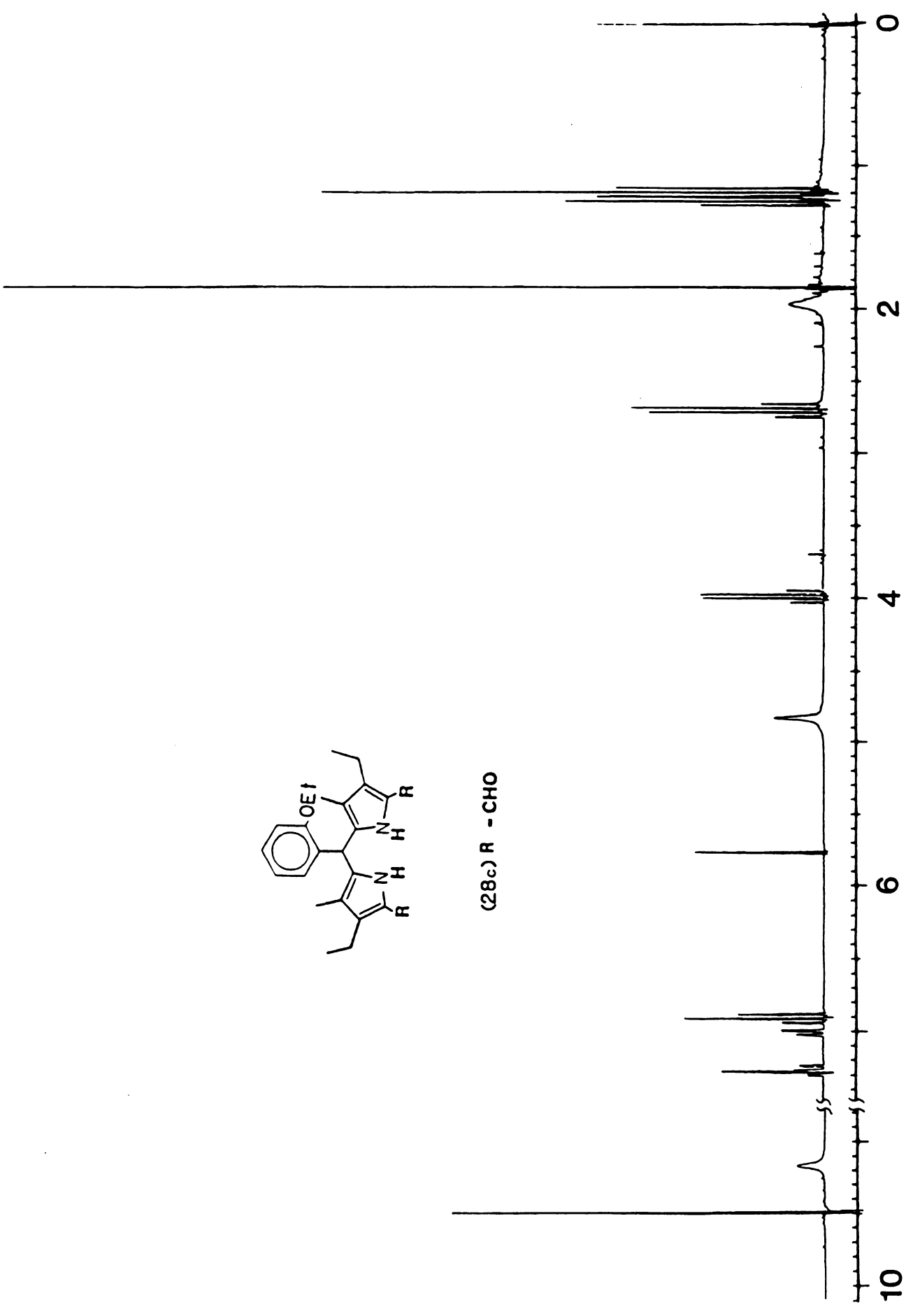

Figure 3-17 'H-NMR spectrum of dipyrromethane 28c

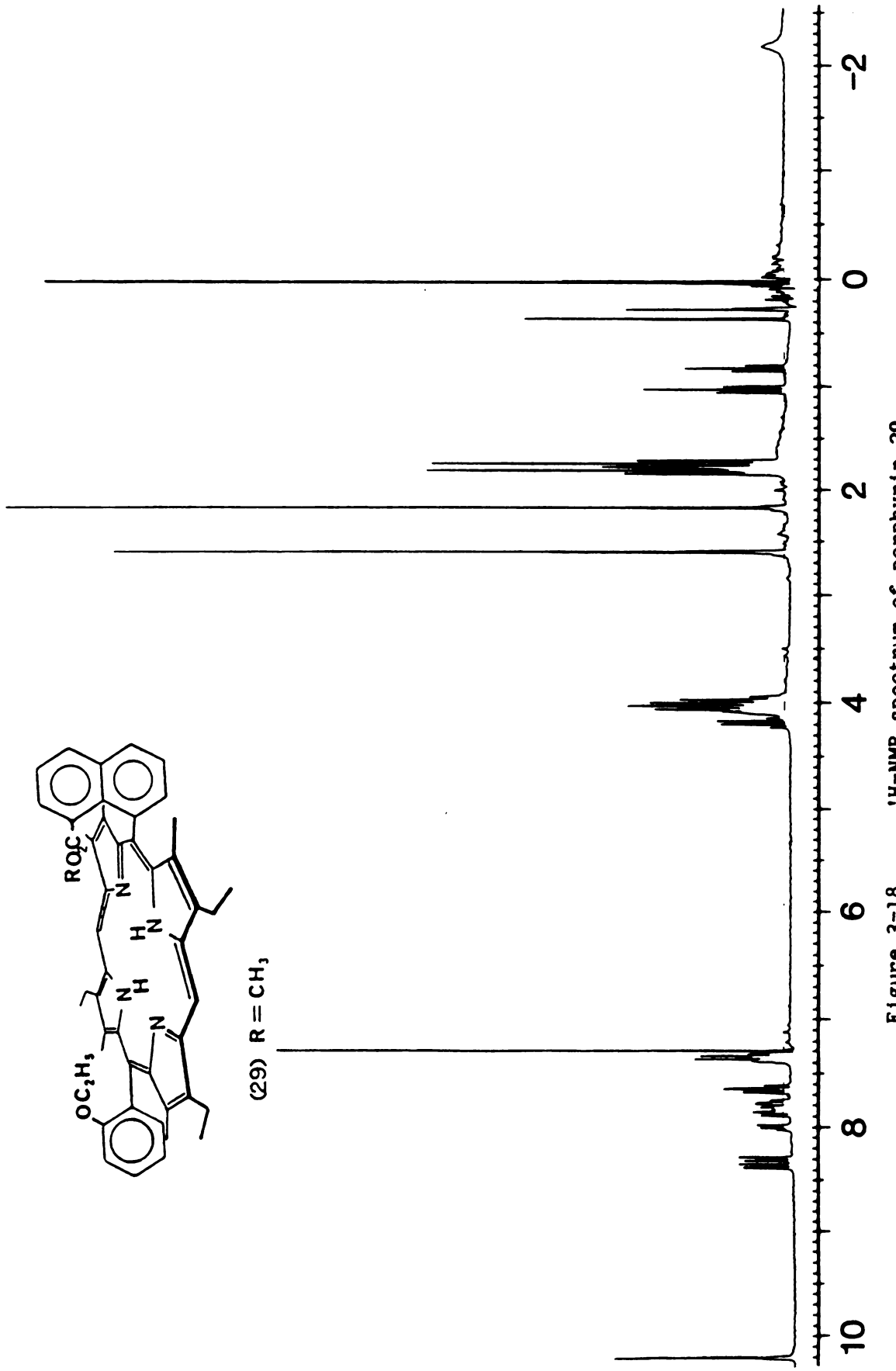

(29) R = CH_3

Figure 3-18 ^{1}H-NMR spectrum of porphyrin 29

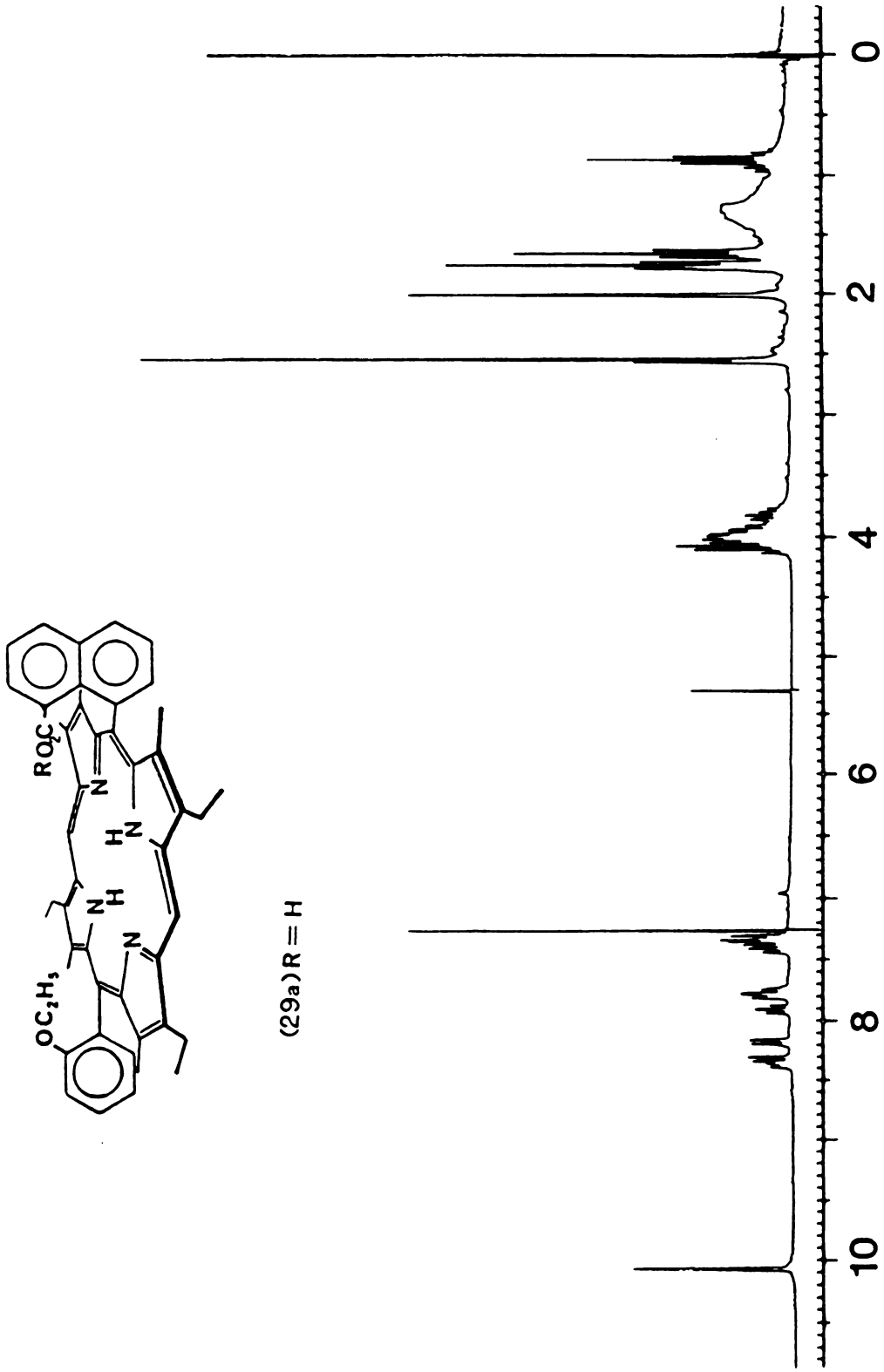

Figure 3-19 'H-NMR spectrum of porphyrin 29a

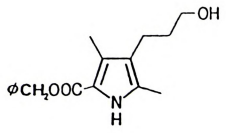

(31)

Figure 3-20 'H-NMR spectrum of pyrrole 31

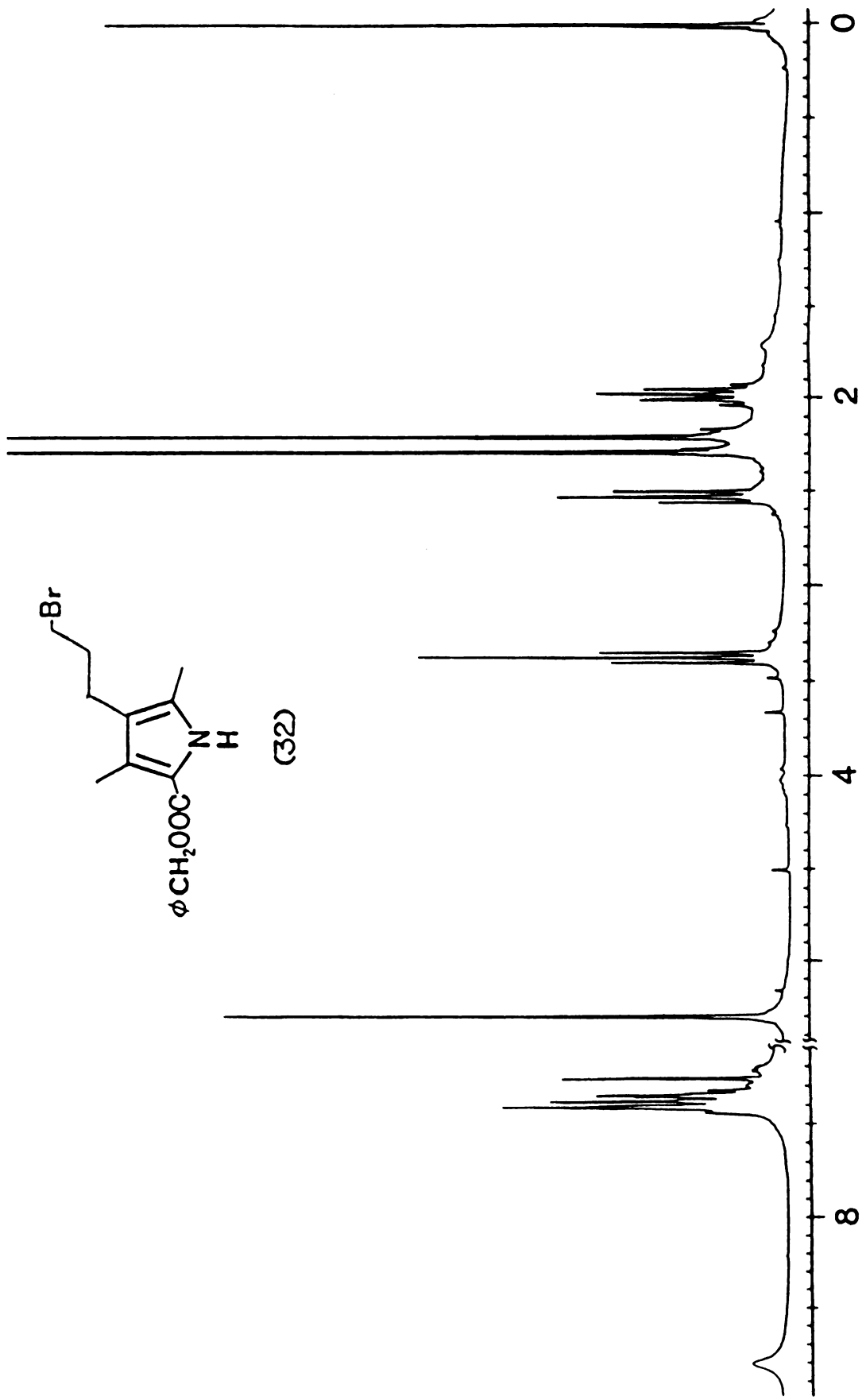

Figure 3-21 'H-NMR spectrum of pyrrole 32

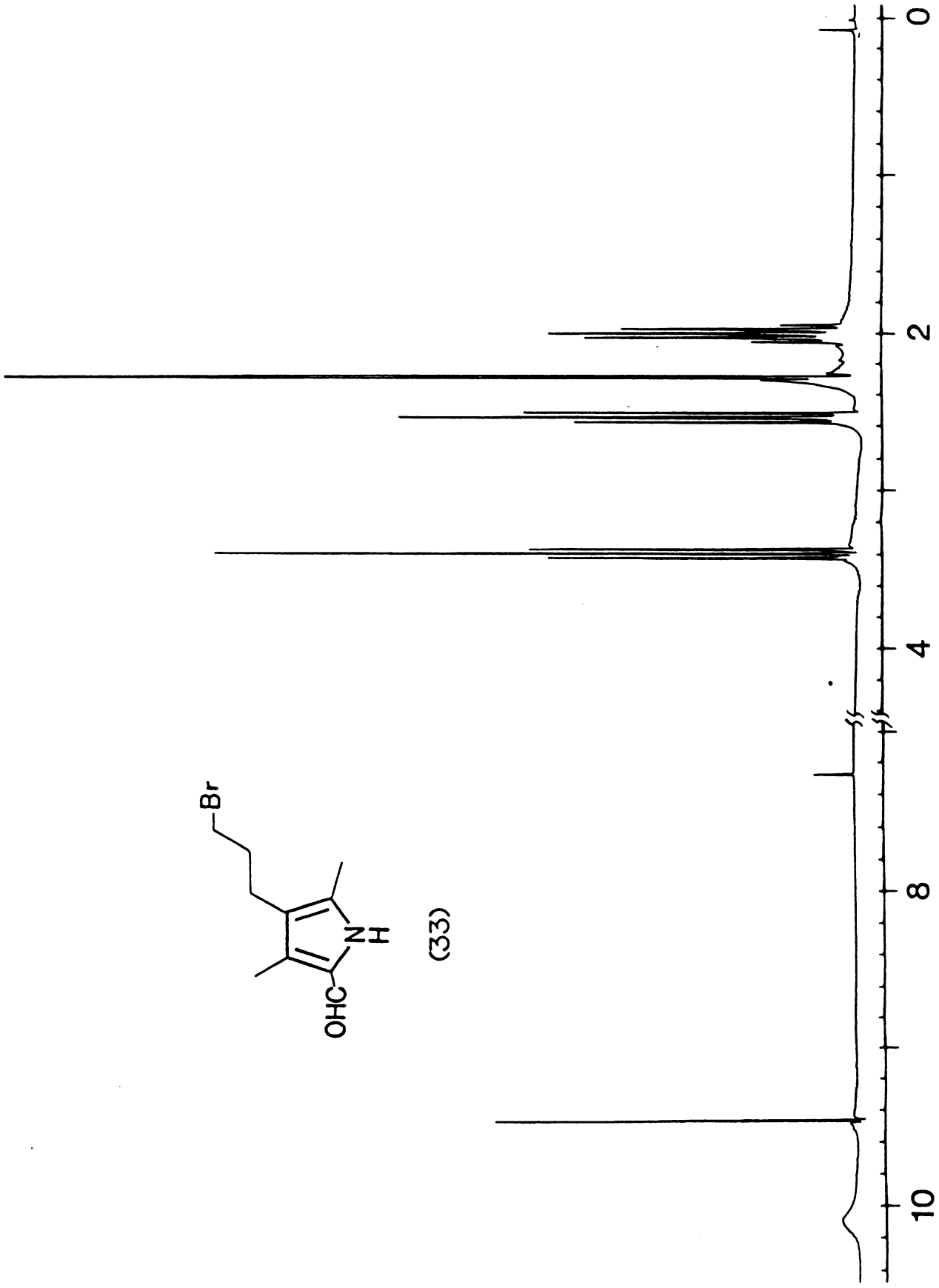

Figure 3-22 'H-NMR spectrum of pyrrole 33

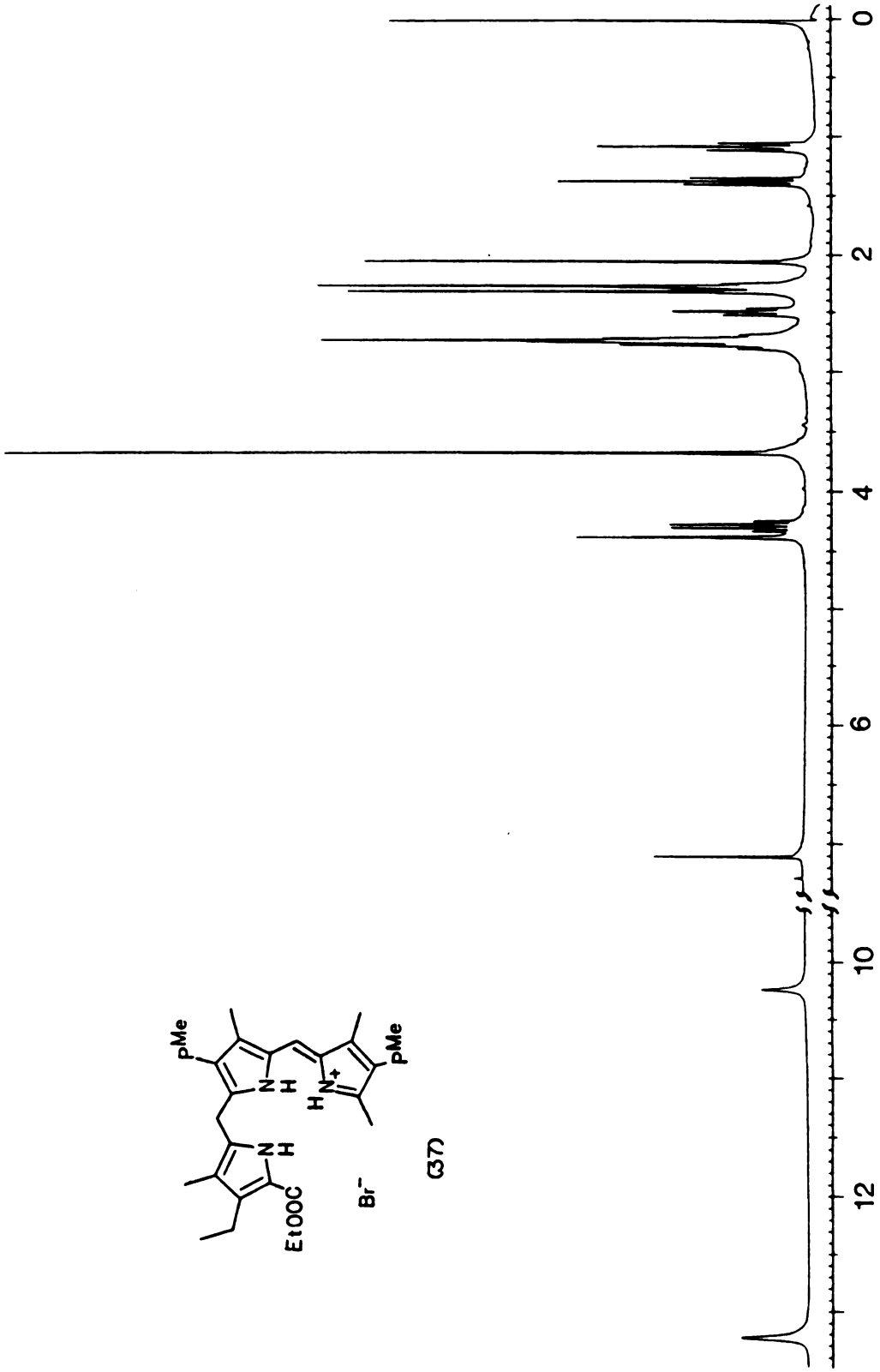

Figure 3-23 'H-NMR spectrum of tripyrrin 37

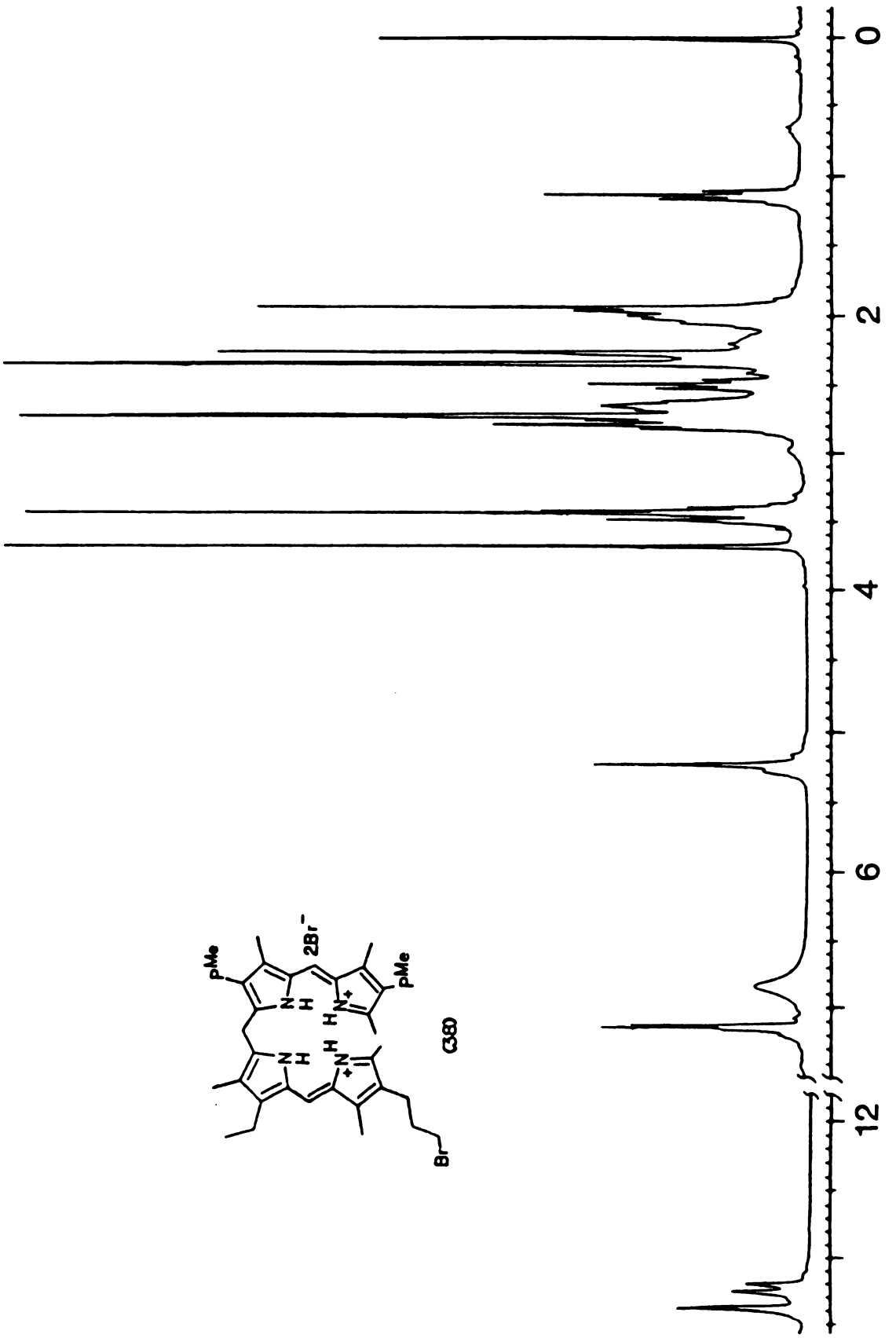

Figure 3-24 'H-NMR spectrum of biladiene 38

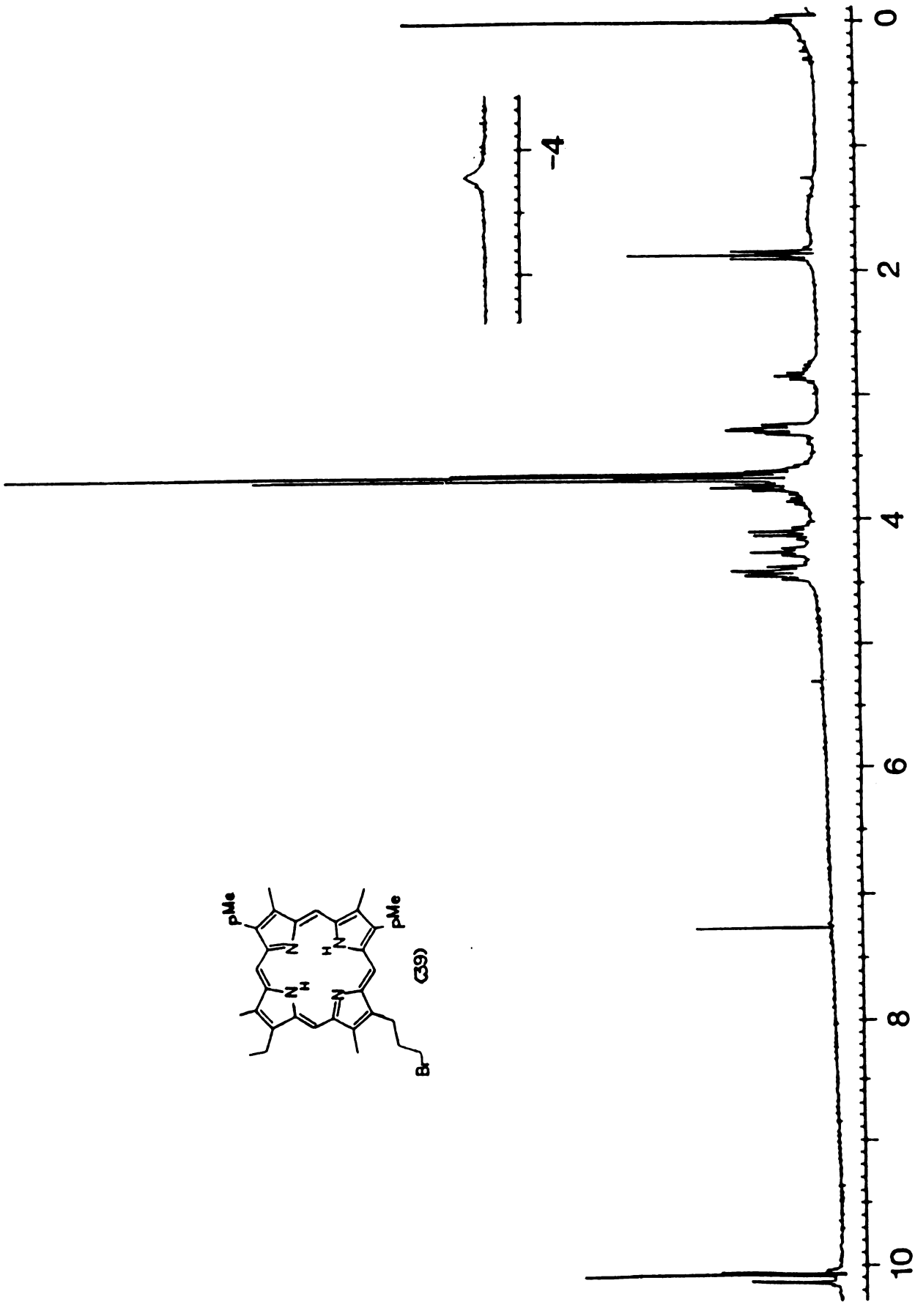

Figure 3-25 'H-NMR spectrum of porphyrin 39

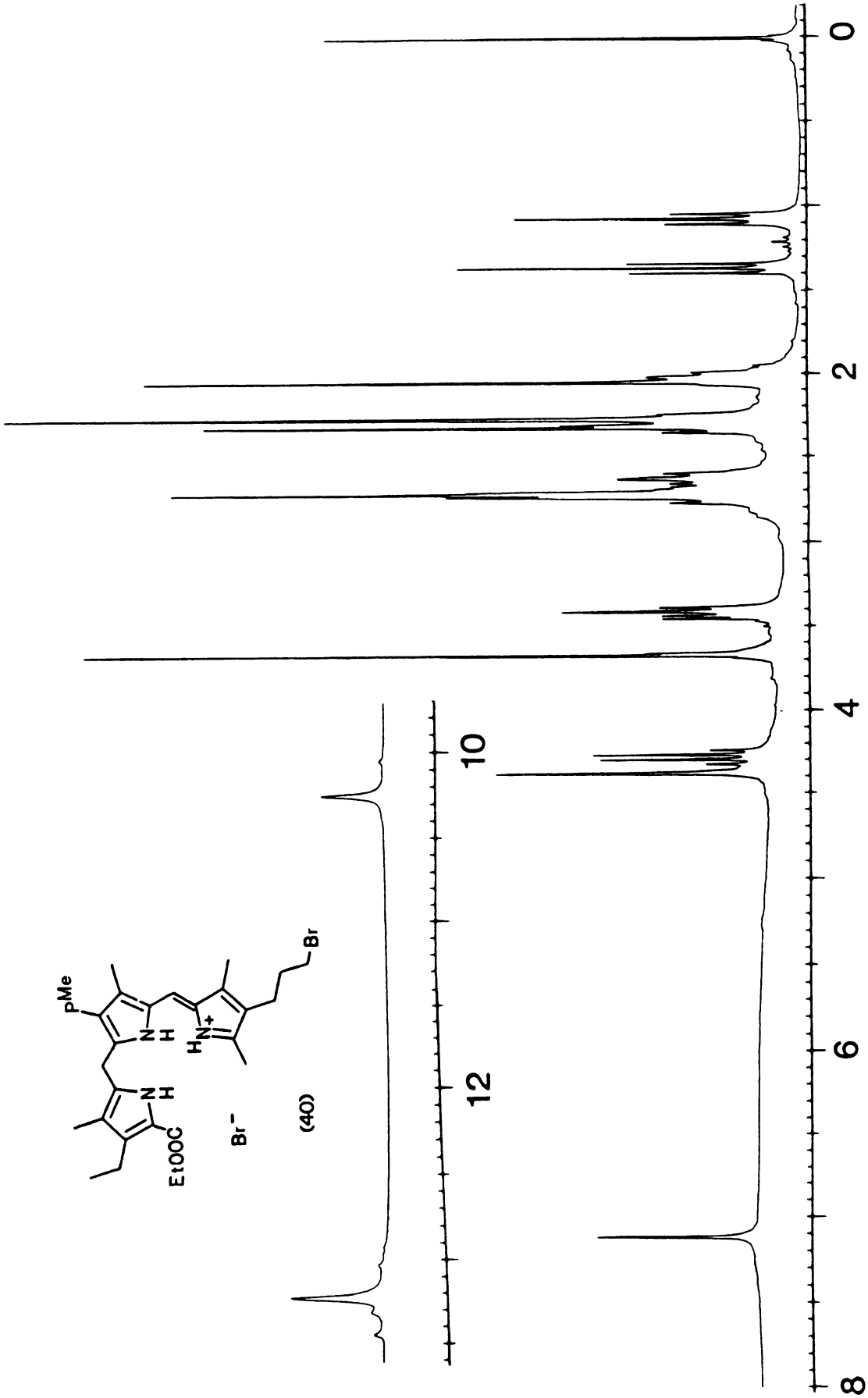

Figure 3-26 'H-NMR spectrum of tripyrrin 40

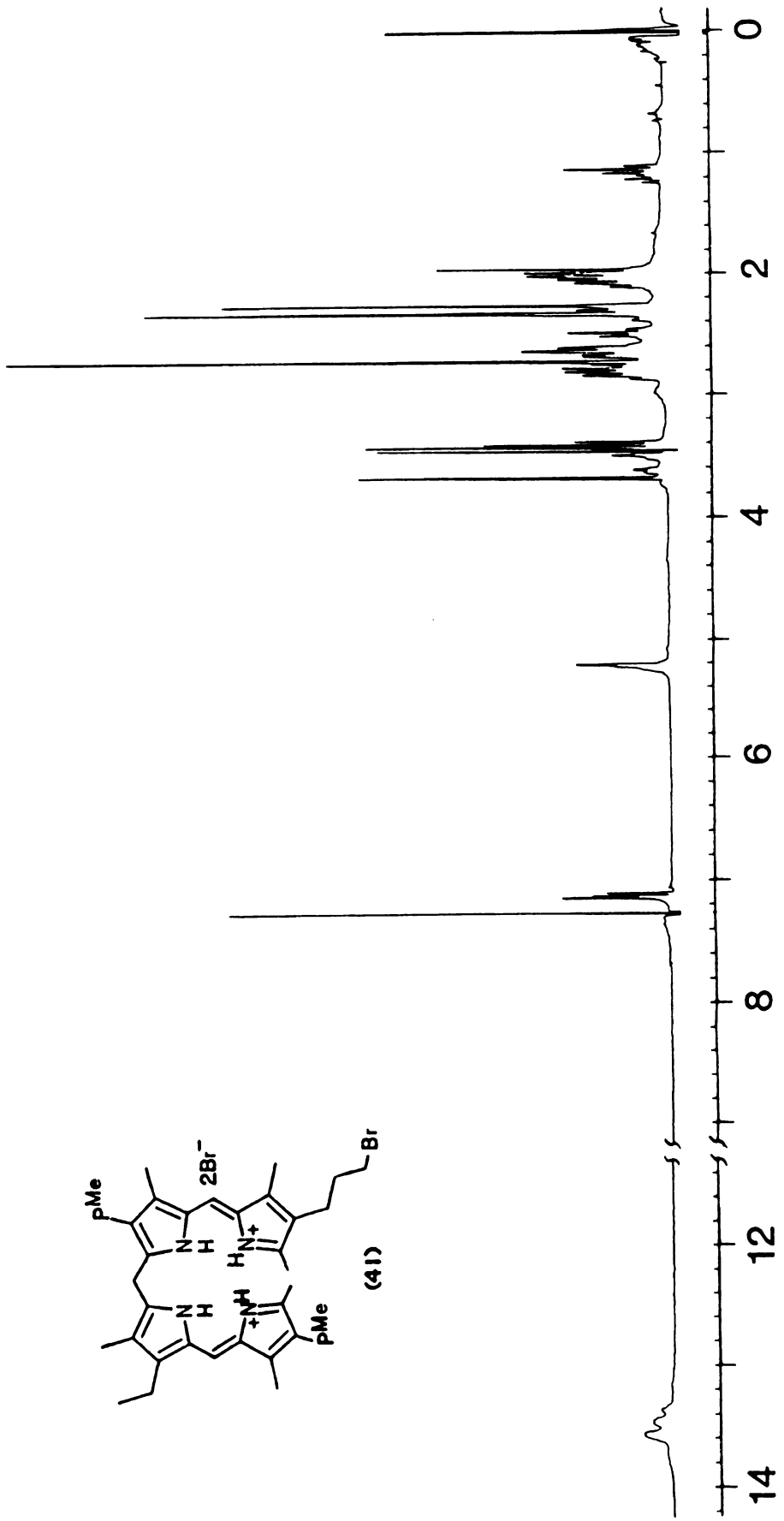

Figure 3-27 'H-NMR spectrum of biladiene **41**

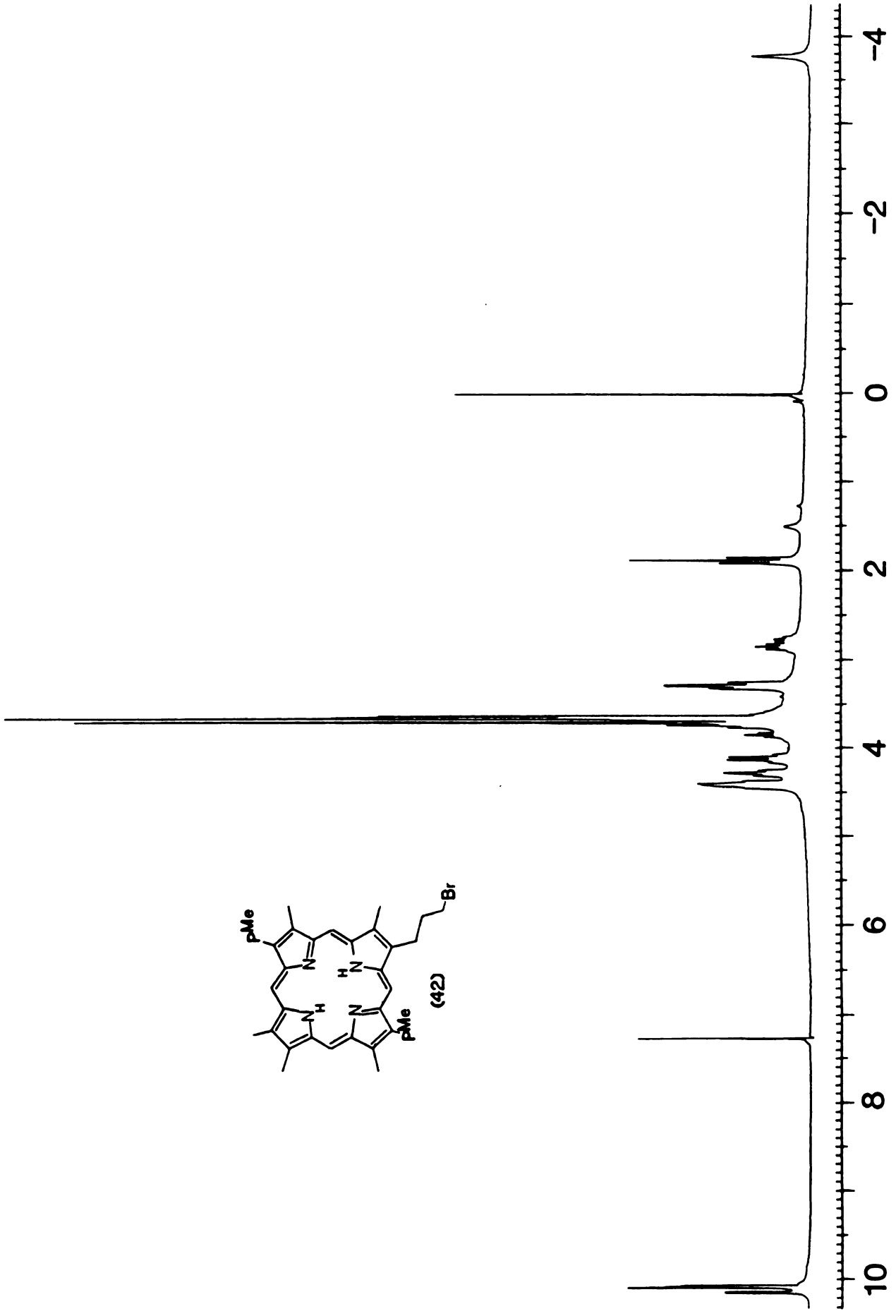

Figure 3-28 'H-NMR spectrum of porphyrin 42

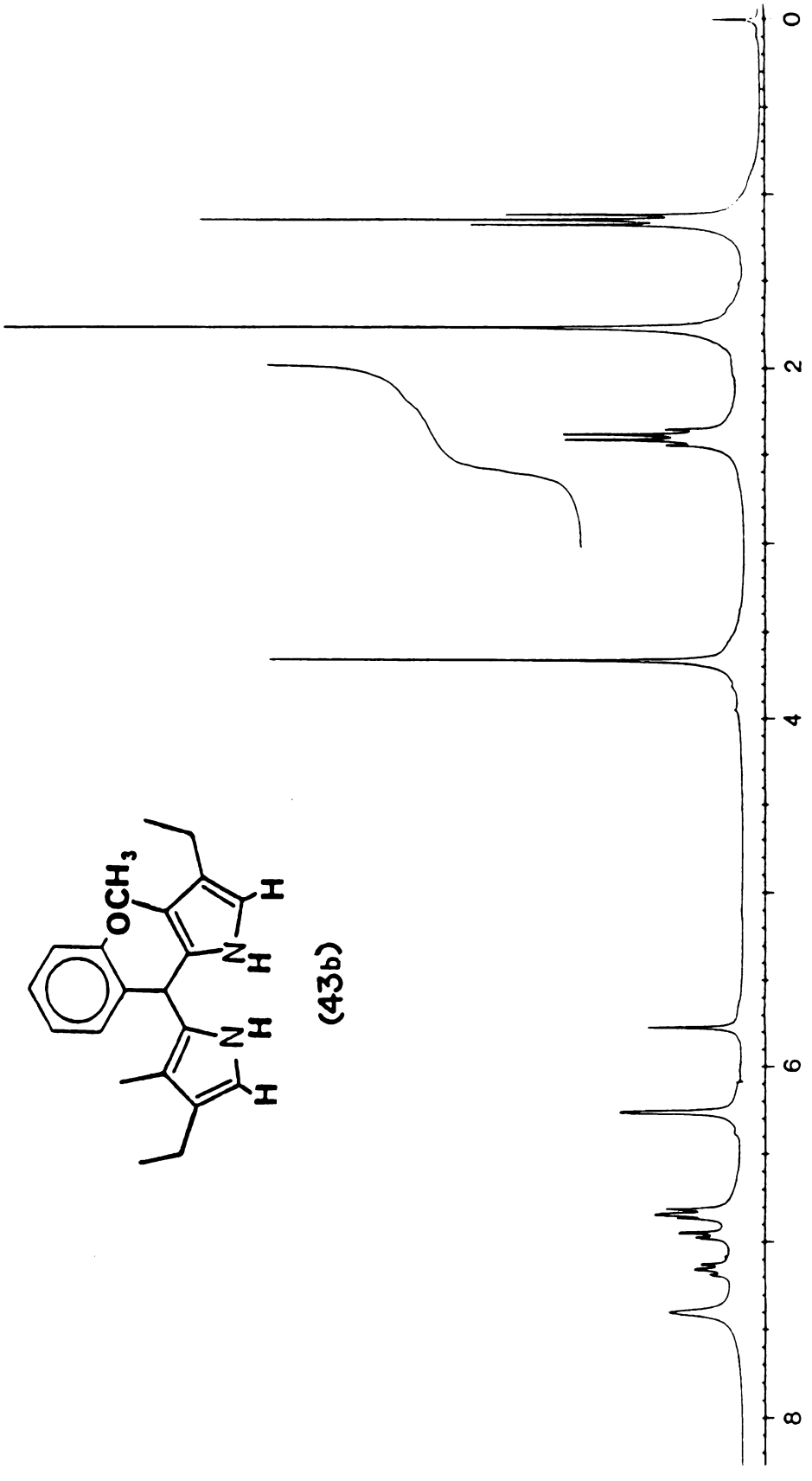

Figure 3-29 'H-NMR spectrum of dipyrromethane **43b**

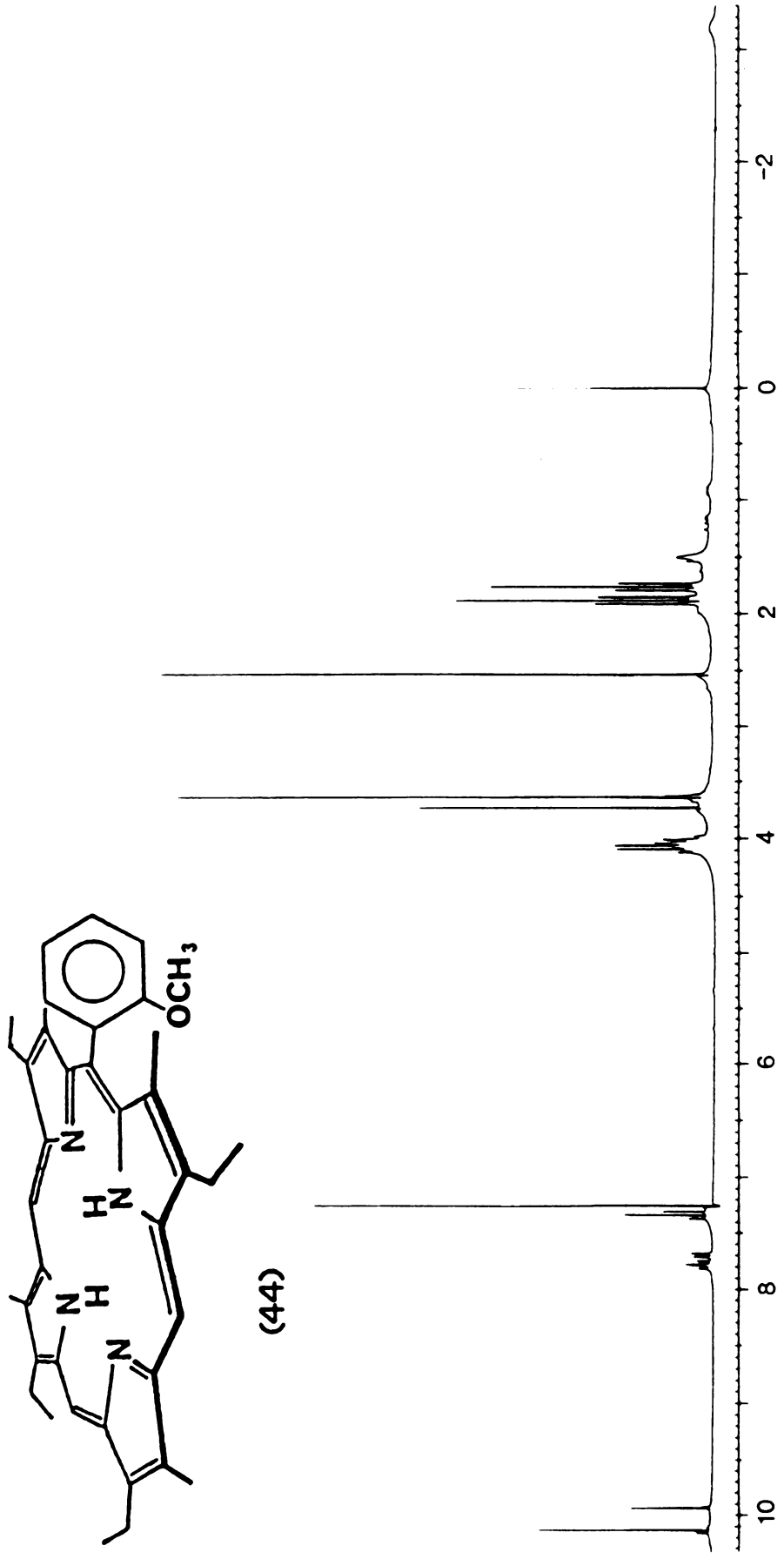

Figure 3-30 'H-NMR spectrum of porphyrin **44**

LIST OF REFERENCES

1. a. Antonini, E. and Brunori, M. (1971) in "Hemoglobin and Myoglobin in their their Reactions with Ligands," North Holland Publishing Co. Amsterdam.
   b. Guengerich, P. F.; MacDonald, T. L. Acc. Chem. Res. (1984), **17**, 9-16.
   c. Metelitsa, D. I. Uspekhi Khim (1981), **50**, 2019.
   d. Dickerson, R. E.; Geis, I. in "Hemoglobin: Structure, Function, Evolution and Pathology" (1983), (Benjamin/Cummings Publishing, Menlo Park, CA.).

2. a. Ibers, J. A.; Holm, R. H. Science (1980), **209**, 223-235.
   b. Collman, J. P.; Halbert, T. R.; Suslick, K.S. in "Metal Ion Activation of Dioxygen", T. G. Spiro, ed. (John Wiley & Sons; 1980) 1-72.

3. a. Phillips, S. E. V.; Schoenborn, B. P. Nature (1981), **292**, 81-82.
   b. Phillips, S. E. V. J. Mol. Biol. (1980), **142**, 531-554.
   c. Shaanan, B. Nature, (1982), **296**, 683.
   d. Chang, C. K.; Traylor, T. G. Proc. Nat'l. Acad. Sci. USA (1975), **72(3)**, 1166.

4. St. George, R.C.; Pauling, L. Science (Washington D.C.) (1951), **114**, 629.

5. a. Huber, R.; Epp, O.; Formanek, H. J. Mol. Biol. (1970), **52** 349.
   b. Heidner, E. J.; Ladner, R. C.; Perutz, M. F. J. Mol. Biol. (1976), **104**, 707.
   c. Norvell, J. C.; Nunes, A. C.; Schoenborn, B. P. Science (Washington D. C.) (1975), **190**, 568.
   d. Steigemann, W.; Weber, E. J. Mol. Biol. (1979), **127**, 309.
   e. Padlan, E. A.; Love, W. E. J. Biol. Chem. (1975), **249**, 4067.

6. a. Peng, S. M.; Ibers, J. A. J. Am. Chem. Soc. (1976), **98**, 8032.
   b. Hoard, J. L. (1975) in "Porphyrins and Metalloporphyrins," Smith, K. M. (ed.), Elsevier: New York, p. 351.

7. a. Moffatt, K.; Deatherage, J.F.; Seybert, D.W. Science (Washington D. C.) (1979), **206**, 1035.
   b. Perutz, M. F. Ann. Rev. Biochem. (1979), **48**, 327.

8. a. Caughey, W. S. Ann N.Y. Acad. Sci. (1970), **174**, 148.
b. Perutz, M. F. Br. Med. Bull. (1976), **32**, 195.
c. Collman, J. P.; Brauman, J. I.; Halbert, T. R.; Suslick, K. S. Proc. Nat'l. Acad. Sci. USA (1976), **73**, 333.
d. Collman, J. P.; Brauman, J. I.; Doxsee, K. M. Proc. Nat'l. Acad. Sci. USA (1979), **76**, 6035.

9. a. Traylor, T.G.; Chang, C.K.; Geibel, J.; Berzinis, A.; Mincey, T.; Cannon, J. J. Am. Chem. Soc. (1979), **101** 6716.
b. Traylor, T. G.; Berzinis, A. Proc. Nat'l. Acad. Sci. USA (1980), **77**, 3171.
c. Hashimoto, T.; Basolo, F. Comments Inorg. Chem. (1981), **1(4)**, 199-205.

10. a. Geibel, J.; Cannon, J.; Campbell, D.; Traylor, T. G. J. Am. Chem. Soc. (1978), **100**, 3575.
b. Traylor, T. G.; Campbell, D.; Sharma, V.; Geibel, J. J. Am. Chem. Soc. (1979), **101**, 5376.

11. a. Traylor, T. G.; Campbell D.; Tsuchiya, S. J. Am. Chem. Soc. (1979), **101**, 4748.
b. Battersby, A. R.; Hamilton, A. D. J. Chem. Soc. Chem. Commun. (1980), 117.
c. Collman, J. P.; Brauman, J. I.; Collins, T. J.; Iverson, B.; Sessler, J. L., J. Am. Chem. Soc. (1981), **102**, 2450.
d. Traylor, T. G.; Mitchell, M. J.; Tsuchiya, S.; Campbell, D. H.; Stynes, D. V.; Koga, N. J. Am. Chem. Soc. (1981), **103**, 5234.
e. Ward, B.; Wang, C. B.; Chang, C. K. J. Am. Chem. Soc. (1981), **103**, 5236.
f. Collman, J. P.; Brauman, J. I.; Iverson, B.; Sessler, J. L.; Morris, R. M.; Gibson, Q. H. J. Am. Chem. Soc. (1983), **105**, 3052.
g. Suslick, K. S.; Fox, M. M.; Reinbert, T. J. J. Am. Chem. Soc. (1984), **106**, 4522-25.
h. Traylor, T. G.; Koga, N.; Deardurff, L. A.; Swepston, P. N.; Ibers, J. A. J. Am. Chem. Soc. (1984), **106**, 5132.

12. Chang, C. K.; Ward, B.; Young, R.; Kondylis, M. P. J. Am. Chem. Soc. Submitted.

13. Lexa, D.; Momenteau, M.; Rentien, P.; Rytz, G.; Saveant, J-M.; Xu, F. J. Am. Chem. Soc. (1984), **106**, 4755-65.

14. a. Asakura, T.; Sono, M. (1979) in "Porphyrin Chemistry Advances," Longo, F. R. (Ed.), Ann Arbor Science.
b. Traylor, T. G.; Tsuchiya, S.; Campbell, D.; Mitchell, M.; Stynes, D.; Koga, N. J. Am. Chem.

Soc. (1985), **107**, 604-614.
c. Traylor, T. G.; White, D. K.; Campell, D. H.; Berzinis, A. P. J. Am. Chem. Soc. (1983), **103**, 4932-4936.
15. Yound, R.; Chang, C. K. J. Am. Chem. Soc. (1985), **107**, 898.

16. Ward, B.; Chang, C. K. Photochem. Photobiol. (1982), **35**, 757.

17. a. Chang, C. K.; Traylor, T. G. Poc. Nat'l. Acad. Sci. USA (1975), **72**, 1166.
b. Traylor, T. G.; Chang, C. K.; Cannon, J. J. Am. Chem. Soc. (1979), **101**, 6716.

18. Marzilli, G. L.; Marzilli, P. A.; Halpern, J. J. Am. Chem. Soc. (1971) **93**, 1374.

19. a. Diekmann, H.; Chang, C. K.; Traylor, T. G. J. Am. Chem. Soc. (1971), **93**, 4068.
b. Chang, C. K. J. Am. Chem. Soc. (1971), **99**, 2819.
c. Traylor, T. G.; Campbell, D.; Tsuchiya, S. J. Am. Chem. Soc. (1979), **101**, 4748.
d. Baldwin, J. E.; Almog, J.; Dyer, R. L.; Peters, M. J. J. Am. Chem. Soc. (1975), **97**, 226.
e. Baldwin, J. E.; Grossley, M. J.; Klose, T.; O'Rear, E. A.; Peters, M. K. Tetrahedron Lett. (1982), **38**, 27.
f. Battersby, A. R.; Buckley, D. G.; Hartley, S. G.; Turnbull, M. D. J. Chem. Soc. Chem. Commun. (1976), 879.
g. Momenteau, M.; Lavalette, D. J. J. Chem. Soc. Chem. Commun. (1982), 341.
h. Ogoshi, H.; Sugimoto, H.; Yoshida, Z. Tetrahedron Lett. (1976), 4477.
i. Collman, J. P.; Gagne, R. R.; Halbert, T. R.; Marchon, J. C.; Reed, C. A. J. Am. Chem. Soc. (1973), **95**, 7868.
j. Collman, J. P.; Brauman, J. I.; Doxsee, K. M.; Halbert, T. R.; Brunnenberg, E.; Linder, R. E.; Lamar, G. N.; DelGaudio, J.; Lang, G.; Spartalian, K. J. Am. Chem. Soc. (1980), **102**, 4182.
k. Collman, J. P.; Brauman, J. I.; Collins, T. J.; Iverson, B. L.; Lang, G.; Pettman, R. B.; Sessler, J. L.; Walters, M. A. J. Am. Chem. Soc. (1983), **105**, 3038.
l. Momenteau, M.; Loock, B.; Mispelter, J.; Bisagni, E. Nouv. J. Chem. (1979), **3**, 77.
m. Tabushi, I.; Sasaki, T. J. Am. Chem. Soc. (1983), **105**, 2901.

20. Paine, J. B.; Chang, C. K.; Dolphin, D. Heterocycles (1977), **7(2)**, 831.

21. Abchibald, J. L.; Walker, D. M.; Shaw, K. B.; Markovac, A.; MacDonald, S. F. Can. J. Chem. (1966), **44**, 345.

22. Chong, R.; Clezy, P. S.; Liepa, A. J.; Nichol, A. W. Aust. J. Chem. (1969), **22**, 229.

23. Chang, C. K.; Abdalmuhdi, I. J. Org. Chem. (1983), **48**, 5388.

24. Fuson, R. C.; Munn, G. J. Am. Chem. Soc. (1949), **71**, 1870.

25. a. Crumbliss, A. L.; Basolo, F. J. Am. Chem. Soc. (1970), **92**, 55.
    b. Hoffman, B. M.; Spilburg, C. A.; Petering, D. H. Cold Spring Harbor Symp. Quant. Biol. (1971), **36**, 343.
    c. Stynes, H. C.; Ibers, J. A. J. Am. Chem. Soc. (1972), **94**, 1559.
    d. Stynes, H. C.; Ibers, J. A. J. Am. Chem. Soc. (1972), **94**, 5125.
    e. Synes, D. V.; Stynes, H. C.; Ibers, J. A.; James, B. R. J. Am. Chem. Soc. (1973), **95**, 1142.
    f. Stynes, D. V.; Stynes, H. C.; James, B. R.; Ibers, J. A. J. Am. Chem. Soc. (1973), **95**, 1796.

26. a. Ibers, J. A.; Stynes, D. V.; Stynes, H. C.; James B. R. J. Am. Chem. Soc. (1974), **96**, 1358.
    b. Drago, R. S.; Beugelsdijk, T.; Breese, J. A.; Cannady, J. P. J. Am. Chem. Soc. (1978), **100**, 5374.
    c. Drago, R. S.; Stahlbush, J. R.; Kitko, D. J.; Breese, J. J. Am. Chem. Soc. (1980), **102**, 1884.
    d. Drago, R. S.; Corden, B. B. Acc. Chem. Res. (1980), **13**, 353-360.
    e. Collman, J. P.; Browman, J. I.; Boxsee, K. M.; Halbert, T. R.; Hayes, S. E.; Suslick, K. S. J. Am. Chem. Soc. (1978), **100**, 2761.

27. Jameson, G. B.; Drago, R. S. J. Am. Chem. Soc. (1985), **107**, 3017-3020.

28. a. Jackson, A. H.; Smith, K. M. In "Total Synthesis of Natural Products", ApSimon, J. W., Ed., Wiley, New York, (1973), pp. 143-278.
    b. Smith, K. M. In "Porphyrins and Metalloporphyrins," Smith, K. M.; ed.; Elsevier, Amsterdam, (1975), Chapter 2.

29. Smith, K. M.; Graig, G. W. J. Org. Chem. (1983), **48**, 4302-4306.

30. Suckling, G. J., Ph.D. Thesis, Liverpool, (1970).

31. Clezy, P.S.; Fookes, C. J. R.; Liepa, A. J. Aust. J.

Chem. (1972), **25**, 1979.

32. Paine, J. B. In "The Porphyrins," Dolphin, D., Ed., Academic Press, (1978), Vol. 1, pp. 107-115.

33. Drago, R. S.; Cannady, J. P.; Leslie, K. A. J. Am. Chem. Soc. (1980), **102**, 6014.

34. Molenaro, F. S.; Little, R. G.; Ibers, J. A. J. Am. Chem Soc. (1977), **99**, 5628.

35. Guryanova, E. N.; Goldshtein, I. P.; Perepelkova, T. I. Russ. Chem. Rev. (1976), **45**, 792.

36. Spilburg, C. A.; Hoffman, B. M.; Petering, D. H. J. Biol. Chem. (1972), **247**, 4219.

37. Ikeda-Sato, M.; Yamamoto, H.; Imai, K.; Kayne, F. J.; Yonetani, T. J. Biol. Chem. (1977), **252**, 620.

38. a. Dolphin, D.; Felton, R. H.; Borg, D. C.; Fajer, J. J. Am. Chem. Soc. (1970), **92**, 743.
    b. Bonnett, R.; Dimsdale, M. J. J. Chem. Soc. Perkin I (1972), 2540.

39. O'Carra, P. in "Porphyrins and Metalloporphyrins," Smith, K. M., ed., Elsevier Scientific Publishing Company, (1975), p. 123-153.